MODELLING OF A LATHE STRUCTURE

MODELLING OF A LATHE STRUCTURE FOR THE COMPUTATION OF DYNAMIC CHARACTERISTICS

By

CEDRIC PARK, B.Sc.(Eng.)

A Thesis

Submitted to the School of Graduate Studies

in Partial Fulfilment of the Requirements

for the Degree

Master of Engineering

McMaster University

September 1973

MASTER OF ENGINEERING (1973) McMASTER UNIVERSITY
Hamilton, Ontario

TITLE: Modelling of a lathe structure for the computation of dynamic characteristics

AUTHOR: Cedric Park, B.Sc.(Eng.) (University of London)

SUPERVISOR: Dr. J. Tlusty

NUMBER OF PAGES: x, 146

ABSTRACT

As part of a general programme of machine tool research, this work initiates development of mathematical models of machine tool structures.

The lumped-parameter method is employed in modelling a lathe spindle assembly, importance being attached to the effect of components in contact with the spindle proper. For the complete lathe structure, the finite element approach is used and computations are carried out on a commercially-available computer programme.

In both cases the dynamic behaviour of the model is determined and compared with the behaviour of the actual structures obtained directly by measurement. The measurements belong to related studies in the general programme.

The work also includes an introductory study of the static and modal characteristics of a model milling machine adopted by several universities in an international co-operative programme in machine tool research.

ACKNOWLEDGEMENTS

The author gratefully acknowledges the valuable guidance and advice of Dr. J. Tlusty, given consistently throughout the course of this work.

The author also acknowledges the support of the National Research Council in making it possible to carry out the computations.

Thanks are also expressed to Mrs. A. Smith and Mrs. S. Mountain whose valuable assistance in preparing this document is greatly appreciated.

TABLE OF CONTENTS

LIST OF FIGURES

INTRODUCTION

1. INTRODUCTION

1.1 General Introduction

Only in this decade has an attempt been made to apply digital computing methods to machine tool design. Such methods are well-established in the aircraft and civil engineering industries but it was not until 1964 that the digital computer was first used in the investigation of static and dynamic characteristics of machine tool structures. The investigators at that time were Taylor and Tobias [1].* Since then the computer has not only been adopted in machine tool research in the universities but also in more applied research and in design in the machine tool industry in several countries.

1.2 A Problem in Dynamics

The design of a machine tool must include consideration of its rigidity and stability as a structure. Deformations can occur due to various factors, cutting forces; weight forces; forced vibrations from unbalanced rotating parts; self-excited vibrations at the cutting point. It follows therefore that the quality of the machined work depends appreciably upon the static and dynamic

---

*Numbers in square brackets indicate references given in bibliography.

stiffness characteristics of the tool and workpiece. The machine tool structure as a vibratory system determines chatter stability, which has been defined as the maximum width of cut which can be taken without causing the machine to chatter. Chatter phenomena has been the subject of considerable investigation [2,3].

A detailed treatment of the theory of chatter and associated self-excited vibrations is given in reference [4]. The mechanism of chatter is shown as a closed-loop system having these fundamental components:

(i) the cutting process

(ii) the vibratory system of the machine structure

(iii) the mutual directional orientation of these two components.

The cutting process, characterized by the feed, the cutting speed, the tool geometry and the material of the workpiece, will not be considered in this thesis.

As a vibratory system, the machine tool structure has an infinite number of degrees of freedom and with this, in turn, is associated an infinite number of natural frequencies and mode shapes. From these, together with the related mass and stiffness characteristics of the structure, can be obtained the appropriate equations of motion and hence the dynamic response of the tool and workpiece to harmonic excitation. This is dealt with in more detail in Chapter III, where it is shown that not all modes are of

practical importance and usually only the lower modes are considered. The discrete model in Chapter III has over 400 dynamic degrees of freedom, yet only the first ten modes are computed.

The mutual directional orientation of the cutting process with respect to the vibratory system occurs because the machined surface has a definite location in space, the cutting forces have a definite direction and because also the vibratory system of the machine has a definite location in space, with definite directions of vibrations in its individual modes. By changing the mutual directional orientation of both basic components, their mutual influence is changed and also the limit conditions for stable machining change [5].

1.3 A Brief History

The original computer-aided work carried out by Taylor and Tobias [1] covered two types of machines; a radial drill and a lathe. The flexibility method was used in the matrix formulation on 'lumped-parameter' models and the results obtained were compared with those obtained from measurements made with plexiglass models. Results were encouraging, although it must be realized that the comparison was not made with the actual machines.

In 1967 Cowley [6] reported on a computer anlysis of a plano-milling machine structure. His method of analysis was similiar to that just described but in his study, amongst other refinements, he took into account the contributions various machine elements made to deflection.

In January 1970, six universities from five countries embarked on a co-operative programme of work concerned with computer-aided design of machine tool structures. Under the auspices of the C.I.R.P. Group Ma they selected a model milling machine in use at the University of Leuven. The primary objective of the first phase of the work was to establish the nature of the computational procedures adopted by the various contributors and to compare the results obtained from their individual computations of the static and dynamic properties of the model [7]. When the results were in and the comparison made, one or two modifications to the model were agreed and the computations repeated. The first phase has now concluded satisfactorily and the computer programs created, and regarded as now thoroughly tested, wil be used in subsequent phases for computations on actual machine tools [7,8].

In 1968 Stephens used the stiffness matrix method in the form of the finite element technique in the analysis of machine tool sections. Further studies employing this method were made by Wilson [9] and Hinduja [10]

in 1971. In his study, Wilson included a finite element treatment of the C.I.R.P. model milling machine.

1.4 The Case for Computing

Prior to the introduction of the digital computer in machine tool design, the most reliable method of predicting static and dynamic behaviour before manufacture was by construction and testing of a physical model, usually made of plastic. Model testing has produced much valuable information and, no doubt, has on many occasions led to modifications in design [11]. Brown et al report [3] that as a result of model testing of hobbing machine structures, the quasi-static stiffness was increased by 100%. Model-testing fails through its limitations. Between the model and the prototype there are serious differences in properties of materials and in the tolerances of manufacture. Model analysis cannot truly reflect small changes since the effects of minor modifications are lost in differences in manufacture for the different materials and in tolerance differences. Moreover, a small modification in design is not necessarily followed by correspondly small shop cost.

The computer as a design tool has much to commmend it and its principal value is the ease with which it allows comparison of alternative designs to be made. The design of a new machine model is based on the previous one.

Measurements made on the old model indicate which parts of the machine should be made stiffer. It is here that the computing of static stiffness of these parts in a preliminary design in several variants, helps considerably in choosing the best variant. However, one cannot, at this stage, reliably determine dynamic stability of the machine mainly because of an inability to determine damping as related to design. Prediction of the dynamic behaviour is also inhibited by the lack of knowledge of the characteristics of such machine elements as joints, bearings and irregular sections.

Therefore, it is necessary to wait until the prototype is constructed and measured. Then the natural frequencies, mode shapes and receptances are computed for a mathematical model of the machine. This computational model is modified until it matches the measured one. The final computed model is then an important basis for checking any proposed changes in design between the prototype and the machine to be manufactured. In this stage because the changes will affect the structure only partly, it is assumed that the damping remains as measured. References [12,13,14] report on comparison of computations made on alternative designs.

1.5 Object and Scope

This study on the mathematical modelling of machine tools falls into three parts:

(i) Development of a model of a lathe spindle complete with chuck, workpiece and mounted parts such as gears. The study includes the case of the spindle held in bearings. By making refinements to the model an attempt is made to match the computed natural frequencies and mode shapes with those measured on the actual spindle. The lumped-parameter method is used in the computations.

(ii) Development of a model for the complete lathe. Natural frequencies and mode shapes are computed and also the relative receptance between the tool and the workpiece is determined. A comparison is made with results obtained from measurements on the lathe. The problem is formulated using the finite-element method.

(iii) Using the dimensional, inertia and stiffness data supplied to the various universities, computations are made on the C.I.R.P. model to determine the static deflections due to certain cases of loading and also to determine the lower natural frequencies and mode shapes. The lumped-parameter method is used.

The three parts are dealt with in Chapters II, III and IV respectively.

The experimental work, with which the results in Chapters II and III are compared comprised harmonic excitation tests on the lathe. The experimental work is reported in reference [5].

LATHE SPINDLE

II. LATHE SPINDLE

2.1 Introduction

It was noted in Chapter I that one of the reasons for the computer not playing a greater role in machine tool design is the present lack of factual data on the structural elements which make up the machine. Elements having simple cross-sections, for example tubular or thin-walled box-type sections, admit to theoretical treatment and close agreement with experimental results can be achieved in static or modal analysis. Such elements can be readily represented when modelling the complete machine. However, when cutaways, ribbings, irregular sections or bearings are encountered in machine elements, the complexity of the structure does not lend itself easily to theoretical analysis.

In recent years a start has been made in solving this problem with the aid of computers, in conjunction with experimental investigation [13,14,20]. This chapter deals with the development of a mathematical model for a lathe spindle complete with chuck and workpiece. This type of spindle is more complex than most and Section 2.2 describes these complexities.

The lumped-parameter method is used to determine natural frequencies and mode shapes of the model. These results are compared with those obtained by measurement on the actual spindle in similiar configuration and refinements then made to the model with the purpose of obtaining good agreement between measured and computed mresults. In the lumped-parameter method, the structure under consideration is represented by a number of lumped masses located at points, known as nodes and connected by weightless, elastic beams. The accuracy of the results obtained by this method depends largely on how well the stiffness of the structure is represented by the stiffness of the connecting beams and also how well the distribution of the mass of the actual structure is represented by the distribution of the lumped masses.

2.2 Developing the mathematical model

Obtaining a suitable discrete model of a lathe spindle, without any attachments, presents little difficulty as it is a simple matter to calculate the inertias and stiffnesses involved. But when the spindle is considered completely assembled as it would be when functioning normally, then the assembly represents a complicated substructure. The following elements in the assembly must then be considered:

(a) The basic spindle, comprising various cross-sections, collar and nose;

(b) The chuck with its jaws, a complicated structure whose rotary inertia could be significant if transverse vibrations are present. Of great importance here is the contact between jaws and workpiece. This is characterized by small contact area and large local deformation and suggesting the possibility of certain relative rotation between chuck and workpiece.

(c) The attached masses on the spindle, including gears, dog clutch and bearings. These items constitute additional mass but what is more difficult to gauge is by how much they increase the stiffness of the spindle.

(d) The bearings. The unknown here, - the stiffness of a system of the two rings with a row of balls between, - is not easy to determine and is further complicated by such factors as, the accuracy of the bearing, the diametrical clearance and the pre-load.

The investigation is based on these four elements. Each of the last three is taken in turn and its effect on the modal behaviour of the spindle isolated from the others and thereby examined. The work is therefore carried out in three phases, both experimentally on the actual spindle and by computation on the model. Details of the experimental work are given in Section 7.5 while an outline of the three phases is given below.

(i) The spindle was removed from the lathe and suspended, complete with chuck and workpiece but without any other attached masses and without bearings, from ropes. Natural frequencies and mode shapes were obtained experimentally as it vibrated as a 'free-free' beam. When this was simulated on the computer, the important parameters referred to the chuck. They were chuck stiffness and clamping of the chuck jaws. These two were studied together in the first phase and the optimum values resulting from the study were used in the second phase. Optimum values were those values which gave best agreement between the computed and measured frequencies and mode shapes.

(ii) The gears and other masses which are normally part of the spindle assembly were mounted on the spindle and the procedure as in (i) was repeated. However, in the computations the parameter under investigation was now the stiffening effect of the masses on the spindle.

(iii) The final phase was with the spindle back in the lathe. The effects of the chuck stiffness, clamping and of the mounted masses had been assessed and were incorporated into the input data in the final computations. The final parameter to be examined was the stiffnesses of the two bearings.

During the investigation described in the three phases above, actually two workpieces were used, - one, long and heavy compared with the other. In this way, the

modelling procedure had to accommodate correctly the two stiffnesses on the chuck (the body of the chuck and the jaws in contact with the workpiece) for more than one type of workpiece.

Figure 2.1 (a) is a drawing of the actual spindle while below in Figure 2.1 (b) is shown the initial version of the mathematical model. The selection of the location of station points or nodes was determined by changes in cross-section of the spindle and location of the two bearings. The mass of the attached gears, dog clutch and bearings was apportioned between appropriate nodes. The chuck represented the greatest concentration of mass. Its mass was initially divided between two nodes and connected by a rigid beam. The clamping of the workpiece in the chuck was assumed to allow certain relative rotation and was represented by a torsion spring located at the face of the chuck. Two springs located between the appropriate nodes and ground represented the bearings.

To obtain closer agreement between the computed and measured results certain modifications were later made to the model. Mode shapes disallowed the assumed rigidity of the chuck, necessitating the rigid link be replaced by a beam of finite stiffness. The torsion spring was replaced by a short flexible beam. The flexible beam

provided the necessary relative rotation between workpiece and jaws yet, as it was short, contributed little to nodal displacements. This produced an improvement in mode shape but, more important, it resulted in a model which offered wider application (Figure 2.1 (c)).

2.3 Analysis

There is one equation of motion for each degree of freedom and for each degree of freedom there is one generalized co-ordinate. Thus the matrix embodying the equations of motion will be square. The equations can be set up using influence coefficients. The stiffness influence coefficient, k_{ij} is defined as the applied force associated with x_i (see Figure 2.2) required to hold the system in static equilibrium when x_j is given unit displacement; the displacement of the other co-ordinates being zero. Then, for a system of static forces and displacements, the applied forces are:

$$\begin{aligned} F_1 &= k_{11}x_1 + k_{12}x_2 + \cdots + k_{1j}x_j + \cdots + k_{1n}x_n \\ &\vdots \\ F_i &= k_{i1}x_1 + k_{i2}x_2 + \cdots + k_{ij}x_j + \cdots + k_{in}x_n \\ &\vdots \\ F_n &= k_{n1}x_1 + k_{n2}x_2 + \cdots + k_{ng}x_j + \cdots + k_{nn}x_n \end{aligned} \quad \ldots (2.1)$$

$$\text{or} \quad (F) = [K](X) \quad \ldots (2.1a)$$

Where [K] is a square matrix and (F) and (X) are the applied force and displacement vectors respectively. The reactive elastic force vector is then = − [K] (X).

The inertia force on mass m_i is

$$F_i \text{ (inertia)} = -m_i \ddot{x}_i$$

Assuming that the system vibrates harmonically with circular frequency ω , such that

$$x_i = X_i \sin \omega t$$

then the equations of motion can be expressed in the following matrix form for a conservative system:

$$[K] \quad (X) \quad = \omega^2 \quad [M] \quad (X) \qquad \ldots.(2.2)$$

[M] being a diagonal matrix.

(2.2) can be written as follows:

$$\frac{1}{\omega^2} \quad (X) \quad = \quad [K]^{-1} \quad [M] \quad (X)$$

$[K]^{-1}$ being the inverse stiffness or flexibility matrix.

Then if the matrix product $[K]^{-1}\ [M] = [A]$

$$\frac{1}{\omega^2} \quad (X) = [A] \quad (X) \qquad \ldots.(2.3)$$

Equation(2.3) represents the eigenvalue problem which is satisfied for every eigenvector (X_i) with corresponding eigenvalue or characteristic value $\frac{1}{\omega_i^2}$

Once formulated, the eigenvalue problem can be solved using a computer library sub-routine. At one stage in the computing when difficulties developed with mode shapes, or eigenvectors, the problem was re-formulated to give

$$\omega^2 (X) = [K] [M]^{-1} (X) \quad \ldots\ldots(2.4)$$

As the mass matrix contained several zeros, a reduced mass matrix method had to be used. Details of this method are given in the appendix.

Consideration will now be given to the determination of stiffness influence coefficients. A simple method for a beam having many degrees of freedom is given in reference [15]. In Figure 2.3 each node is shown having two co-ordinates, one translational and one rotational. By including the rotational co-ordinates the effects of a single displacement when determining the coefficients are confined to the immediate neighbourhood of that displacement. For example, - referring to Figure 2.3, if unit displacement is given to co-ordinate 3 only, then reactive forces are introduced at co-ordinates 3 and 4 and at the neighbouring nodes only, i.e. at co-ordinates 1,2,5 and 6. This limits the number of non-zero terms in Equations (2.1) to six.

By giving each co-ordinate in turn unit displacement, the necessary reactive forces and moments can be found from flexural analysis. In Figures 2.4 (a) and 2.4 (b) the beam is given unit translational and unit rotational deflections, respectively, at the free end of the beam. This gives the following influence coefficients taking unit deflection at co-ordinate No. 3 (Fig. 2.3)

$$k_{33} = 12\frac{EI_1}{L_1^3} + 12\frac{EI_2}{L_2^3}$$

$$k_{13} = -12\frac{EI_1}{L_1^3} \quad ; \quad k_{53} = -12\frac{EI_2}{L_2^3}$$

$$k_{23} = -6\frac{EI_1}{L_1^2} \quad ; \quad k_{63} = 6\frac{EI_2}{L_2^2}$$

$$k_{43} = 6\frac{EI_2}{L_2^2} - 6\frac{EI_1}{L_1^2}$$

These coefficients then become the elements of the stiffness matrix as shown (overleaf)

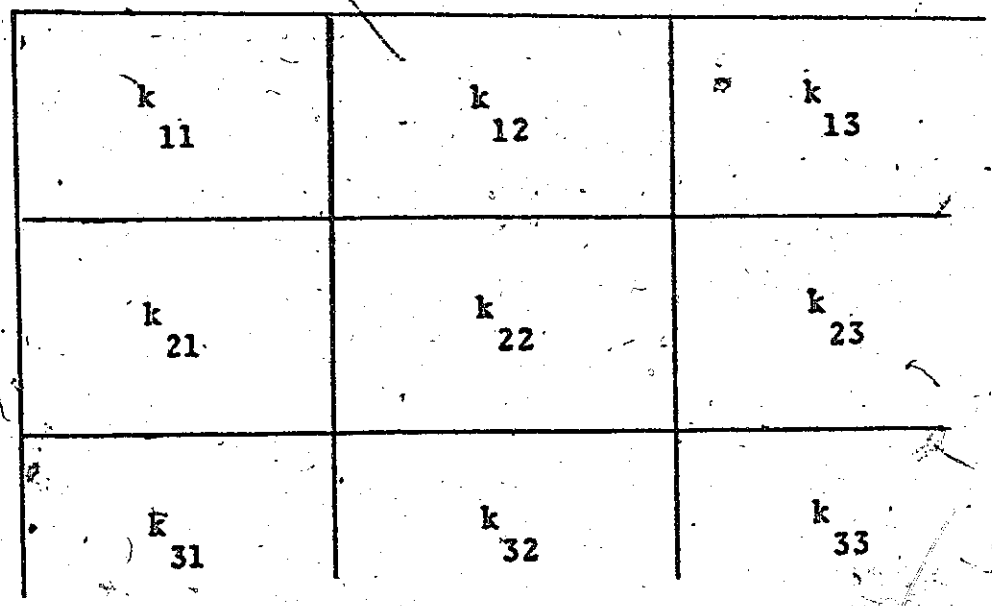

On a practical note, the construction of the matrix is simplified on account of its symmetry. For example $k_{21} = k_{12}$, as stated in Maxwell's Reciprocal Theorem.

2.4 Computer Programme

The programme includes two sub-routines. INVMAT inverts a general non-singular matrix, using a modification of the Gauss pivotal method. EIGENP finds all the eigenvalues and corresponding eigenvectors of a real general matrix. Because we do not take into account any damping this is a suitable sub-routine. During the second phase of the computations an overall 'do' loop allowed trials to be made on the stiffening effect of mounted parts. A similiar 'do' loop was used in phase 3 for trials on bearing stiffness.

In the preparation of the data, the elastic and inertia properties were obtained mainly from manufacturer's drawings or by weighings. Rotary inertias of the chuck and large gear were determined from the frequency of small oscillations when the part was suspended from a peripheral point, i.e. the oscillations were about a non-centroidal axis.

When the beam is computed as a 'free'free' beam (during phases 1 and 2) it is capable of rigid body motion. As there are no restraints there can be no reactive forces. The unit forces necessary in the flexibility method of structural analysis cannot therefore be applied and hence the flexibility matrix, implicit in Eqn. (2,3), cannot exist. This difficulty was overcome by artificially introducing very soft bearings as springs between this body and the "ground", by which the reality of the model is not changed in any substantial way. The stiffness matrix form of the eigenvalue problem, as in Eqn. (2.4), was the alternative solution. This was also done, as stated in the Analysis.

An estimate of the clamping stiffness of the chuck was obtained by a quasi-static testing of the work-piece in the chuck. From a measurement of the amplitudes in the lower two modes, the inertia forces were determined. Torsional stiffness of clamping was then calculated from

the moments of the exciting and inertia forces and the angular deflection. This checked sufficiently well with the value obtained by static deflection to be used as a starting trial value in the computing.

The programme was first tested on a uniform beam. The programme test model is shown in Fig. 2.5. The theoretical analysis for a continuous system gives

$$\frac{d^4y}{dx^4} - n^4y = 0$$

as the form of the equation of motion for the beam in lateral vibration. The natural frequencies are

$$\omega_n = n^2 \sqrt{\frac{gEI}{w}}$$

where w = weight per unit length and for a 'free-free' beam [16],

$(n_1L)^2 = 22.4$ in fundamental mode

$(n_2L)^2 = 61.7$ in second mode, etc.

L = length of beam

The mode shapes for this beam are:

displacement,

$$y = \cosh k_nx + \cos k_nx - B_n(\sinh k_nx + \sin k_nx)$$

For fundamental mode, $k_n = \frac{4.73}{L}$; B= 0.9825

For second mode, $k_n = \frac{7.853}{L}$; B= 1.0008

The beam will also act as a rigid body with zero frequency and displacement, y = 1.

2.5 Experimental work

Figure 2.6 shows the experimental set-up to obtain natural frequencies and mode shapes. The oscillator, OS, fed a sinusoidal signal through the power emplifier, PA, to the electro-dynamic exciter, EX, in turn applying a harmonic force to the workpiece through the force link, FL. Feedback of the charge generated in the force link was amplified in the charge amplifier, CA, and fed back as a voltage to the oscillator. A Philips velocity pick-up was used in measuring the vibration amplitudes. The output voltage from the pick-up, which was proportional to the vibrational velocity at the point being sensed, was taken direct to an oscilloscope.

Figure 2.7 shows the spindle being measured in the machine, with the exciter resting on the lathe, while Figure 2.8 shows the spindle being measured as it hung freely, with the exciter resting on the ground. To identify the natural frequencies, the vibration signal on the scope was observed as the frequency of

excitation was slowly swept from 10 to 500 Hz. All frequencies at which the magnitude of vibration reached a maximum were natural frequencies. Each frequency represented a mode of vibration and with the excitation frequency set at each natural frequency in turn, the amplitudes and sense (i.e. either in phase or out-of phase) of vibration at selected locations on the spindle were measured.

Reference [5] gives a full description of the equipment used.

2.6 Results

Computations made on the initial model consistently produced unrealistic mode shapes, in the form of 'kinks' in the curves. When the problem was reformulated according to Eqn. 2.4 frequencies obtained were identical to previous results but the mode shapes were still unsatisfactory. Removing the rigid link produced a slight improvement. Results for the programme test model (see Fig. 2.5) gave frequencies within 1.5% of the theoretical values. However, when the first three mode shapes were plotted, 'hooks' appeared at the ends of the curve in each case (Fig. 2.9), though the rest of the curve agreed closely with the theoretical shape.

After all other possibilities were exhausted, suspicion focused on the sub-routine used to extract the

eigenvalues and eigenvectors (the parameters of the sub-routine having already been examined). EBERVC, the sub-routine being used, was suitable for a non-symmetric matrix and was based on the iterative method of Eberlein. This sub-routine was replaced by EIGENP, which computes the eigenvalues by the QR Double-Step Method. The eigenvectors are computed by inverse iteration. This sub-routine gave completely satisfactory results for the programme test model, Fig. 2.10. As before, the computed first natural (non-zero) frequency was 177 Hz as compared with 179 Hz for the theoretical value.

On using this new sub-routine on the spindle model, the mode shapes became more realistic, but agreement with the measured mode shapes was still not acceptable. It was decided to use the modified model (the short flexible beam replacing the torsion spring) and try-out various combinations of chuck stiffness and clamping stiffness. This was tried out first on a more uniform beam (Fig. 2.11) to see if any pattern emerged. The results are shown in Figures 2.12 and 2.13. For the 5" 'workpiece' there is a sharp increase in the value of the second natural frequency as the clamping stiffness increases, but this is less marked for the larger 'workpiece'. Figures 2.14 and 2.15 show how the ratio of the second to the first frequency varies in the two cases. If

compared with the ratio of the measured frequencies for the actual spindle an interesting convergence is seen. With the 5" workpiece the family of chuck stiffness curves for all but the least stiffness, converge towards the value of the measured frequencies ratio. For the 11" specimen the lines converge, rising towards the experimental value at a much lower value of clamping stiffness

This procedure was then carried out on the model of the actual spindle. Figure 2.16 shows the results for the 5" specimen. Optimum value for the clamping stiffness appears to be 0.17 and for the chuck stiffness, - 6.0. For these values of the stiffnesses the two lower computed frequencies are 455 and 772 Hz as compared with measured frequencies of 405 and 820 Hz, - a discrepancy of 10% and 6%, respectively. The results for the longer specimen are shown in Fig. 2.17. Again, the chuck stiffness of 6.0 appears to be the more reasonable, although chuck stiffness has little effect in the second mode frequency. With this frequency there is less agreement with the measured frequency than there is in the first mode or, than there is in the case of the smaller workpiece. The clamping stiffness selected for the longer workpiece was 0.102 which gave 1% and 17-1/2% discrepancy respectively for the first two modes. As in the trials on the more uniform beam, the clamping stiffness selected was considerably less for the longer workpiece than for the

shorter one.

Mode shapes for the 5" specimen with the above clamping stiffness are shown in Fig. 2.18. Close agreement will be noted between the measured and computed shapes. Good agreement can also be seen for the 11" specimen, Fig. 2.19, although the measured second mode shape shows more deflection of the workpiece and less deflection of the outer end of the spindle than is shown in the corresponding computed shape.

In Phase 2, the spindle was measured with the gears and other parts mounted on the shaft. The longer workpiece only, was used in this phase. As regards the computational model, it was assumed that the effect of sliding members on the stiffness of the spindle assembly was not significant. In fact, the only part that was likely to contribute to any extent was the inner ring of the outer bearing, which would be a light interference fit on the spindle, (the inner bearing was never removed from the spindle and so was already included in the stiffness of the spindle). The area moment of inertia I_2, at this point on the spindle was given various values from the original value of 6.76 up to 15.0 inch^4 units in computations on the model, with the mass of the mounted parts added to the model masses.

Figure 2.20 shows a comparison of computed and measured results. The first mode shows good agreement on both frequency and mode shape, - the computed frequency being 189 Hz compared with 175 Hz measured. The effect of the stiffening due to the bearing ring is insignificant, - merely raising the frequency to 190 Hz. With the second mode there is a greater discrepancy in frequency, - 482 Hz computed compared with the measured frequency of 700 Hz. That the second measured frequency had not decreased with additional mass, suggested that some of the other mounted parts made a considerable contribution to the spindle assembly stiffness, thereby compensating for the additional inertia. An examination of the computed and measured shapes for the second mode would seem to confirm this. The effect of including the bearing ring, increased the frequency from 482 to 516 Hz., - still a 26% discrepancy with the measured frequency. Figure 2.21 shows how the frequencies of the two modes vary with moment of inertia, I_2.

In Phase 3, measurement were taken with the spindle in the lathe Fig. 2.7. Natural frequencies and mode shapes were measured for both workpieces. In the computations, to facilitate plotting and to establish a basis for comparison the ratio of the stiffness of the two bearings was considered. Using this ratio as a parameter and also the stiffness of one of the bearings, computed

frequencies were obtained over a wide range of bearing stiffness. The results are shown in Fig. 2.22. It was found that closest agreement with measured frequencies was obtained with bearings having a stiffness of 8 x 10^4 lb./in. for the outer bearing. Computed mode shapes for these values of bearing stiffness are shown compared with the measured modes in Fig. 2.23. The first mode shows very good agreement but the second and third modes show very little agreement.

The difference in the shapes can be attributed to an assumption made in Phase 3. This was that the lathe proper which was supporting the spindle, would act as a rigid structure and that the only displacements would be those of the spindle. This apparently was not the case. The lathe itself was vibrating and so Phase 3 of the spindle study was extending into an area that is dealt with in Chapter III of this thesis. A comparison of the measured results for the cases of the spindle (i) in the bearings and (ii) suspended freely show the frequencies for the latter to be greater which would not be the case if the lathe frame was rigid. On the other hand, the computations on the model assumed the lathe frame to be rigid and the bearing 'ground' to have no displacement. It is clear that the optimum values of bearing stiffness obtained are softer than those on the actual spindle.

To summarize, the results show that the model developed for the basic spindle assembly is satisfactory, giving close agreement with the actual spindle as far as modal behaviour is concerned. As to the attached masses, their effect on the stiffness of the system can be under-estimated. Results indicate that they have some influence on the second mode and it was in this mode that the discrepancy (between computed and measured results) was noticeable. Finally, a more fundamental problem arises when determining bearing stiffness. With the lathe frame as flexible as it was, the experimental measurements with the spindle in the machine led to no valid determination of bearing stiffness. The problem was entering the preserve of Chapter III.

THE COLCHESTER LATHE

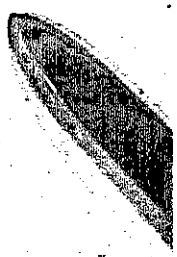

III. THE COLCHESTER LATHE

3.1 Introduction

In the previous chapter a model was developed for a lathe spindle assembly, treating it as an entity rather than an integral part of the lathe. This chapter covers a study of the whole lathe, setting up a model and examining its dynamic behaviour as a machine structure.

Previous computer studies of a lathe have employed the lumped-parameter method. The accuracy of this method depends largely on the accuracy of the stiffnesses assigned to the beams representing the various elements in the lathe structure. Assessing the static stiffnesses of these elements is not an easy task as the shapes are both complicated and diverse. Valuable contributions in this area have been made by Kaminskaya et al [17] in their theoretical studies on box sections and apertures. Also in the same area is the extensive treatment by Gorbatov and Valenta in reference [4]. Formulae derived from these theoretical studies have been the standard for comparison adopted by several investigators in computer studies on the static stiffness of the more regular machine sections [9,18].

The finite element method has been developed in machine tool study to better represent the geometry of the structure when computing static deformations. In this

method the structure is considered as a mathematical assemblage of individual structural elements. Common elements used are, triangular and rectangular plates, beam and solid elements. The smaller the element size, the more accurate the result but the greater the number of elements used, the greater the computer storage required and also the computing costs.

The elements are assumed to be interconnected at a discrete number of nodal points situated on their boundaries. The displacements of these nodal points will be the basic unknown parameters of the problem. A function (or functions) is chosen to define uniquely the state of displacement within each element in terms of its nodal displacements. The stiffness properties of the individual elements are first expressed in a convenient local (element) coordinate system. The element stiffness matrix is then transformed from its local coordinate formulation to a form relating to the general coordinate system. The individual element stiffnesses contributing to each nodal point are superimposed to obtain the total assemblage stiffness matrix, [K]. Eqn. 2.1a may be solved to determine the nodal displacements, given a set of applied nodal forces. Reference [19] is a standard work on the finite element method.

In this chapter, however, the finite element method is used to solve the dynamic problem. The formulation of the problem expressed in Eqn. 2.4 is the basis upon which natural frequencies and mode shapes are computed. From these, in turn, the dynamic responses of the tool and workpiece to harmonic exciting forces are determined. Unlike the static stiffness, the dynamic stiffness and also its reciprocal, the dynamic compliance, are frequency-dependent. Dynamic compliance, - the ratio of the amplitude of displacement to the amplitude of the exciting force, is known as 'receptance'. It is effectively mechanical admittance and can be evaluated for a single mass or for a combination of discrete elements. This is developed in more detail is section 3.2. The only vibration of concern to the designer is that of the tool and workpiece relative to each other. It is therefore only the relative receptance between these two stations that is considered in this chapter.

Machine details

Manufacturer:	Colchester Lathe Co. Ltd. Colchester, Essex, England	
Model:	'Dominion 17'	17" x 72"
Spindle Bearings:	'Garnet' Taper Roller	

A diagram of the lathe is shown in Figure 3.1

3.2 Analysis

The value of the concept of receptance is that in a linear multi-degree-of-freedom (D.O.F.). system the receptance at a particular frequency is the sum of the factored responses in the individual modes. In other words, the system is treated as a series of single D.O.F. systems. To develop this a single D.O.F. system is first considered.

(i) Single degree-of-freedom system

Figures 3.2 (a) and (b) show two different single D.O.F. systems which are identical in treatment. The masses, m, being restrained by the spring, of spring rate or stiffness, k. In case (b) the massless flexible beam is the spring. The system in both cases has a damping coefficient, c.

When performing natural vibrations, the displacement of the mass is

$$x = X_o e^{(-\delta + j\nu)\, t} \qquad \ldots\ldots(3.1)$$

in the direction (x).

where $\delta = \frac{c}{2m}$; $\nu^2 = \omega_n^2 - \delta^2$

and $\omega_n = \sqrt{\frac{k}{m}}$

The damping ratio, $\zeta = \frac{c}{c_c}$ where c_c is the critical damping, $c_c = 2m\omega_n$.

If an external force $p = Pe^{j\omega t}$ acts on the mass in the direction (X), the system vibrates, adapting to the forcing frequency, ω. The steady state motion is

$$x = Xe^{j\omega t} \quad \text{where } X = Ae^{j\phi}$$

where A is the amplitude and ϕ is the phase shift

$$X = \frac{P}{(k - m\omega^2) + jc\omega} = \frac{P}{k} \cdot \frac{\omega_n^2}{\omega_n^2 - \omega^2 + 2j\delta\omega} \qquad \ldots(3.2)$$

$$= P \cdot \phi(\omega)$$

$\phi(\omega)$ is the receptance of the system. As the receptance is a complex quantity it can also be written as

$$\phi(\omega) = \left[\frac{k - m\omega^2}{(k - m\omega^2)^2 + c^2\omega^2}\right] - i\left[\frac{c\omega}{(k - m\omega^2)^2 + c^2\omega^2}\right] \qquad \ldots(3.3)$$

The real part of $\phi(\omega)$ is called the 'real receptance', Re (ϕ),

$$\text{Re}(\phi) = G = \frac{k - m\omega^2}{(k - m\omega^2)^2 + c^2\omega^2} = \frac{\omega_n^2(\omega_n^2 - \omega^2)}{k[(\omega_n^2 - \omega^2)^2 + (2\delta\omega)^2]} \qquad \ldots(3.4)$$

The imaginary part of $\phi(\omega)$, - the 'imaginary receptance',

$$= \text{Im}(\phi) = H = -\frac{c\omega}{(k - m\omega^2)^2 + c^2\omega^2} = -\frac{2\omega_n^2\,\delta\omega}{k[\omega_n^2-\omega^2)^2 + (2\delta\omega)^2} \qquad \ldots(3.5)$$

The real receptance is in phase with the applied force P, while the imaginary receptance is in quadrature with P. The absolute value of the receptance is then the absolute value of the vectoral sum of the real and imaginary parts.

$$|\phi(\omega)| = \frac{1}{k\sqrt{(\omega_n^2 - \omega^2)^2 + (2\delta\omega)^2}} \qquad \ldots(3.6)$$

The phase shift, ϕ, of X with respect to P is

$$\phi = \tan^{-1}\left(\frac{H}{G}\right) = -\frac{2\delta\omega}{\omega_n^2 - \omega^2} \qquad \ldots(3.7)$$

Equations (3.4) to (3.7) are shown plotted against forcing frequency, ω, for various values of the damping ratio, ζ, in Figures (3.3) to (3.6).

(ii) Unidirectional system with two degrees of freedom.

In Figure 3.7(a) a two D.O.F. system is represented with the two masses m_a and m_b free to move only along the parallel lines, (X_a) and (X_b), respectively. Damping and elastic properties, c_a, c_b, k_a and k_b refer.

If the system is initially disturbed and then allowed to vibrate freely, the resulting motion will be the sum of two simultaneous motions pertaining to the two modes of vibration. The modal shape for either mode can be defined as the ratio of the displacements of the two masses:

$$\lambda_1 = \frac{X_{b1}}{X_{a1}} \quad \text{and} \quad \lambda_2 = \frac{X_{b2}}{X_{a2}}$$

where subscripts 1 and 2 refer to modes 1 and 2, respectively. The mode shapes are represented by full lines in Figures 3.7(b) and (c). When the system is vibrating, the displacement at any instant will be the sum (Fig. 3.7(d)) of two factored modal displacements (shown by dashed lines in Figures 3.7(b) and (c)). The shape of the deformed system will be changing continuously because of the difference in the mode frequencies. The instantaneous displacement of mass m_b is:

$$x_b = x_{b1} + x_{b2}$$

where $$x_{b1} = X_{b1} \cdot e^{(-\delta_1 + j\nu_1)t}$$

and $$x_{b2} = X_{b2} \cdot e^{(-\delta_2 + j\nu_2)t}$$

$$\nu_1^2 = \omega_{n1}^2 - \delta_1^2$$

$$\nu_2^2 = \omega_{n2}^2 - \delta_2^2$$

Using the shape coefficients λ_1 and λ_2 the displacement of mass m_a will be

$$x_a = \lambda_1 x_{b1} + \lambda_2 x_{b2}$$

As the values of λ_1 and λ_2 depend only on the parameters of the system, the motion of the system can be described in terms of the two partial co-ordinates, x_{b1} and x_{b2}, thus replacing the original co-ordinates. Initial conditions will determine the two vectors, X_{b1} and X_{b2}.

If one of the masses, say m_b, is subjected to an exciting force $p = Pe^{j\omega t}$ acting in the direction (X_b), the vibration will be

$$x_b = X_b . e^{j\omega t}$$

where $X_b = A_b . e^{j\phi}$

$$= P\left(\frac{1}{k_{b1}} \cdot \frac{\omega_{n1}^2}{\omega_{n1}^2 - \omega^2 + 2j\delta_1\omega} + \frac{1}{k_{b2}} \cdot \frac{\omega_{n2}^2}{\omega_{n2}^2 - \omega^2 + 2j\delta_2\omega}\right) \qquad \ldots(3.8)$$

$$= P \cdot \phi_b(\omega)$$

Eqn. (3.8) may be re-written as

$$X_b = X_{b1} + X_{b2}$$

with $$X_{b1} = \frac{P}{k_{b1}} \cdot \frac{\omega_{n1}^2}{\omega_{n1}^2 - \omega^2 + 2j\delta_1\omega} = P.\phi_{b1}(\omega)$$

and $$X_{b2} = \frac{P}{k_{b2}} \cdot \frac{\omega_{n_2}^2}{\omega_{n2}^2 - \omega^2 + 2j\delta_2\omega} = P.\phi_{b2}(\omega)$$

again, $x_b = x_{b1} + x_{b2}$

$$= X_{b1}e^{j\omega t} + X_{b2}e^{j\omega t} = P.(\phi_{b1} + \phi_{b2})e^{j\omega t}$$

The sum,

$$\phi_{b1} + \phi_{b2} = \phi_b$$

signifies that the receptance of the system can be obtaining by summing the receptances of the first and second modes.

Or considering the components

$$\phi_b = (G_{b1} + G_{b2}) + j(H_{b1} + H_{b2}) \qquad ...(3.9)$$

i.e. the simple arithmetic sum in both cases, (see Figure 3.8).

In steady state vibration, every point on the system experiences harmonic motion of the same frequency as the excitation. If the frequency is in the neighbourhood of a natural frequency, then the corresponding mode contributes largely to the resulting vibration. The contribution from the other mode is relatively small.

In the computational work on the lathe, summation of this kind was made to obtain the resulting

response from the contributions of individual modes, whereas in the case of the experimental work, the resulting receptance was resolved to determine the contributions of the modes.

It was stated in Chapter I that a machine tool is a structure with an infinite number of degrees of freedom, with an infinite number of modes, and natural frequencies. The infinite number would make it impossible to sum or resolve receptances were it not for the fact that with the higher modes both the stiffness and the damping is greater than with the lower modes. That is to say, mode contribution decreases with mode number and in practice it is sufficient to consider the lower modes only.

3.3 Computer Programmes

3.3.1 STARDYNE Programmes

The STARDYNE System developed by Mechanics Research Inc. of California, consists of a series of digital computer programmes designed to analyse linear elastic structural models. The following programmes are included in the system:

(i) STAR

STAR has two distinct functions:

(a) Static load analysis. Once the structural model has been defined, the reaction to any general type of static load may be investigated.

(b) Modal analysis. For any stiffness matrix and associated mass matrix, the programme will extract eigenvalues and eigenvectors in a desired frequency range. Two sub-programmes are available, one using inverse iteration and the other, the Householder Q-R method.

The following types of elements are available in STAR:

1. Beam elements with shear stiffness
2. Two triangular plate elements. Thick plate and thin plate.
3. Quadrilateral plate element
4. Infinitely rigid members
5. Springs

6. Hexahedron element

7. Tetrahedron element

(ii) DYNRE1

Transient response to imposed dynamic loadings are treated in DYNRE1. Input forcing functions may be in the form of forces, initial displacements, initial velocities and base accelerations.

(iii) DYNRE2

Steady state frequency response to imposed dynamic loadings are computed by DYNRE2. Further details on this and STAR programmes are given later.

(iv) DYNRE3

Response of multi-degree-of-freedom linear elastic structural models subjected to stationary random dynamic loading. DYNRE3 will compute the rms nodal responses, rms element stresses and generate response power spectral density curves for selected nodal degrees of freedom.

(v) DYNRE4

Response of multi-degree-of-freedom, linear elastic models subjected to an arbitrarily oriented foundation shock input. The user may enter shock spectra for any of the directions of motion or call for some ratio of the 1940 El Centro (California) earthquake

spectra. DYNRE4 will compute the absolute and/or rms sum of the nodal responses, and/or element stresses.

(vi) DYNRE5

Computes shock spectrum values from a transient base acceleration time history digitized at equal or unequal time intervals. The user may specify frequencies at which shock spectrum values for displacement, velocity and acceleration will be computed, in turn for each value of damping entered.

An analysis summary chart of the Stardyne System is given in Fig. 3.10. For both types of plate elements, the displacement of the element was defined by three translations and two notations at each corner.

The dimensional capability of the STAR programme with 6 D.O.F. per node is as follows:

Number of degrees of freedom (static)	15000
Number of degrees of freedom (other)	6000
Number of nodes and maximum node number (static)	2500
Number of nodes and maximum node number (other)	999
Number of beams (rigid, pinned, elastic)	9999
Number of tri-plates	9999
Number of quad-plates	9999
Number of cubes	9999

Number of tetrahedrons	9999
Number of elements into one node	no limit
Number of rigid systems	no limit
Number of nodes per rigid system	no limit
Number of rigid bar elements	no limit
Number of static load cases	no limit
Number of entries to material property table	250
Number of entries to beam property table	999
Number of nodes with individual ref. systems	2500
Number of individual reference systems	999
Dynamic DOF for modal extraction	
Householder-QR	330
Inverse Iteration	6000
Matrix Bandwidth - Nodal	no limit
- D.O.F. (after re-numbering)	1185

The following geometry formulation procedure for the STAR programme was used:

1. A nodal diagram of the idealized structure was made (more information is given in Section 3.4)
2. Numbers were assigned to the node points.
3. Section properties, co-ordinates, member identifications restraints and weights were computed.
4. The input data was coded on data sheets and key-punched.

5. The STAR programme was run and terminated after the geometry phase in order to check running time estimates and to inspect the node/element table.

During the geometry formulation, the nodes are re-ordered internally to produce a minimum bandwidth. If requested, the re-formulated geometric data is written on tape.

For triangular and quadrilateral plate elements a choice was available in the type of force the plate would resist. In-plane and bending forces were selected, requiring a minimum of 5 D.O.F. per node. For beam elements, beam shear shape factors were used. These factors when multiplied by the beam area yielded the effective shear areas for two transverse areas of the beam. A 'pin code' option in the beam connectivity table allowed a load carrying capability to be included or released.

In the Inverse Iteration modal extraction subprogramme, the frequency range and the number of eigenvectors desired can be specified. This method is used only when the Householder-QR method maximum for dynamic D.O.F. is exceeded (as in this case) or if only a few modes are desired or when time estimations indicate that the Inverse Iteration Method is more

economic. The procedure attempts simultaneously, during any iteration to converage upon (a) a single eigenvector (b) two close roots (quadratic procedure) and (c) three close roots (cubic procedure). The successful convergence of any of these is dependent upon satisfying the tolerance number associated with each process.

The DYNRE2 programme requires a data tape created during a STAR run. DYNRE2 reads this tape to obtain the required geometry, eigenvalues and eigenvectors for the response history. The input data requirements are specified on the DYNRE2 deck set-up diagram, Fig. 3.11. For the dynamic response a list of possible exciting frequencies is determined by the following:

(a) Each natural frequency selected and one point midway between each pair of adjacent natural frequencies will become a possible exciting frequency.

(b) A finer distribution of exciting frequencies between adjacent natural frequencies may be generated.

(c) A list of specific frequencies may be entered.

A damping factor must be entered for every mode used. If damping data is omitted, a damping ratio of 0.04 is entered.

The forcing function input may be one of three types:

(i) Sinusoidal motion of the base of the structure. These may be accelerations, velocities or displacements.

(ii) A force may be distributed over the structure and given a sinusoidal variation; the amplitude changing as the frequency of excitation changes.

(iii) A unit sinusoidol excitation may be applied at a specific point on the structure and transfer functions computed for all of the remaining co-ordinates.

Type (ii) was adopted to allow equal and opposite forces to be applied simultaneously to the workpiece and the tool. The amplitude of the exciting forces was kept constant over the frequency range selected.

3.3.2. Programme for real and absolute receptance

DYNRE2 computes the response of any selected station or stations to given input forces. The final step then in determining tool and workpiece dynamic behaviour is the determination of the relative receptance at these two station points. The real receptance G (ω) of each point is computed by taking the cosine component of the dynamic response per unit exciting

force, using the DYRNE2 programme output. The algebraic difference of these two values then gives the relative dynamic behaviour of tool and workpiece in terms of real receptance, $G(\omega)_{rel.}$ A similiar procedure, but taking the sine component instead, gives the imaginary receptance $H(\omega)_{rel}$ of the tool relative to workpiece. The absolute value of receptance of one to the other is determined from:

$$\left|\Phi(\omega)\right|_{rel.} = \sqrt{[G(\omega)]^2_{rel.} + [H(\omega)]^2_{rel.}}$$

A simple programme for computing these relative receptances is shown in Fig. 3.12.

3.4 Preparation of the model

The preparation of the model was based on a set of drawings obtained from the manufacturer. From these, tracings were made of parts with non-regular plane areas and the areas were then divided up into finite elements, either triangular or rectangular. All other plane areas were divided up in like manner,

for the three-dimensional structure. To minimize the risk of overlooking an element (and hence leaving a weak spot in the structure model) the elements lying in the differentplanes were drawn on different isometric drawings of the lathe. Flanges around castings, the top part of the bed and generally parts that could not be considered as plate elements were represented by beam elements. The model can be seen in Figure 3.1(b), which is actually one of the mode shapes. The quadrilateral elements that can be seen were introduced as an additional Stardyne facility after the initial preparation of the model. Its introduction resulted in a decrease in the number of nodes and hence, in the number of D.O.F. The elliptical cross-ribbing shown in Fig. 3.13 was represented by rectangular plates. The spindle of Chaper II had to be located at appropriate nodes in the headstock. The bearings could not be represented by springs between the spindle and 'ground' as the bearing housing could not be considered rigid. Neither was there provision in Stardyne for springs to be located between nodes. However, the matter was simply settled by placing pairs of beams between appropriate nodes on the spindle and on the headstock. The longitudinal stiffness of the beam was made equal to

that of the bearing it represented. The two beams per bearing allowed for bearing stiffness in the horizontal and vertical directions. Load bearing capabilities in the other co-ordinates were released. One beam representing one of the bearings was given certain transverse stiffness to prevent free axial float of the spindle model.

A similiar provision was made for the bearing in the 'live' centre on the tailstock. Rotation of the spindle was fully restrained at the outer bearing but the torque capability of the workpiece, where it was held by the 'live' centre, was released. Where the legs of the lathe were in contact with the ground, the nodes were constrained in the three translational co-ordinates. As drawings and information were not available relating to the saddle and tool post, an adjacent point on the top of the lathe bed was taken to represent the tool when considering tool/workpiece dynamic behaviour.

Summary of input:

Number of nodes	=	143
Number of beams	=	115
Number of tri-plates	=	36
No. of quad-plates	=	97
No. of nodes with restraints	=	9

No. of D.O.F./node	6
No. of D.O.F.	833
No. of dynamic D.O.F.	414

3.5 Experimental work

In the harmonic excitation tests carried out on the lathe an electro-magnet was used as the source of excitation. It was used with concave poles of radius 2-3/4 in. acting on a workpiece of diameter 5-1/2 inches. The gap between the poles and the workpiece was kept at 0.04 inch.

The arrangement of the equipment is shown in Fig. 3.14. The automatic sweep oscillator OS supplied a constant harmonic voltage to the E.M. amplifier (amplifier supplying current to the electro-magnet). The frequency of that harmonic voltage was swept from 10 HZ to 500 HZ at a slow sweeping speed. The output of the E.M. amplifier EA was connected to the magnet. Hall probes, which are flux (magnetic) sensing transducers, fed back signal of the force into the E.M. amplifier so as to keep the magnetic force across the gapt at a constant amplitude throughout the whole test. For all the tests, a static force of 50 newtons (11.2 lb.) and a dynamic force of amplitude equal to 10 newtons (2.24 lb.) were used. Force-analogous voltage was employed as one of the inputs to the multiplier MU, part of a standard analogue computer. The vibra-

tion signal was sensed by a capacitive vibration pick-up VP, amplified by Wayne Kerr vibration meter WM. It was used as the other input to the multiplier. Output of the multiplier was then connected to the X-Y plotter PT. Since the plotter was a good AC filter for the purpose, no further filter for the A C signal was required. The product of force and vibration signals was recorded as the Y-component and the log-frequency of excitation as the X-component. This set up gave direct plotting of real-receptance. A full treatment of the experimental work is given in Ref. [5].

3.6 Results

The STAR modal extraction programme computed the first ten eigenvalues and frequencies and these are given in Table 3.15. Corresponding mode shapes for five modes together with the measured mode shapes are shown in Figures 3.16 to 3.28. Because in this phase we still treat the case as of natural vibrations, with no damping, necessarily all the eigenvectors have been normalized and the mode shapes do not differ in the general magnitude of displacements. It is not possible to see which of the modes are dominant on the actual machine. This presents some difficulty when comparing the computed modes with the measured ones. The main

parameter relating the two sets is the natural frequency.

The problem of significance of modes was dealt with by considering the dynamic responses. These responses, computed from the DYNRE2 programme, for the bed and workpiece are shown in Figures 3.29 to 3.32 for horizontal response and in Figues 3.33 to 3.36 for vertical response. Finally, from the output from the dynamic response programme, the relative receptance between the bed and the workpiece was computed. The plotted results for the real receptance, G (ω) in the horizontal and vertical planes are shown in Figs. 3.37 (a) and 3.38. Absolute values of the receptance, $|\Phi(\omega)|$ can be seen in Figures 3.39 and 3.40.

The fifth computed mode has a natural frequency of 97.6 Hz and the horizontal G (ω) curve Fig. 3.37 indicates that this is the dominant horizontal mode. This is very similiar to the principal measured horizontal mode of frequency 97.3 Hz. Fig. 3.37 (b). Comparison of the mode shapes, Figs. 3.18, 3.19 and 3.20 shows good correlation on the distortion of the workpiece spindle and tailstock barrel though there is more flexing of the spindle in the bearings for the model and, secondly, the computed mode shape shows more flexibility in the lathe bed. It also shows the workpiece and bed to be out-of-phase. This is also clear

from the phase shift diagrams, Figs. 3.30 and 3.32.

Comparing Figures 3.22, 3.23 and 3.21 both representing dominant vertical modes (see Fig. 3.38) the spindle bearings for the model again appear not to be as stiff as for the actual machine. The difference in bearing stiffness appears to be more pronounced in the vertical plane and this, coupled with the more flexible bed, could account for the low computed frequency, 76.1 compared with the measured frequency 105.4 Hz.

It will be noted that the two measured natural frequencies are close, 97.3 and 105.4 Hz. This is not uncommon in lathes because of the symmetry of parts along the spindle axis (as many are circular in section). The significance of this is clear when it is realized that the workpiece is the main vibrating mass with the spindle and the tailstock as 'springs'. Further, the geometry of the lathe in the region of the workpiece and bed beneath, would suggest greater stiffness in a plane opposing vertical deflection, than in that opposing horizontal deflection. The higher measured vertical frequency would support this. Examination of the responses in Figures 3.33 and 3.35 shows that the large real receptance in this mode

(third mode with computed frequency 76.1 Hz) is almost entirely due to the workpiece - not to the bed. It would therefore appear that increased bearing stiffness in the model would bring it more 'in line' with the actual machine.

Out of the six lowest computed natural frequencies, five are horizontal modes. This is in agreement with experience, the reason being, as stated, that the vertical stiffness is greater than the horizontal. In the first mode, at a frequency of 53.9 Hz, there is simple bowing of the lathe bed horizontally, (Figs. 3.16 and 3.17) this time in phase with the workpiece. Again the "springs" are the spindle bearings, tailstock barrel and centre. The "spring" acting on the point masses representing the saddle is the lathe bed. The second mode, frequency 60.8 Hz. (Figs. 3.24 and 3.25) shows twisting of the frame about the longitudinal axis, rather than bowing. Both modes 1 and 2 appear on the computed receptance curve, though not on the measured curve. Fig. 3.3 (a) and (b). It is worth noting, however, that the experimenters taking the measurements did identify a mode in the vicinity of 60 Hz but the magnitude of the dynamic responsible was small.

The measured vertical real receptance curve Fig. 3.38 (b) shows a dominant mode at 140 Hz. From the mode shape, Fig. 3.21, it can be seen that the bed is bowing upwards. The corresponding computed mode has a frequency of 126.9 Hz (consistent in that it is somewhat lower than the measured) and the mode shape, Figs. 3.26 and 3.27, indicates the same bowing of the bed. Another feature of the computed shape (not indicated on the measured shape) is the vertical displacement of the workpiece, with the chuck clamping as one of the 'springs'.

This chapter will be concluded with an assessment of the model created. For a first model without any modifications there is good correlation between the dynamic behaviour patterns of the machine and the model. As a vibratory system, the lathe model has as its main 'mass', its workpiece; with the spindle bearings, tailstock barrel and live centre behaving as the 'springs'. The saddle also appears to act as a second mass with the lathe bed as the 'spring'. The first modes are horizontal, which correctly reflects a higher stiffness in the vertical plane. However, some of the lower horizontal modes for the model are much more dominant than for the actual machine.

The results indicate where improvements might be made to the model:

(i) Additional stiffening of the bed. The 'square box' model for the elliptical ribbing could be replaced by one of hexagonal or octagonal section. This would, of course, mean additional nodes.

(ii) The saddle of the lathe, as a major machine element, could be considered to provide both some stiffening and damping to the lathe structure.

(iii) Spindle bearings could be stiffened. This was discussed in Chapter 2.

Modifications to the model can easily be made but cost is a major factor and the largest element in the cost is in the determination of modal behaviour. The time required to extract ten eigenvalues with corresponding eigenvectors was 1170 system second (642 CP seconds), whereas the time to determine the frequency response for the two station points based on 56 exciting frequencies was 37 system seconds (20 CP seconds)

One alternative to the procedure that was followed would be to use the finite element method to create a model and by static analysis of this model determine all stiffnesses necessary to set up a lumped-parameter model. The latter model could then be used to examine dynamic behaviour. The model analysis

would then be performed on a model having a greatly reduced number of degrees of freedom.

MODEL MILLING MACHINE

IV MODEL MILLING MACHINE

4.1 Introduction

The computations of the static and dynamic characteristics of a model milling machine was part of a co-operative programme of work embarked on in January 1970 by members of the C.I.R.P.[a] Group Ma. The following universities participated in the programme:

University of Leuven, Belgium

Eindhoven University of Technology, Holland

Technische Hochschule, Aachen, Germany

University of Kyoto, Japan

University of Birmingham, England

University of Manchester Institute of Science and Technology, England

A common idealized mathematical model was adopted by all participating, so that computational procedures might be compared. Studies on actual machine tools would commence after the computer programmes had been thoroughly tested. The initial phase has been completed and reported [7,8].

---

[a]Collège International pour Récherche de Production mécanique

Computations, similiar to those performed in other universities, were carried out by the author and this chapter is a report on the results. The milling machine model presented an opportunity to try-out the STARDYNE system before commencing the work on the Colchester lathe.

4.2 The work in phase one

The model milling machine was built at the University of Leuven, where it was subjected to static and dynamic tests. The machine is a fabricated steel structure and is shown in Fig. 4.1. The tapered column and the knee assembly are stiffened with diagonal ribbing, the table is constructed from three I-section beams and the spindle is welded both to the column wall and the overarm assembly.

The mathematical model agreed upon, is shown in Fig. 4.2 and consists of twenty uniform beams. The mass of the machine is considered distributed over the nineteen nodes. The beams shown by heavy lines are assumed to be completely rigid and the structure assumed to be connected to a massive foundation. Rotary inertia is neglected in this simple lumped-parameter model.

The programme members were asked to compute the following:

(i) Static deflections of all structural nodes caused by various loadings.

(ii) The natural frequencies of the lowest six modes of vibration.

(iii) The corresponding model shapes.

(iv) The model flexibilities between points 7 and 14.

Information relating to the computer was also requested. This included computer type, storage, cost and time. Input data, by way of nodal masses and the geometric properties of all beams, was made available to all members.

4.3 Results

Two cases of static loading were computed and the results are shown together with loading details in Figs. 4.3 to 4.6. The results from only two other universities are included as only partial results were available from the others.

It will be noted that the McMaster and U.M.I.S.T. results show very close agreement. However, when these computed values are compared with the measured

values (of the very few measured values available, two are shown in brackets in Fig. 4.6), considerable discrepancy is seen. It was found from further study [7], that the discrepancy arose because of local deformation of the front wall of the column of the physical model where the arbor and overarm were connected. This local deformation was confirmed by a finite element analysis.

The computed values of natural frequencies also showed good correlation. The slight discrepancies in the Kyoto results are due to differences in the Kyoto model. No measured values were available for comparison, but reports fromLeuven indicate that the natural frequencies of the physical model were considerably less than the computed values. This was attributed to the flexibility of the mounting of the model on its foundation being ignored in the mathematical model.

Again good correlation in the computed mode shapes from McMaster and U.M.I.S.T. was obtained. The first six modes shapes are shown in Figures 4.8 to 4.11 with the first and fifth U.M.I.S.T. shapes included.

Computational costs reported by the co-operating universities ranged from $9.00 to$150.00. Not including any work on model flexibilities (an unsuccessful feature with the first model in the co-operative programme), the cost of the McMaster computations was approximately $13.00.

APPENDIX

Appendix

It was stated in section 2.2 that at one stage in the study of the lathe spindle, the problem was re-formulated to give

$$\omega^2 (X) = [K] [M]^{-1} (X)$$

Inverting the mass matrix was not immediately possible as it contained some zero rotational inertias. The matrix can be reduced to eliminate the zero masses by the following method, given in Ref. [15].

Eqn. (2.1a) gave $(F) = [K] (X)$

The co-ordinates are re-numbered to allow all non-zero masses to precede zero masses in order. In other words, the zeros are at the bottom of the matrix. The stiffness matrix is correspondingly re-ordered and then partitioned with those elements corresponding to zero masses occupying the lower subdivisions. This is shown below. The vertical portion is selected to make the subdivisions, R and V, square.

$$\begin{pmatrix} f_1 \\ \vdots \\ f_p \\ 0 \\ \vdots \\ 0 \end{pmatrix} = \left[\begin{array}{c|c} R & T \\ \hline U & V \end{array}\right] \begin{pmatrix} x_1 \\ \vdots \\ x_p \\ x_{p+1} \\ \vdots \\ x_n \end{pmatrix} \quad \text{--- A.1}$$

Expanding:

$$\begin{pmatrix} f_1 \\ \\ f_p \end{pmatrix} = \begin{bmatrix} \quad R \quad \end{bmatrix} \begin{pmatrix} x_1 \\ \vdots \\ x_p \end{pmatrix} +$$

$$\begin{bmatrix} \quad T \quad \end{bmatrix} \begin{pmatrix} x_{p+1} \\ \vdots \\ x_n \end{pmatrix} \qquad \text{..... A.2}$$

and

$$0 = \begin{bmatrix} \quad U \quad \end{bmatrix} \begin{pmatrix} x_1 \\ \vdots \\ x_p \end{pmatrix} +$$

$$\begin{bmatrix} V \end{bmatrix} \begin{pmatrix} x_{p+1} \\ \vdots \\ x_n \end{pmatrix} \qquad \text{..... A.3}$$

Premultiplying eqn. 3 by V^{-1} gives

$$\begin{bmatrix} x_{p+1} \\ \vdots \\ x_n \end{bmatrix} = -E^{-1}U \begin{bmatrix} x_1 \\ \vdots \\ x_p \end{bmatrix} \quad \ldots\ldots \text{A.4}$$

and substituting in eqn. 2

$$\begin{bmatrix} f_1 \\ \vdots \\ f_p \end{bmatrix} = R - TV^{-1}U \begin{bmatrix} x_1 \\ \vdots \\ x_p \end{bmatrix} \quad \ldots\ldots \text{A.5}$$

Eqn. 5 contains no co-ordinates associated with zero masses. Comparing A.5 with eqn. (2.1a) shows that the stiffness matrix [K] has been replaced by matrix $[R-TV^{-1}U]$ of an order lower by an amount equal to the number of zero masses. If this reduced stiffness matrix is called K^* and the corresponding reduced mass matrix called M^* then

$$[S^*] \quad (x) = \omega^2 \; [M^*] \; (x)$$

A listing of a programme using this method is given in Fig. A.1.

BIBLIOGRAPHY

BIBLIOGRAPHY

1. Taylor, S. and S.A. Tobias. Lumped Constants Method for the Prediction of the Vibration Characteristics of Machine Tool Structures. Proc. 5th M.T.D.R. Conf. Pergamon Press (1964).

2. Tlusty, J. and M.Polacek. Experience with Analysing Stability of Machine Tool Against Chatter. Proc. 9th Int. M.T.D.R. Conf. Pergamon 1968.

3. Brown, G.M., J.B. Hill, and A.N. Nowicki The Dynamic Characteristics of Hobbing Machine Structures or Hobbing Machine Chatter - A Case History. Proc. 7th Int. M.T.D.R., Conf. Pergamon 1966.

4. Koenigsberger, F. and J. Tlusty. Machine Tool Structures, Vol. 1, Pergamon Press, Oxford 1970.

5. Lau, K.C. Development of Harmonic Excitation Technique for Machine Tool Stability Analysis. A Master Thesis submitted to Engineering Dept., McMaster U., August, 1973.

6. Cowley, A. The Predictions of the Dynamic Characteristics of Machine Tool Structures Ph.D. Thesis, U.M.I.S.T. (1968)

7. Cowley, A. Co-Operative Work in Computer-Aided Design in the C.I.R.P. U.M.I.S.T. (Jan. 1972)

8. Ven Den Noortgate, L. and P. Vanherck, and J. Peters. Third Report on the Computation of a Model Milling Machine. Presented at C.I.R.P. Meeting, Paris, 1971.

9. Wilson, J. The Application of the Finite Element Method to Machine Tool Structural Analysis. M.Sc. Dissertation U.M.I.S.T. 1971.

10. Hinduja, S. Analysis of Machine Tool Structures by the Finite Element Method. Ph. D. Thesis, U.M.I.S.T., 1971.

11. Stansfield, F.M. Some Notes on the Use of Perspex Models for the Investigation of Machine Tool Structures. 6th Int. Mach. Tool Des. Res. Conf. Manchester, 1965.

12. Taylor, S. Computer Aided Design of a Planing Machine Structure. Proc. 9th Int. M.T.D.R. Conf. Pergamon, 1968.

13. Levi, R., S. Rosetto, and A. Verrini. Analytic and Experimental Study of Certain Types of Machine Tool Sub-assemblies. Proc. 9th Int. M.T.D.R. Conf. Pergamon 1968.

14. Opitz, H. and W. Dopper. Development of Digital Computer Programs for the Analysis of Machine Tool Structures and Elements. Proc. 9th Int. M.T.D.R. Conf. Pergamon, 1968.

15. Prentis, J.M. and F. A. Leckie. Mechanical Vibrations an Introduction to Matrix Methods. Longmans, 1963.

16. Anderson, R.A. Fundamentals of Vibrations. New-York: Collier-Macmillan,1967 (in Canada: Collier-MacMillan, Galt, Ontario).

17. Kaminskaya, V.V., Z.M. Levina and D.N. Reshetar. Bodies and Body Components of Metal Cutting Machine Tools. (Translation) Mashgis. 1960.

18. Cowley, A. and S. Hinduja. The Finite Element Method for Machine Tool Structural Analysis. Annals of C.I.R.P. Vol. XVIII, 1970.

19. Zienkiewicz, O.C. The Finite Element Method in Structural and Continuum Mechanics. McGraw-Hill. 1967.

20. Stephen, A.C. and S.Taylor. Computer Analysis of Machine Tool Structures by the Finite Element Method. Proc. 9th Int. M.T.D.R. Conf. Pergamon, 1968.

21. Cowley, A. Co-operative Work on Computer-Aided Design and Analysis of Machine Tool Structures. C.I.R.P. Group Ma Dec 1969.

22. Hurty, W.C. and M.F. Rubinstein. Dynamics of Structures. Prentice-Hall, 1964.

FIGURES

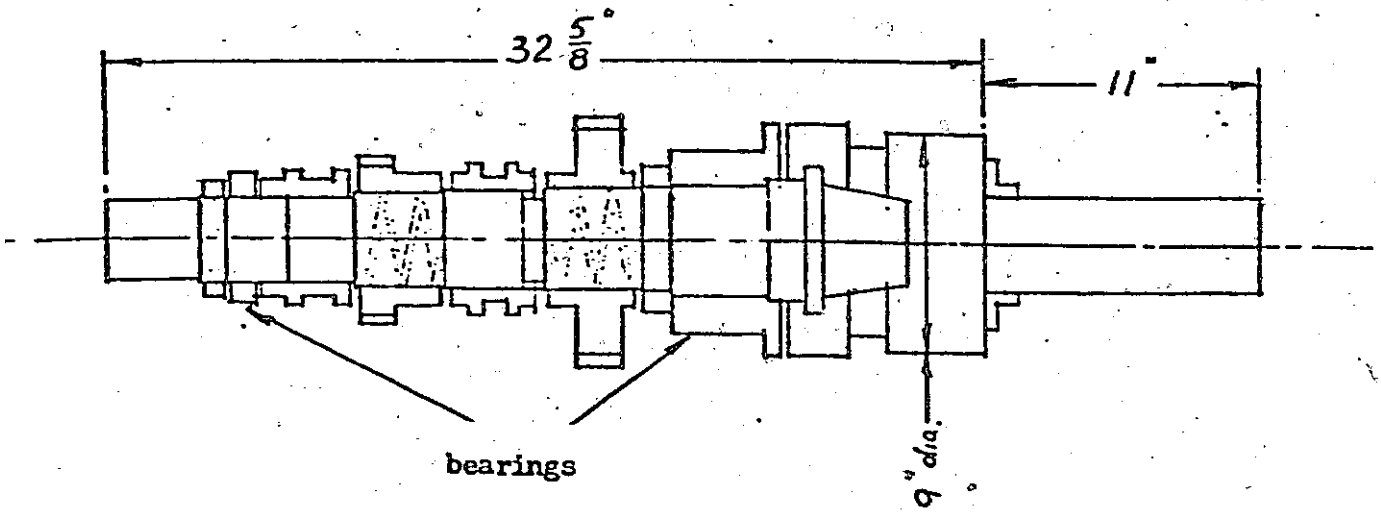

FIG. 2.1a Lathe Spindle

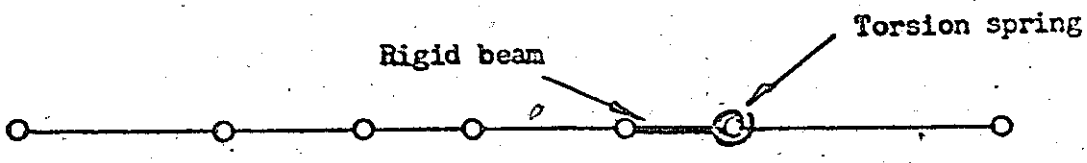

FIG. 2.1b Initial Mathematical Model

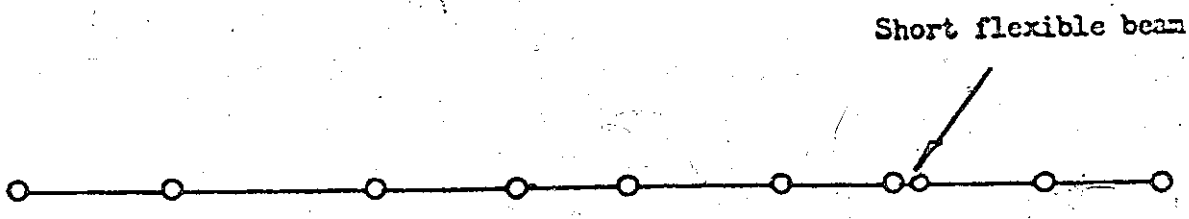

FIG. 2.1c Final Mathematical Model

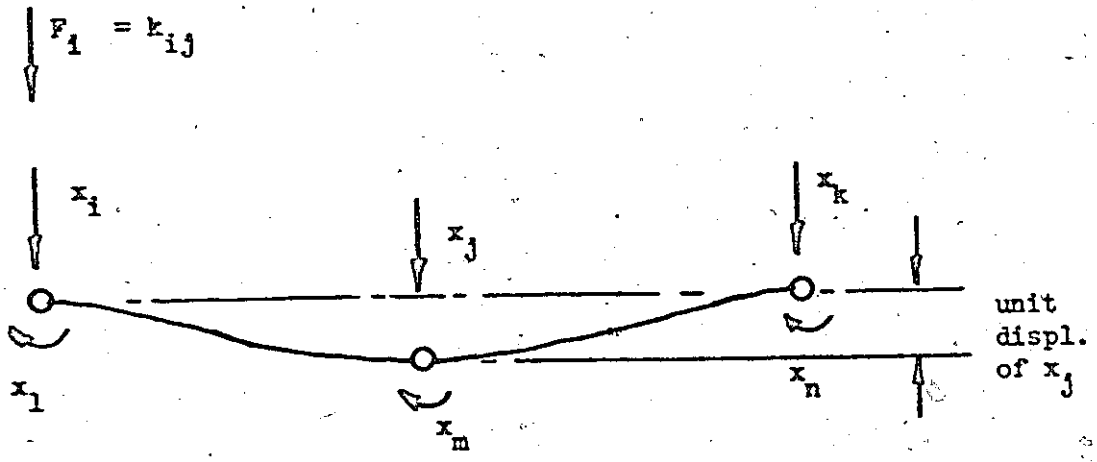

FIG. 2.2 Stiffness Influence Coefficient, k_{ij}

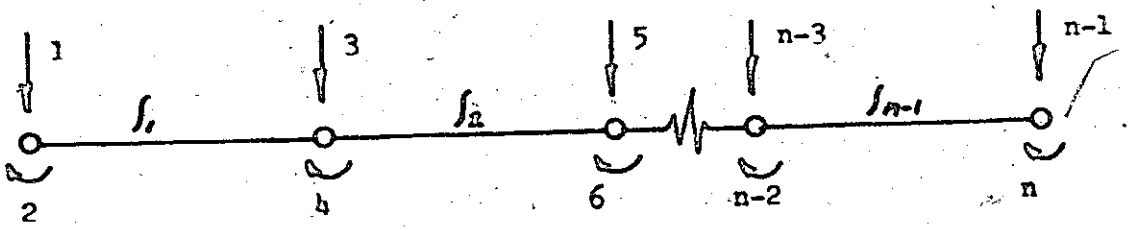

FIG. 2.3 Co-ordinate System for Beam Model

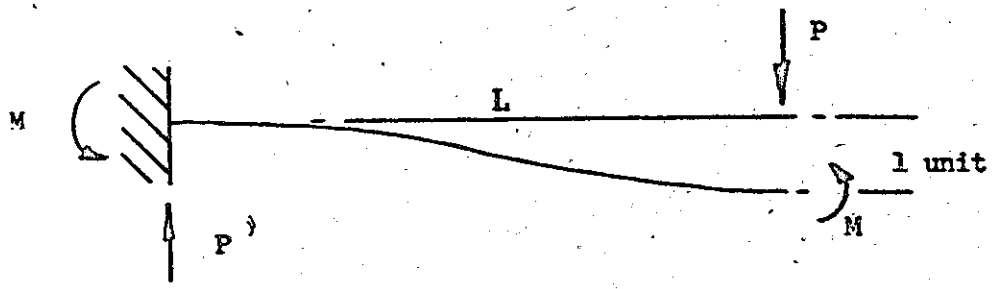

$$P = \frac{12EI}{L^3}$$

$$M = \frac{6EI}{L^2}$$

FIG 2.4a Unit translational displacement

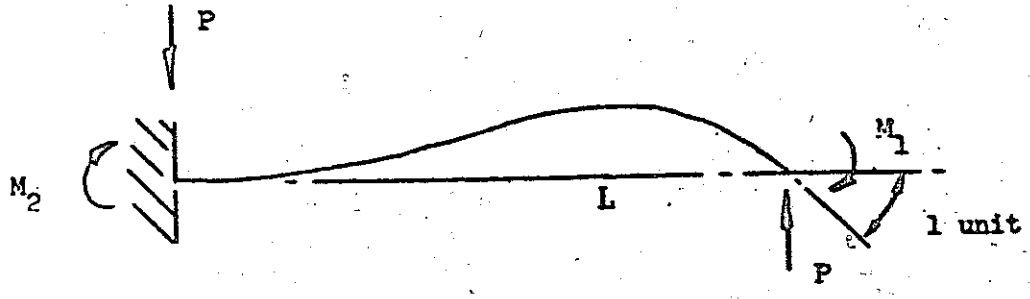

$$P = \frac{6EI}{L^2}$$

$$M_1 = \frac{4EI}{L}$$

$$M_2 = \frac{2EI}{L}$$

FIG. 2.4b Unit rotational displacement

Uniform shaft,

diameter : 3"
length : 45"
No. of Nodes: 16

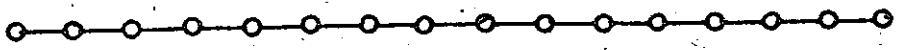

FIG. 2.5 Programme test model

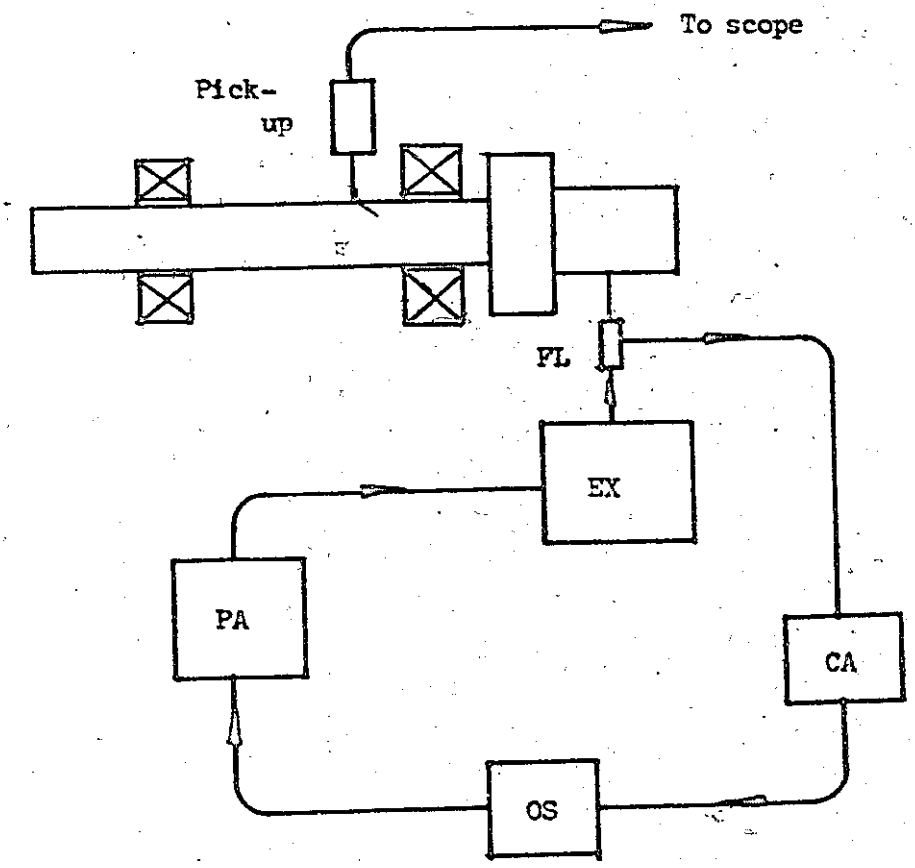

FIG. 2.6 Schematic of experimental set-up for lathe spindle

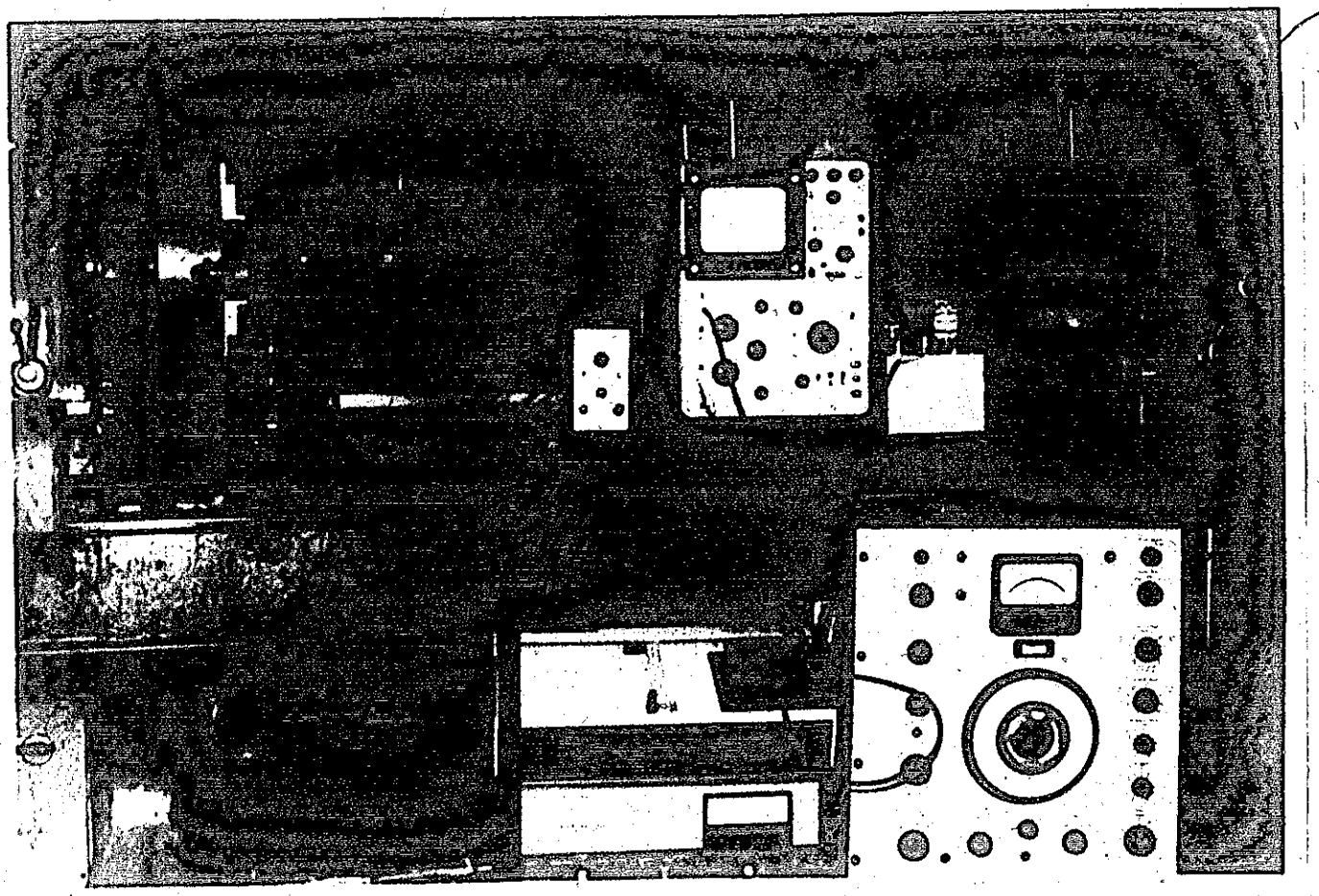

Fig. 2.7 Experimental Set-Up. Spindle in Machine

Fig. 2.8. Spindle Suspended Freely

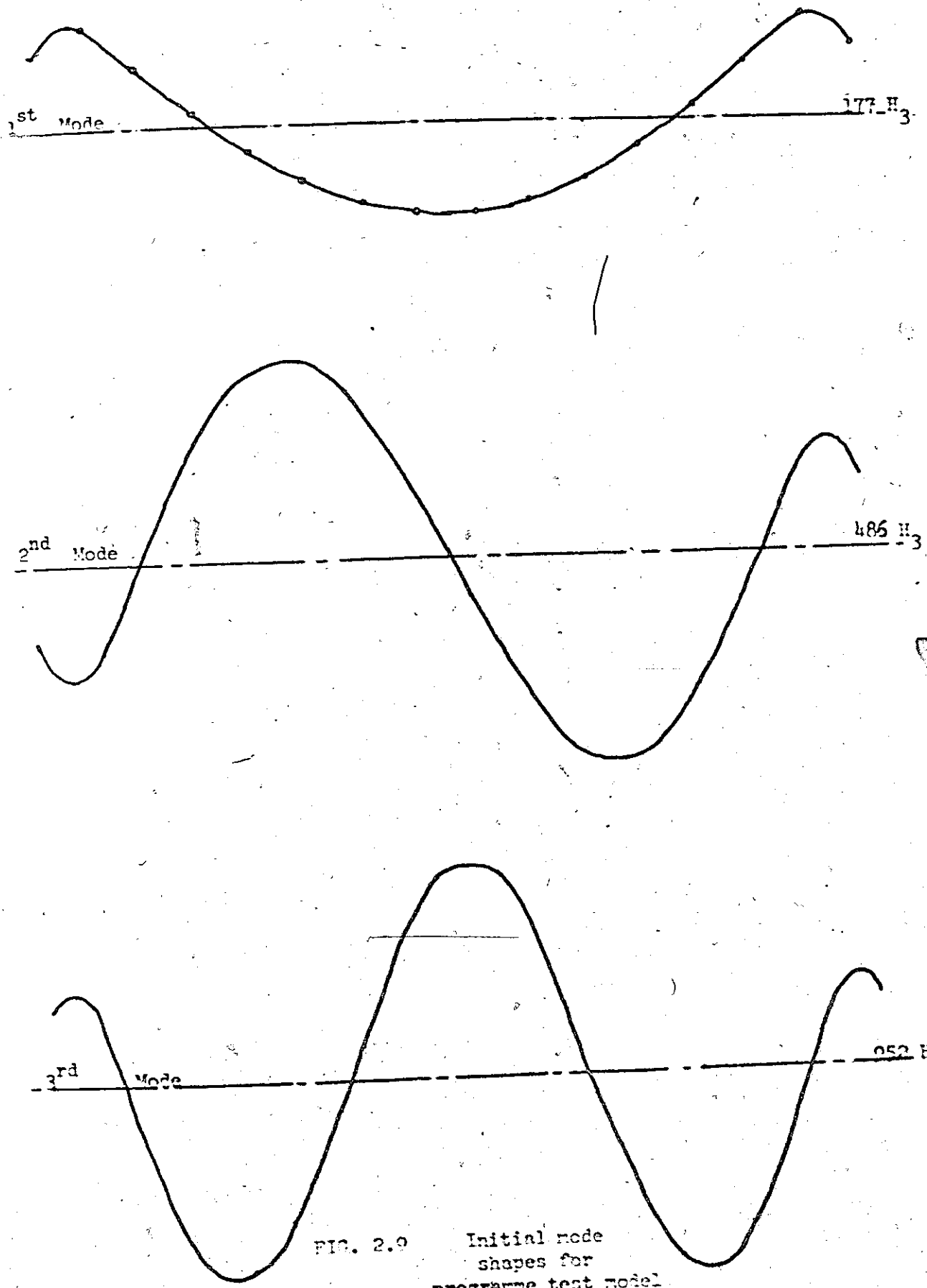

FIG. 2.9 Initial mode shapes for programme test model

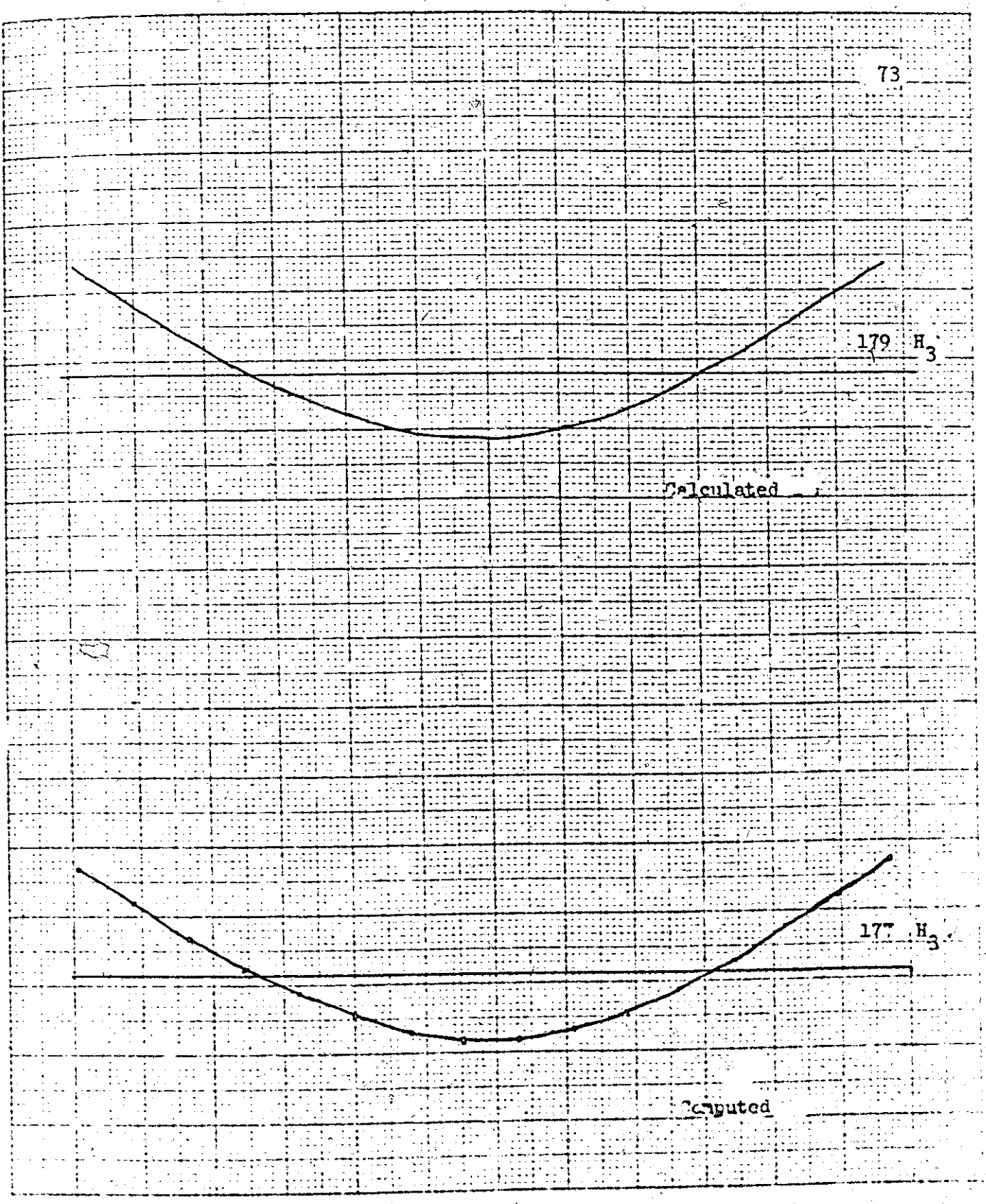

FIG. 3.10 Calculated and final computed mode shapes for programme test model

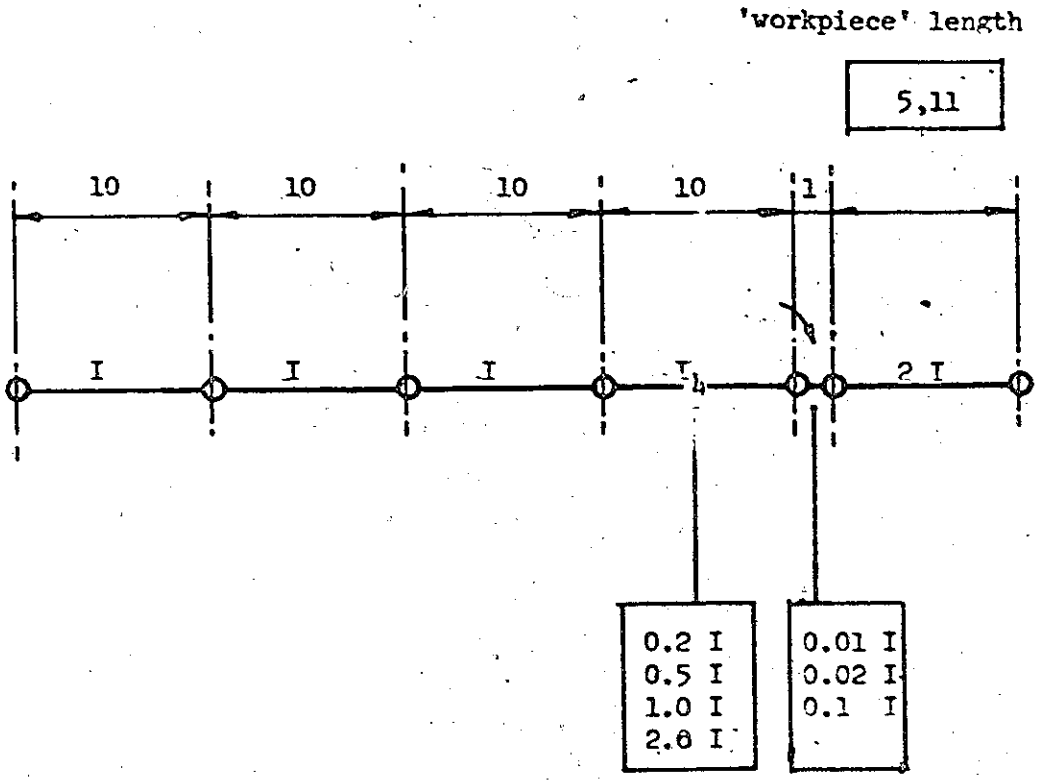

FIG. 2.11 Special model for chuck investigation

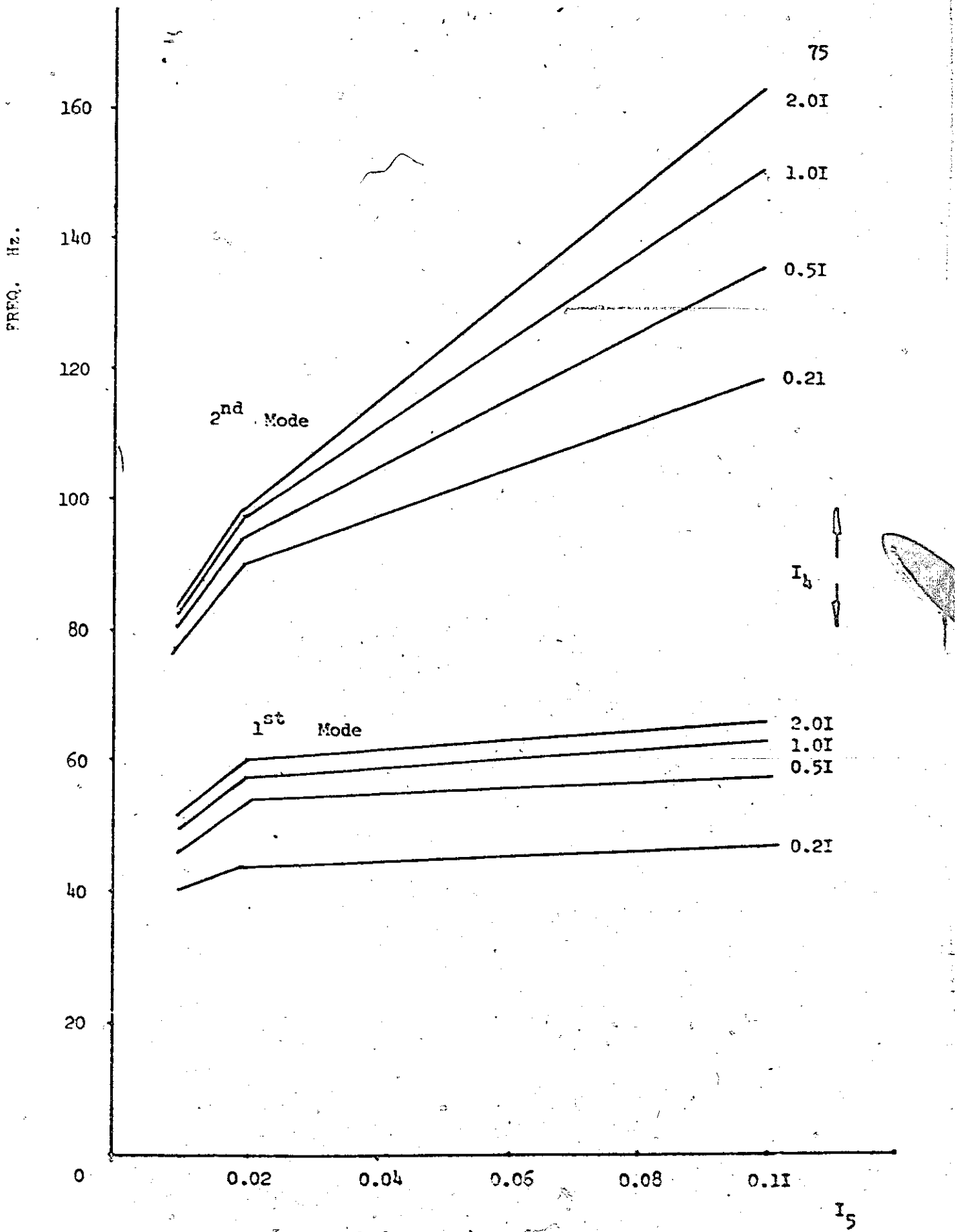

FIG. 2.12 Natural frequencies of special model with 5" 'workpiece'

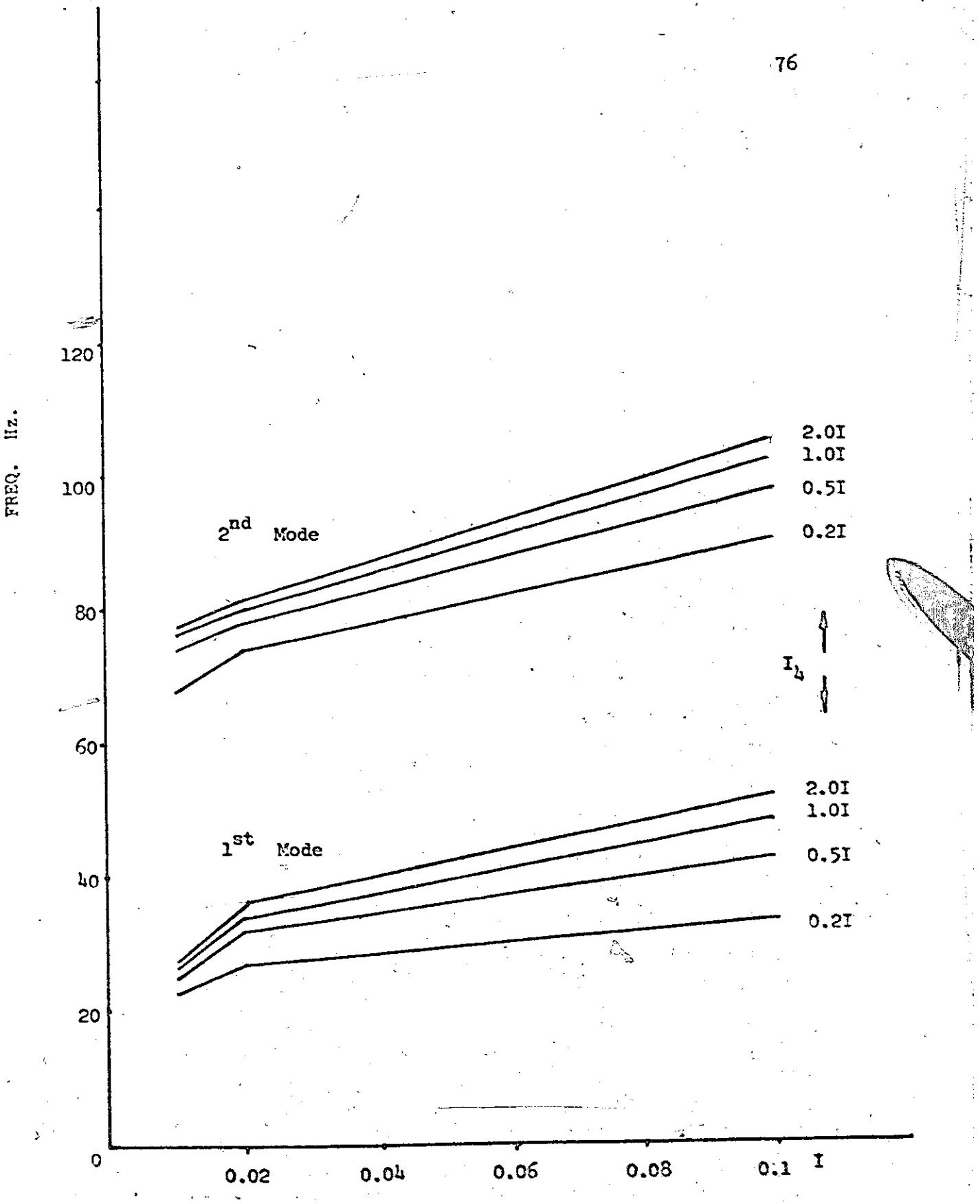

FIG. 2.13 Natural frequencies of special model with 11" 'workpiece'

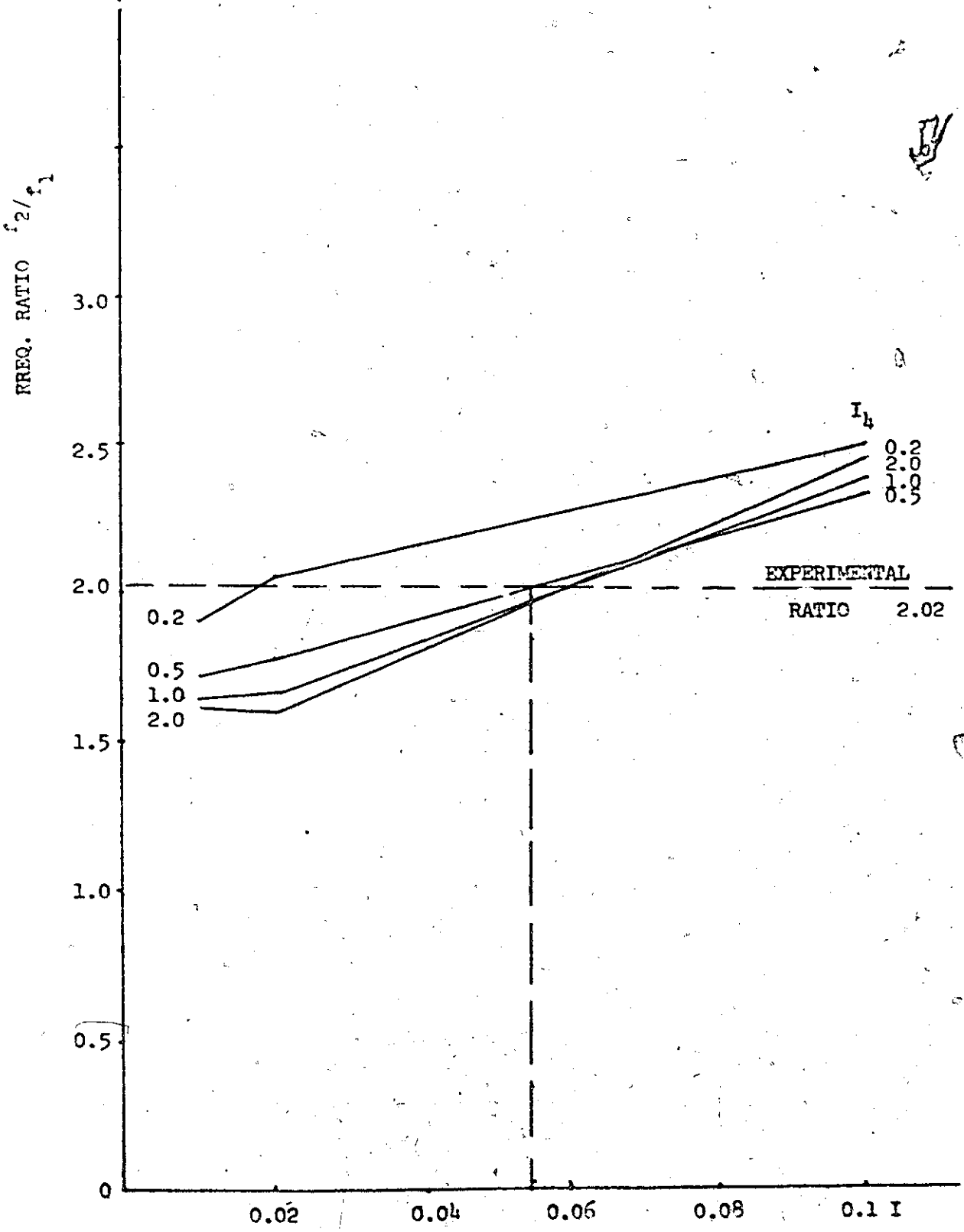

FIG. 2,14 Frequency ratio for special model with 5" 'workpiece'

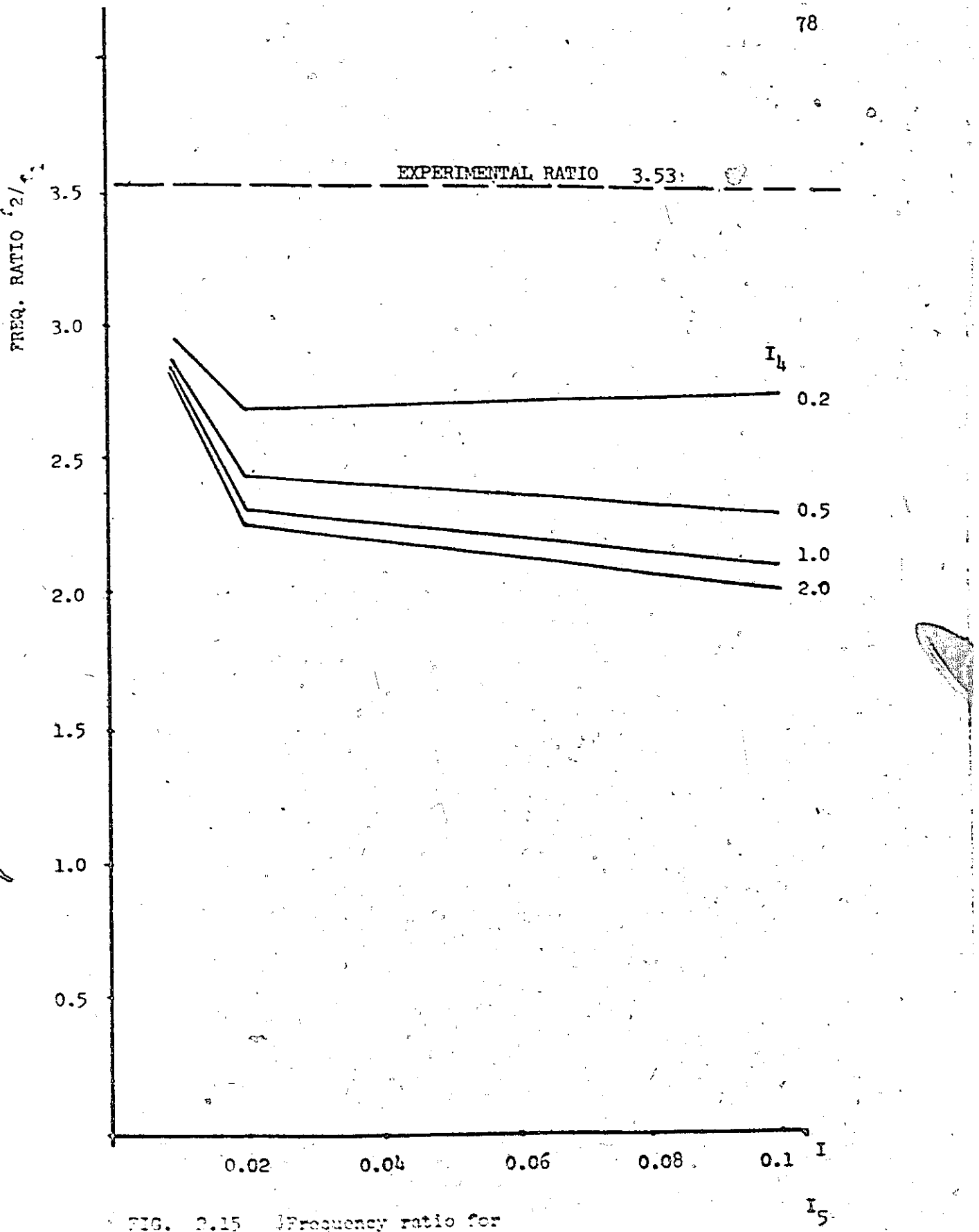

FIG. 3.15 Frequency ratio for special model with 11" 'workpiece'

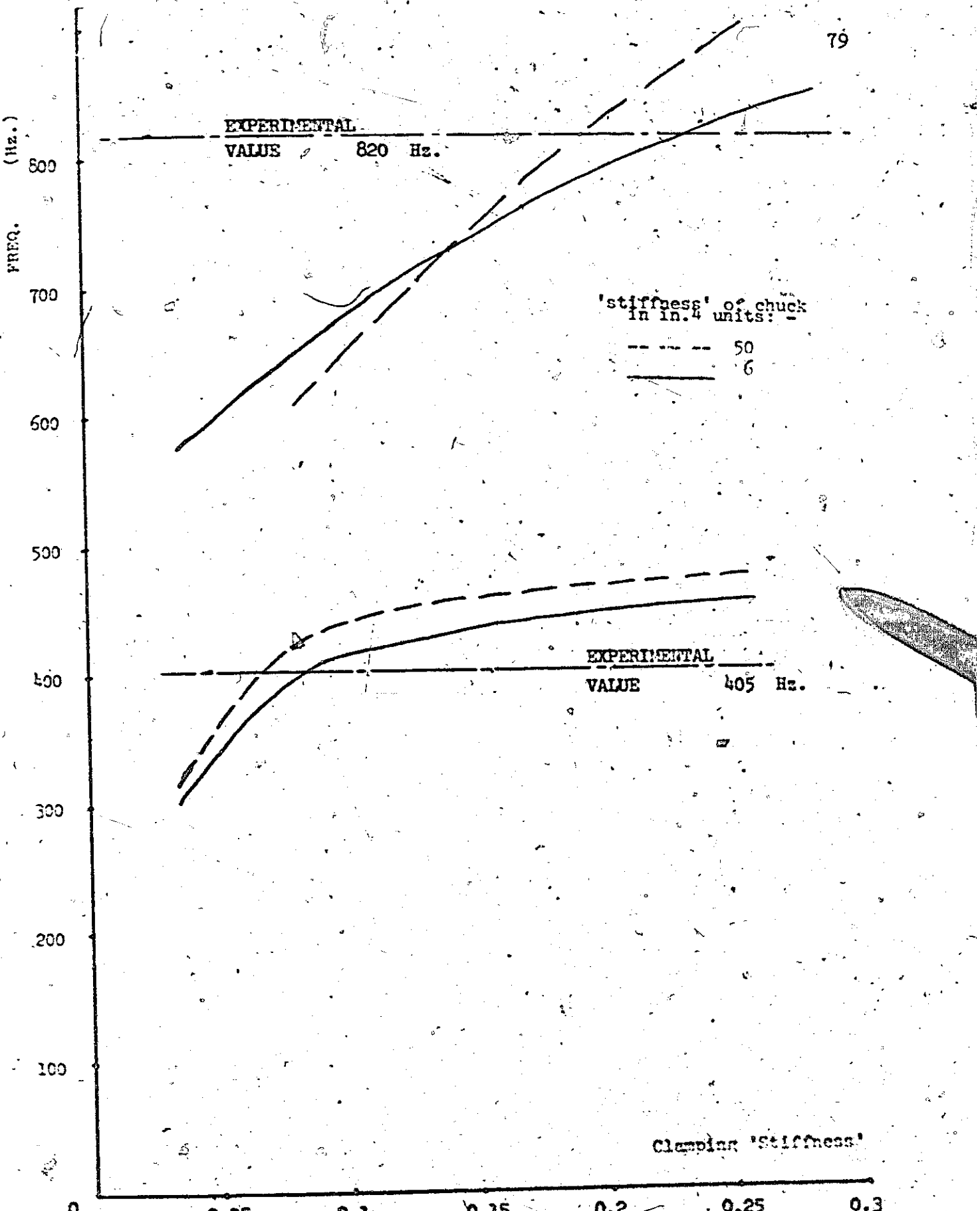

FIG. 2.16 Natural frequencies
Spindle suspended without rear
5" workpiece

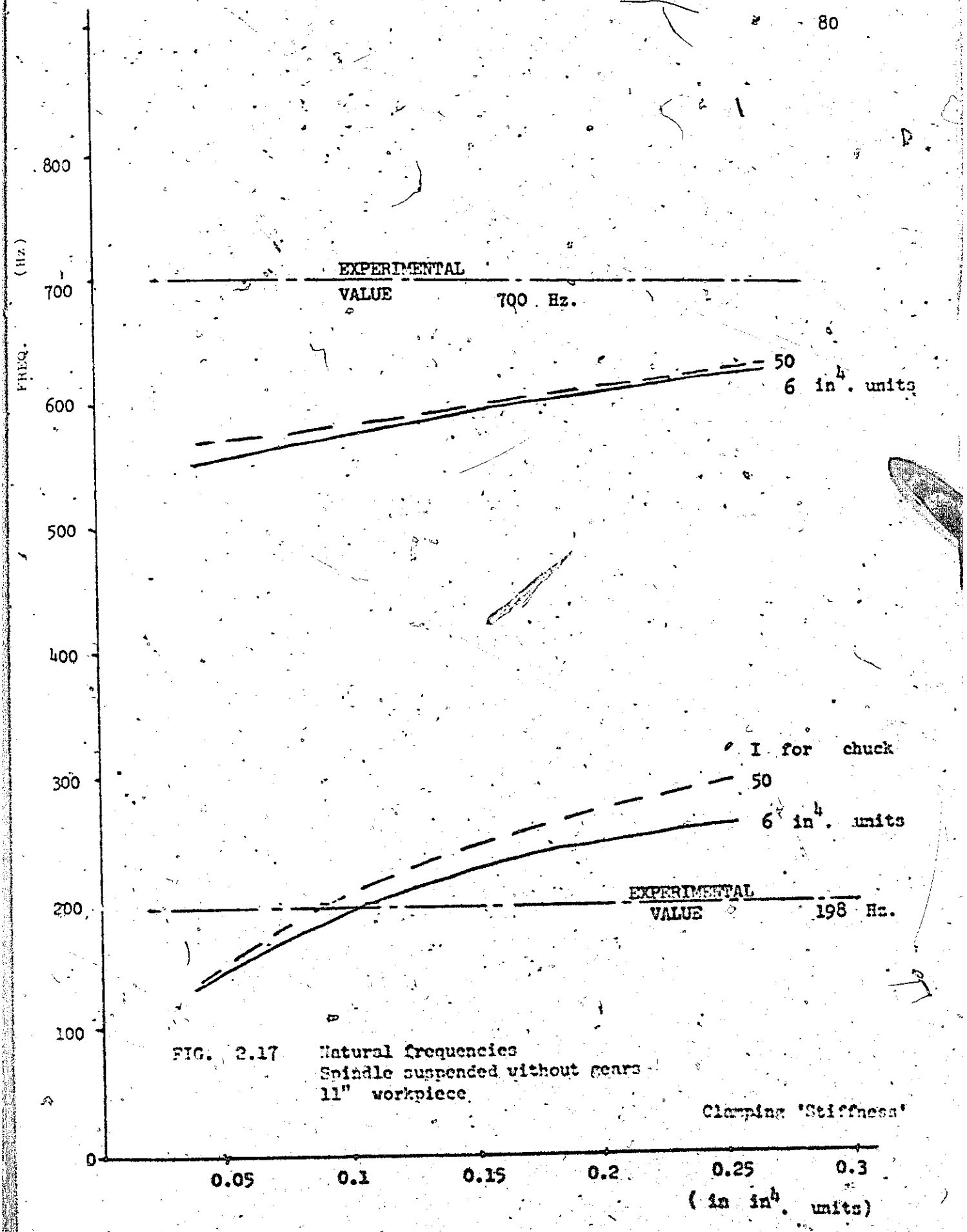

FIG. 2.17 Natural frequencies
Spindle suspended without gears
11" workpiece

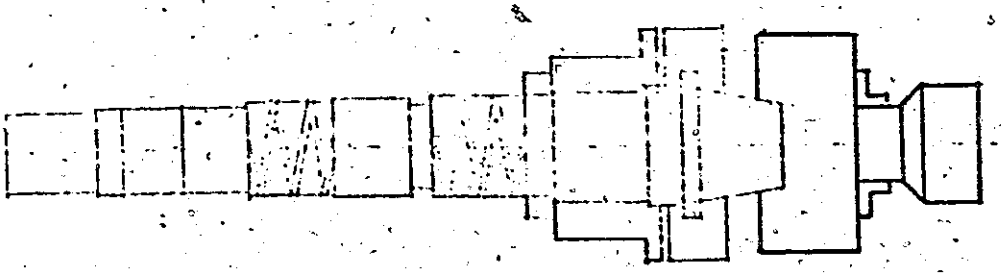

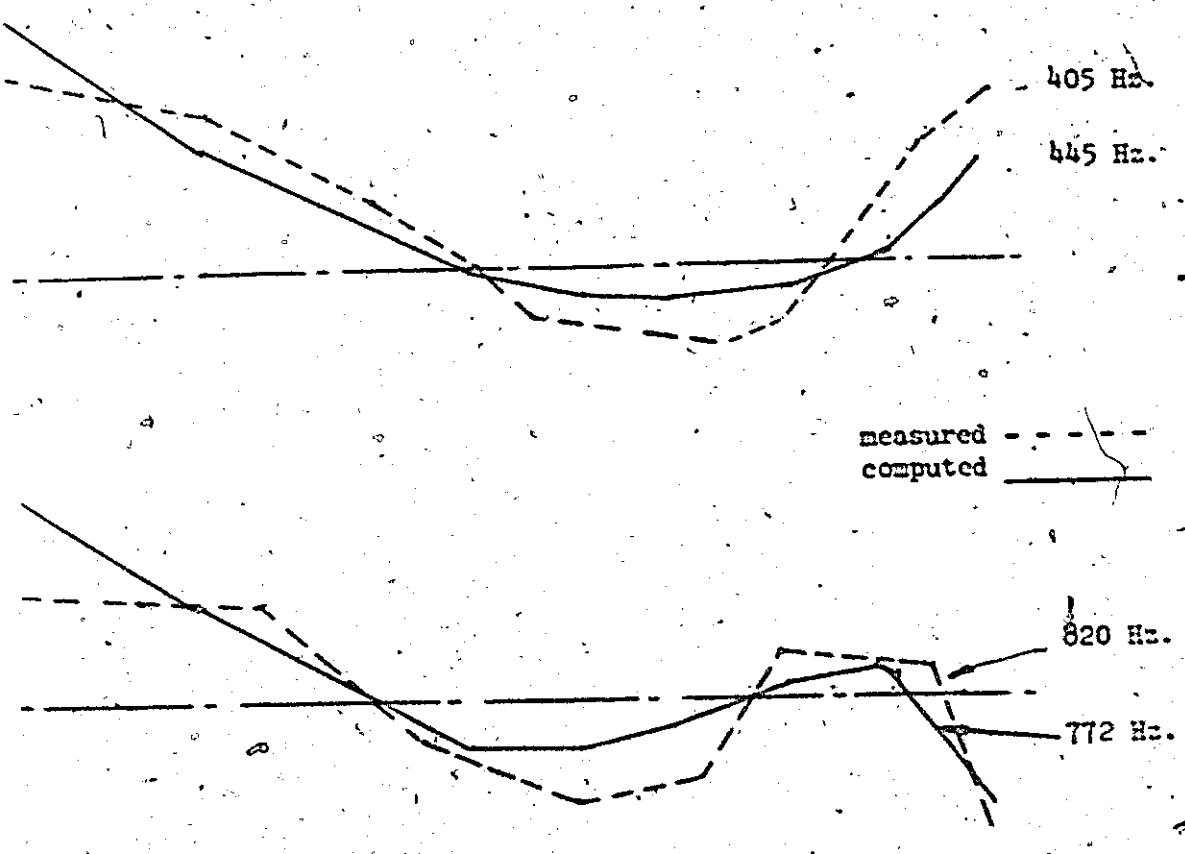

FIG. 2.18 Mode shapes 5" workpiece

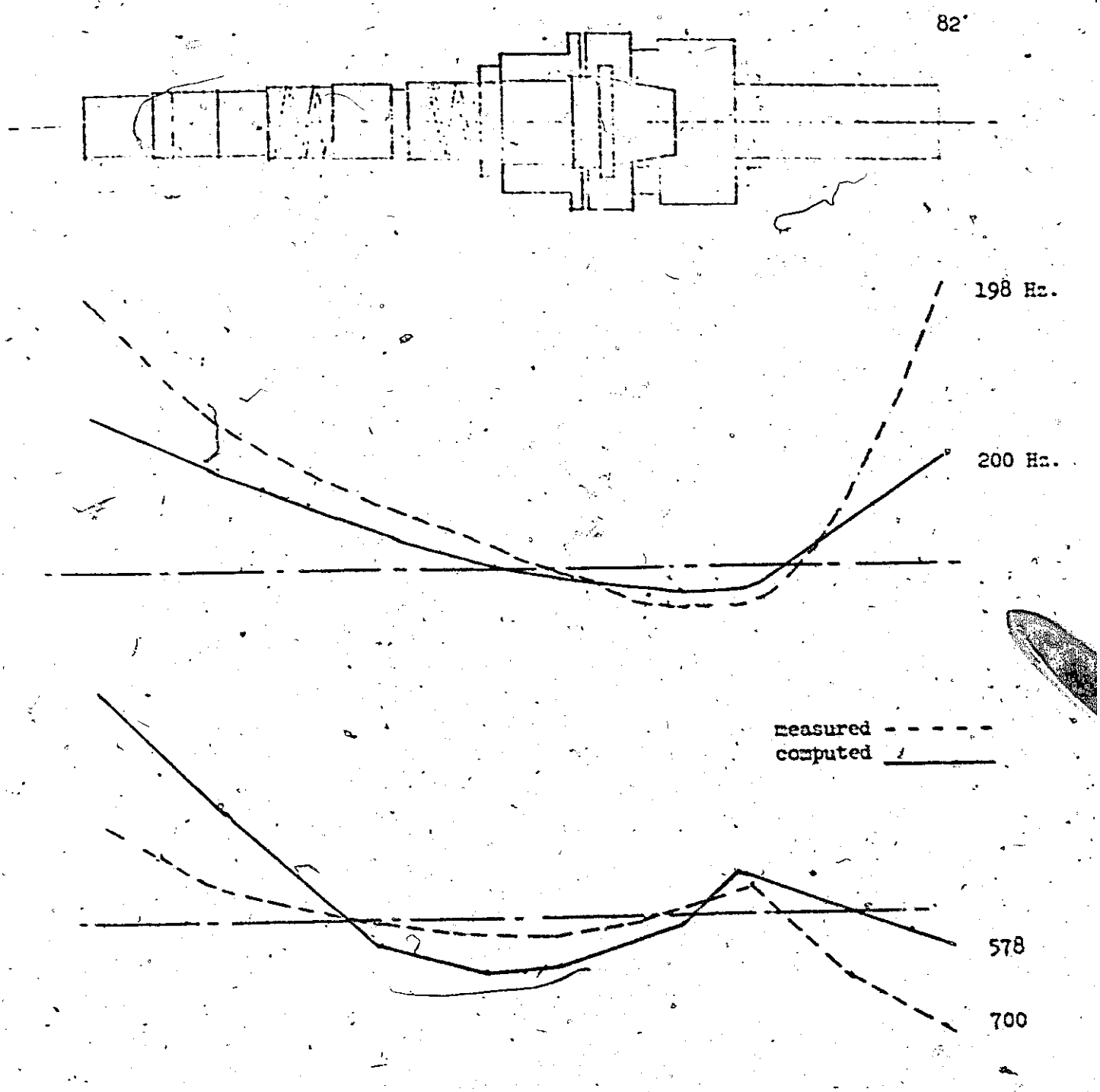

FIG. 2.19 Mode shapes 11" workpiece

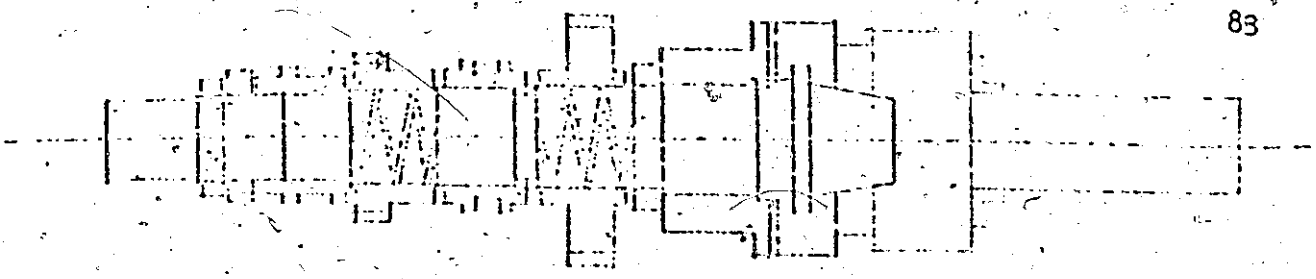

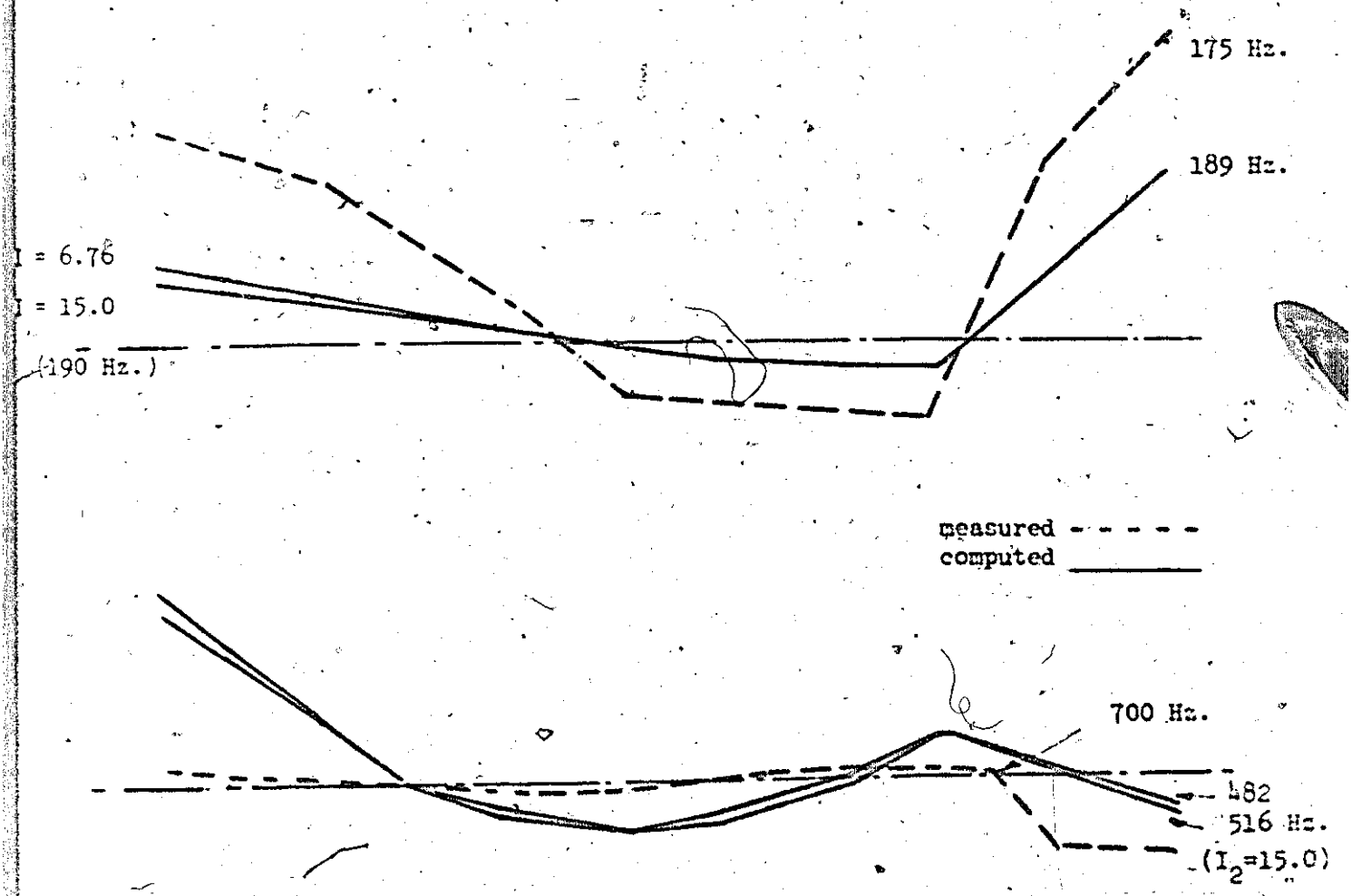

FIG. 2.20 Mode shapes
11" workpiece with gears

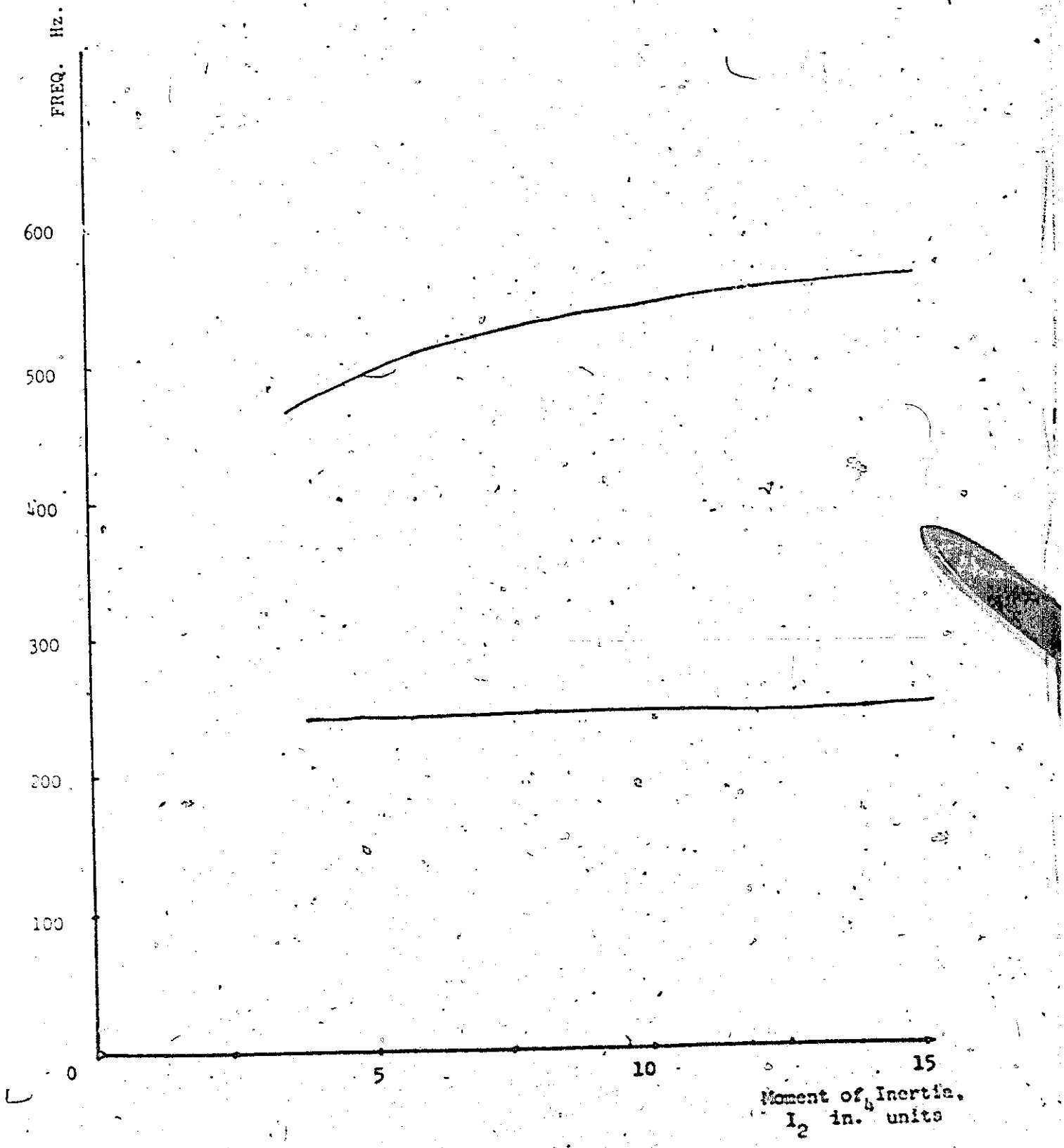

FIG. 2.21 Effect of bearing ring on natural frequencies

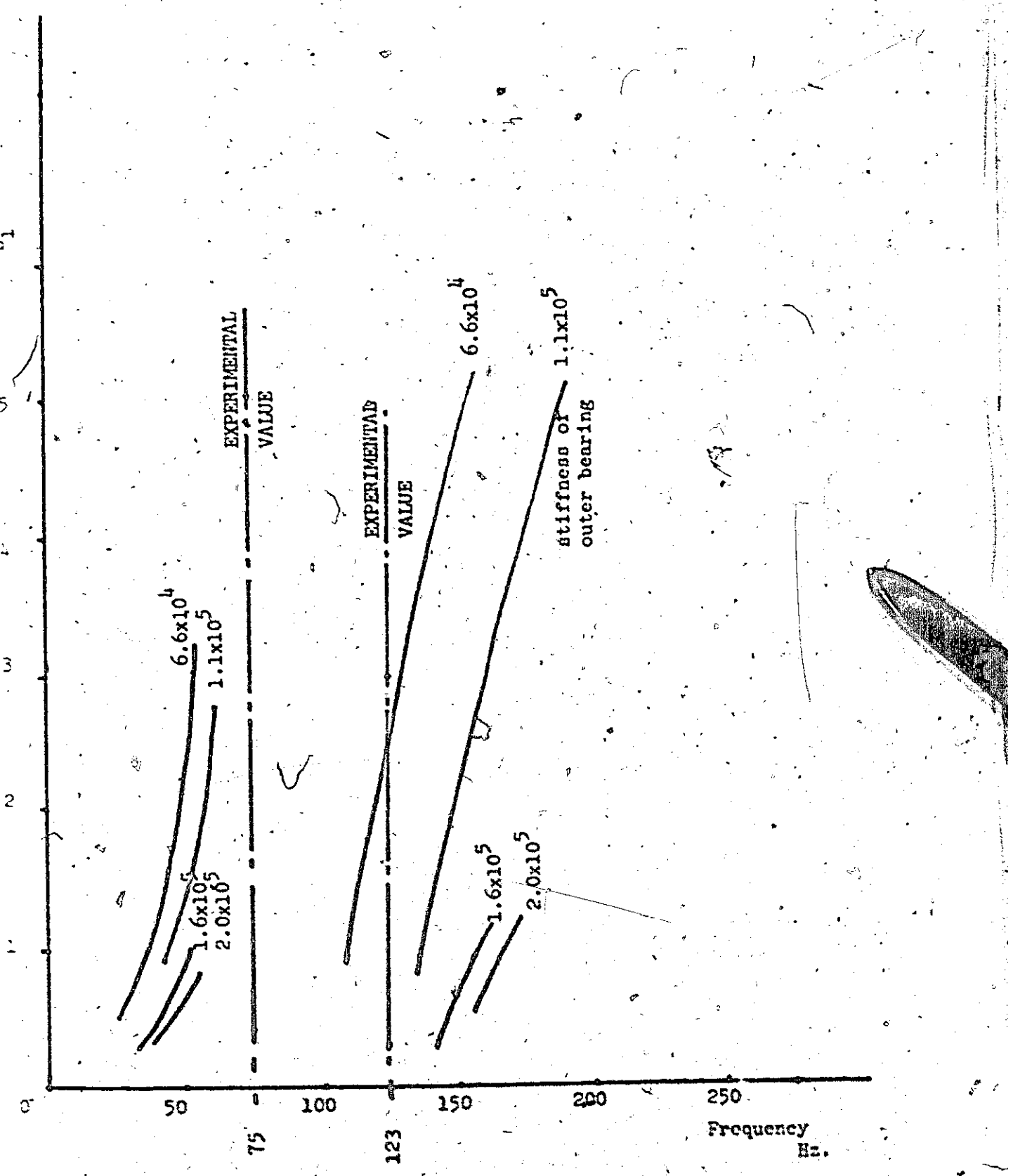

FIG. 2.22 Effect of varying bearing stiffness.

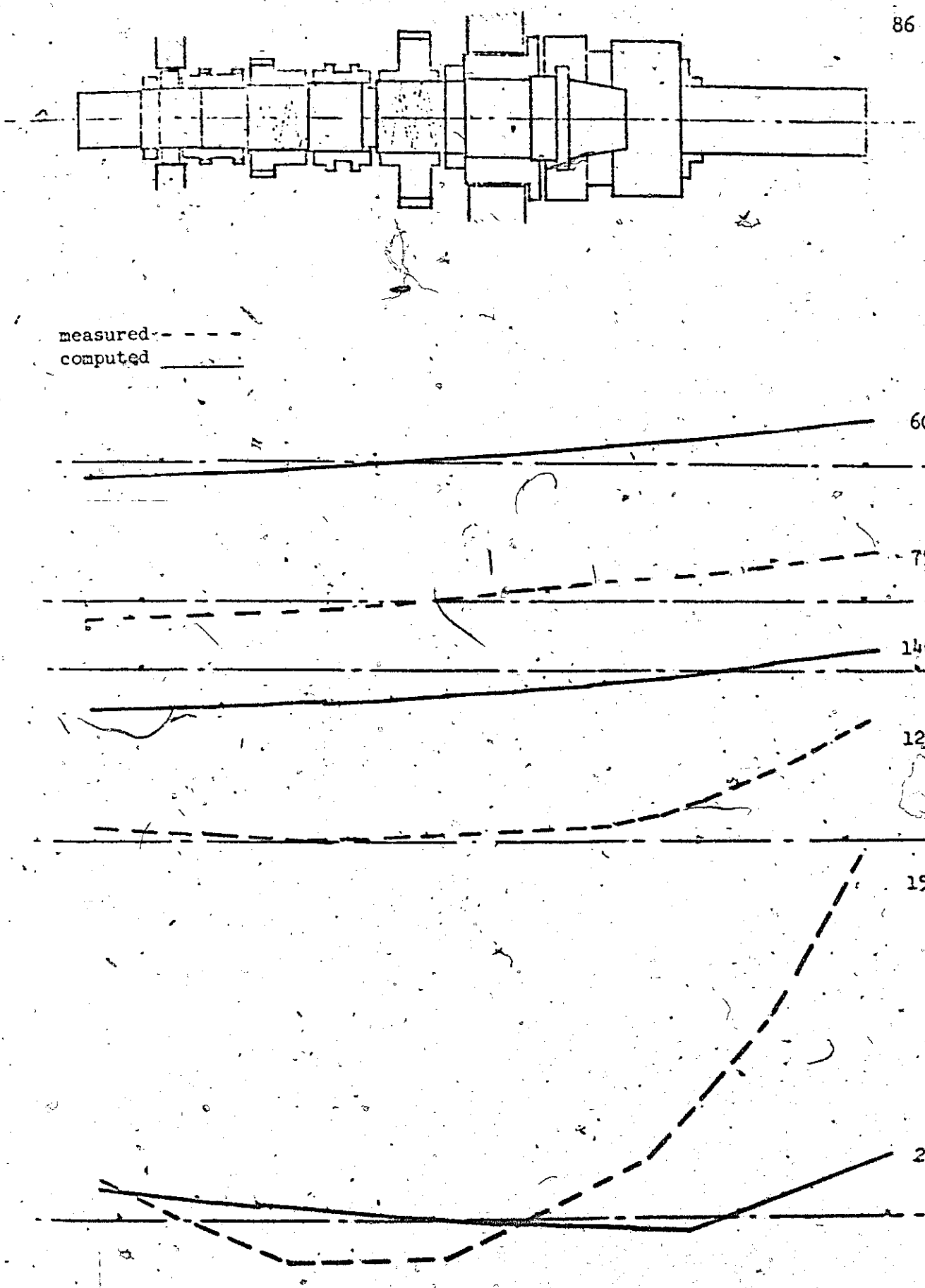

FIG. 2.23 Mode shapes 11" workpiece

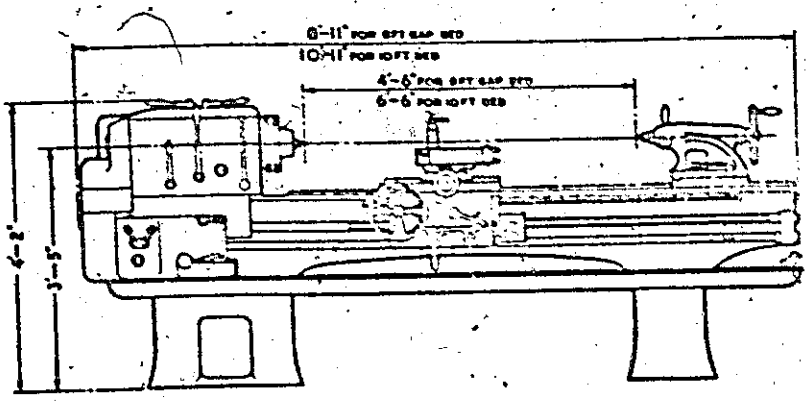

FIG. 3.1a Colchester Lathe

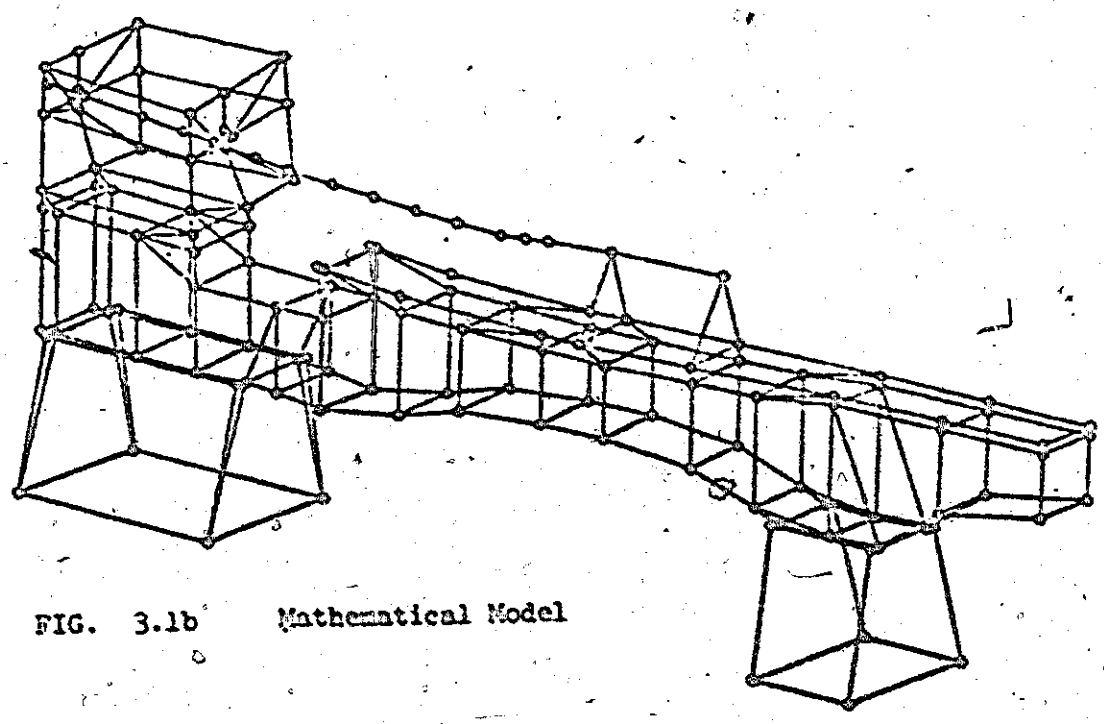

FIG. 3.1b Mathematical Model

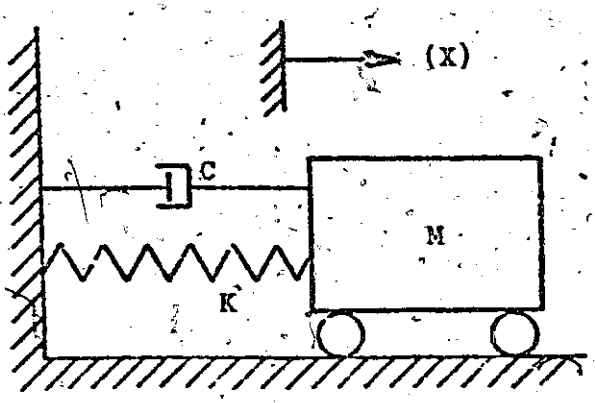

(a)

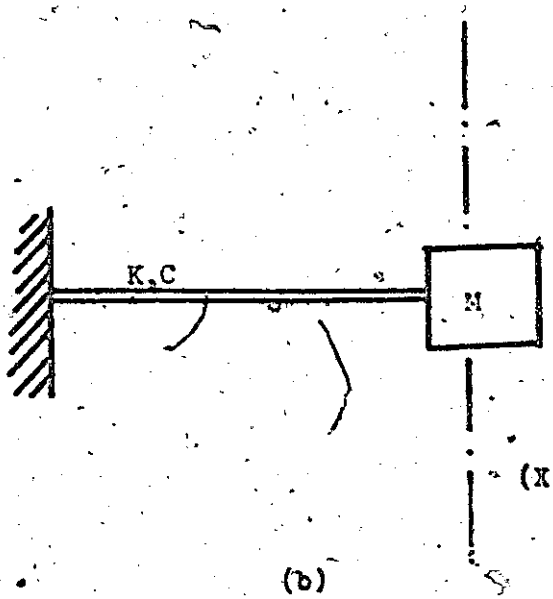

(b)

FIG. 3.2 Single D.O.F. systems

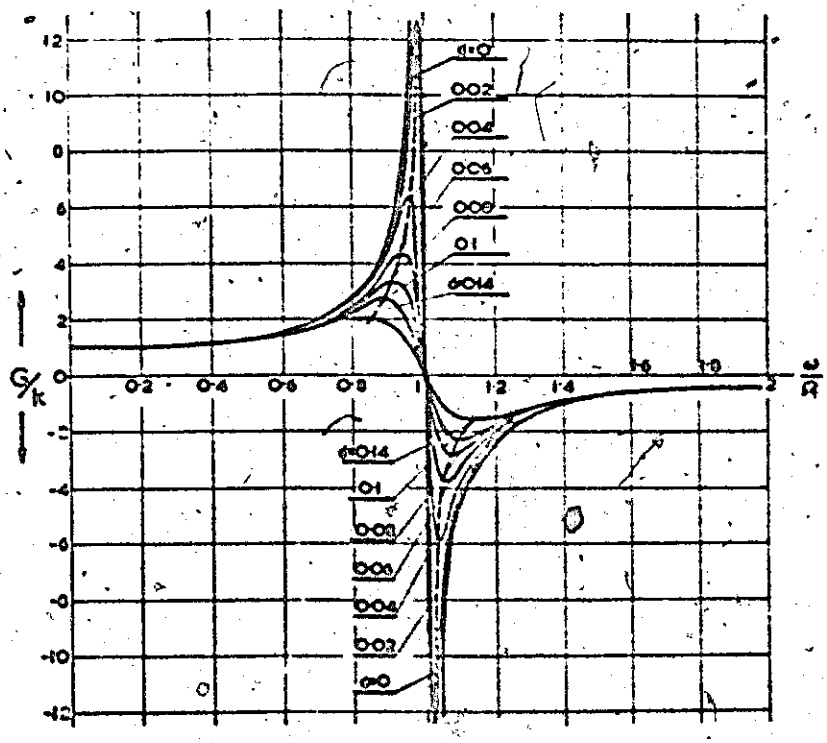

FIG. 3.3 Real receptance

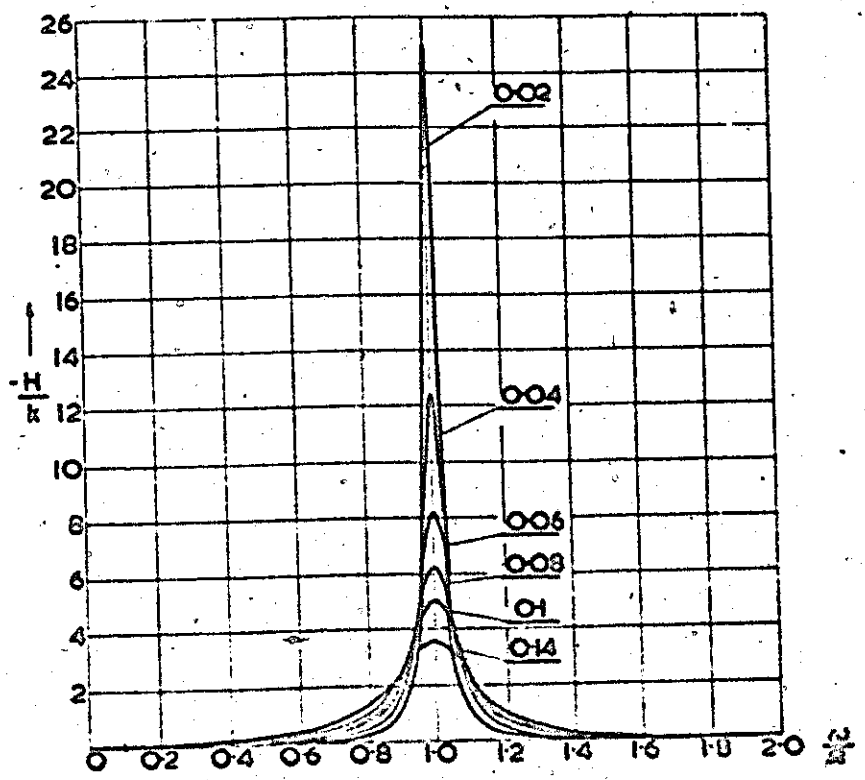

FIG. 3.4 Imaginary receptance

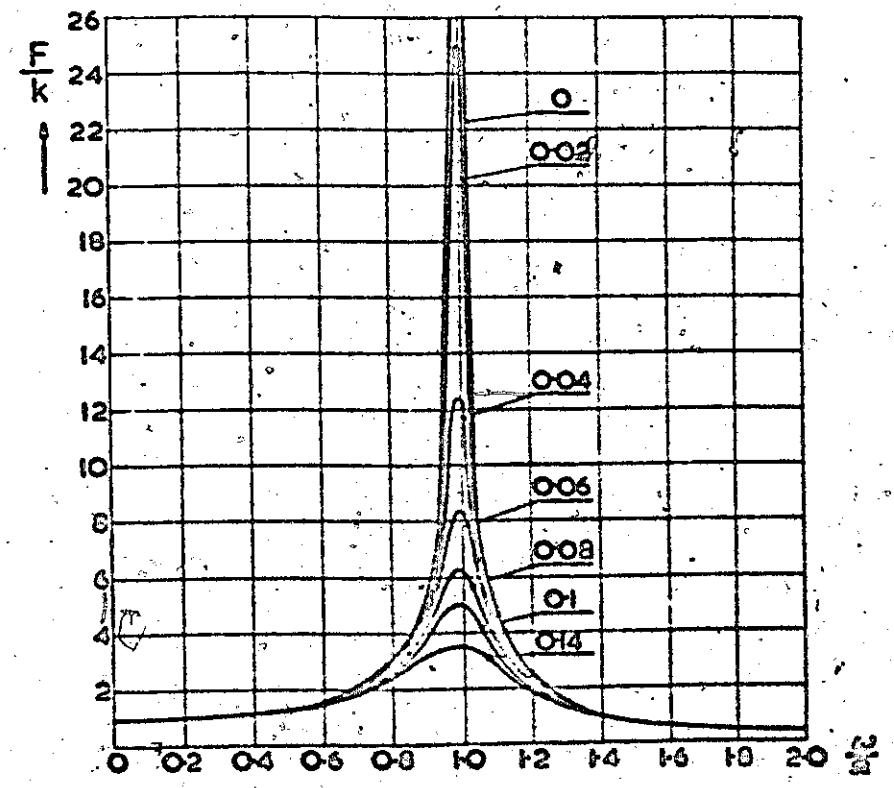

FIG. 3.5 Absolute receptance

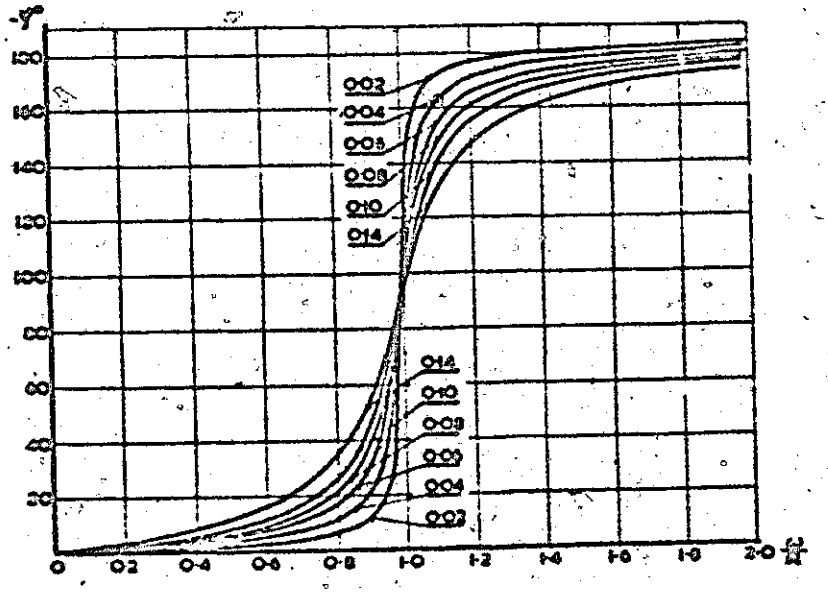

FIG. 3.6 Phase shift

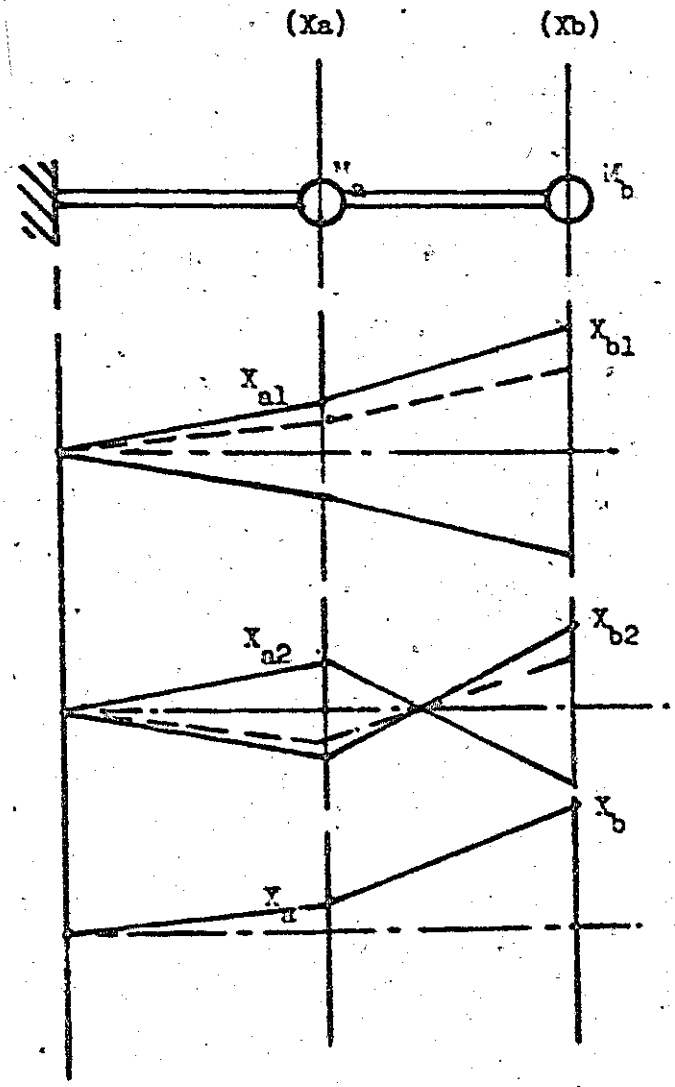

FIG. 3.7 2 D.O.F. System

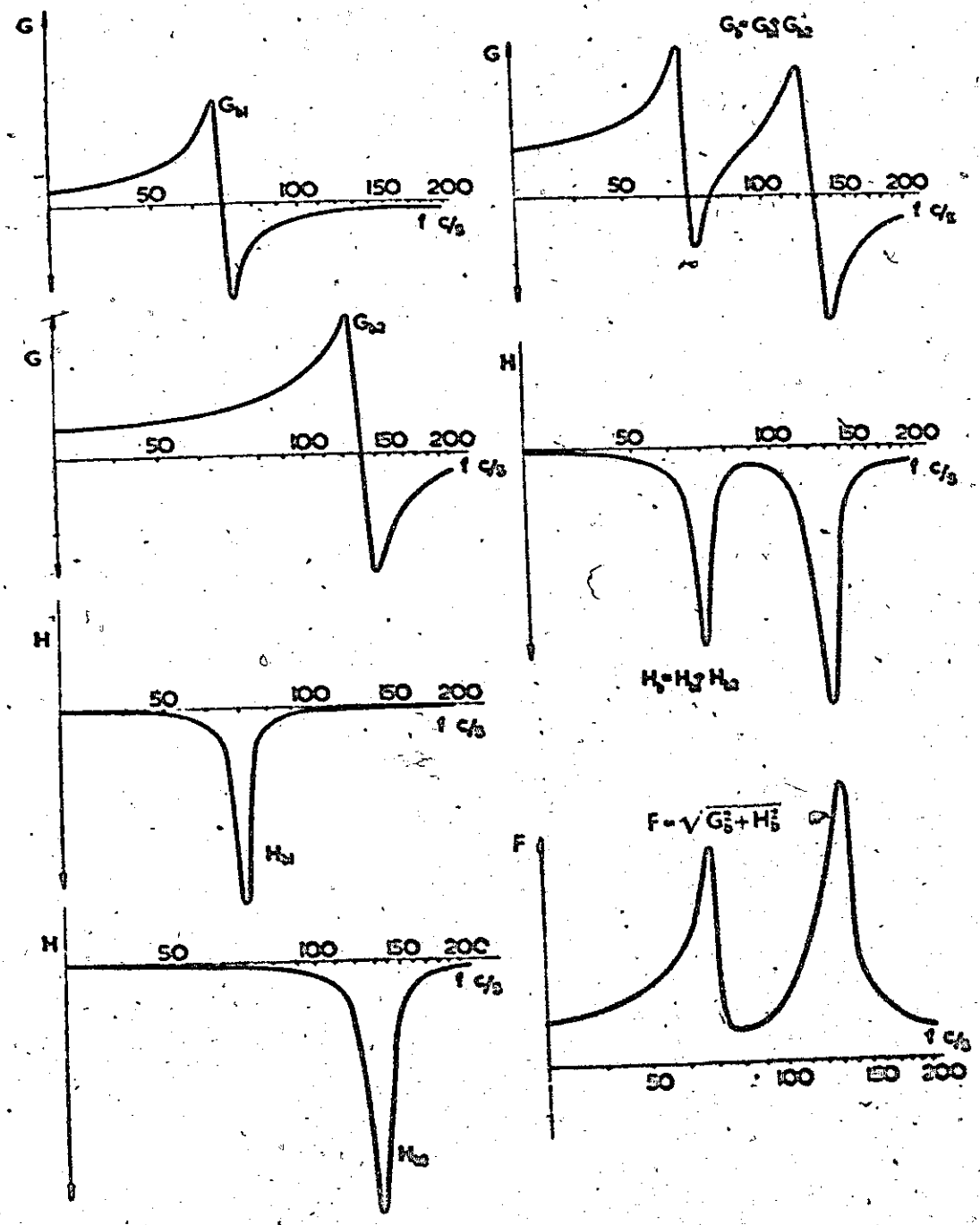

FIG. 3.8 Summation of receptances of individual modes

FIG. 3.9

o Commonly Used Finite Elements

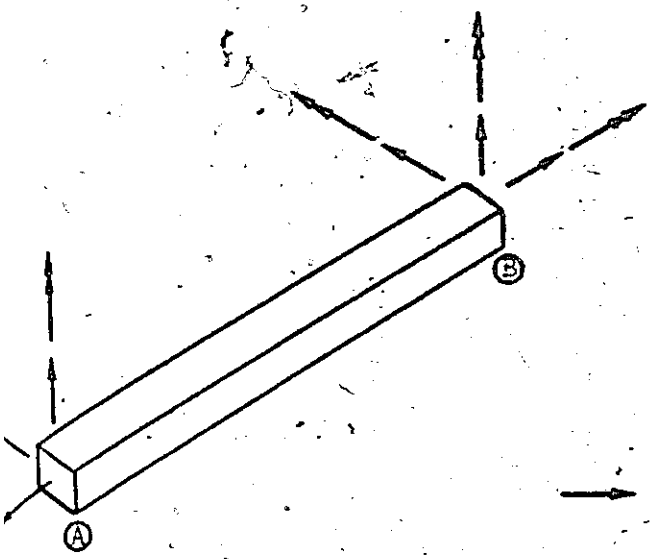

o Bar
(2 nodes)

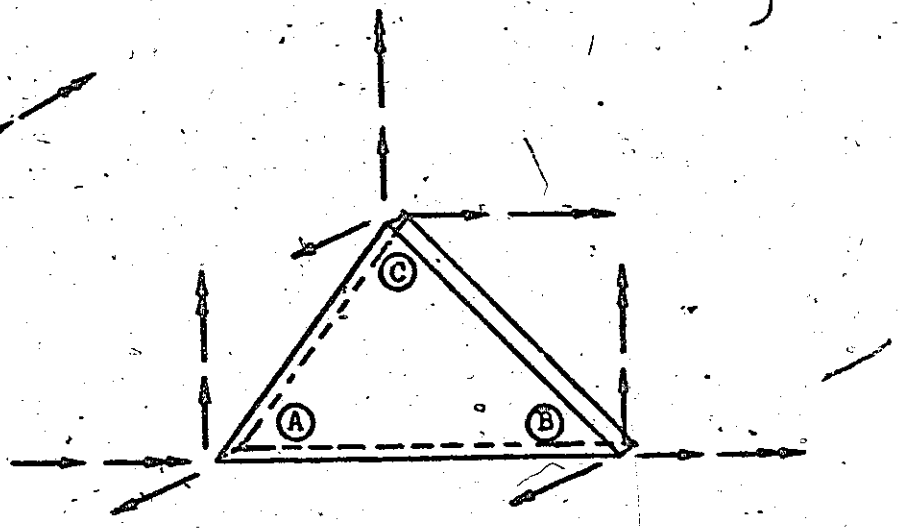

o Triangular Plate(s)
(3 nodes)

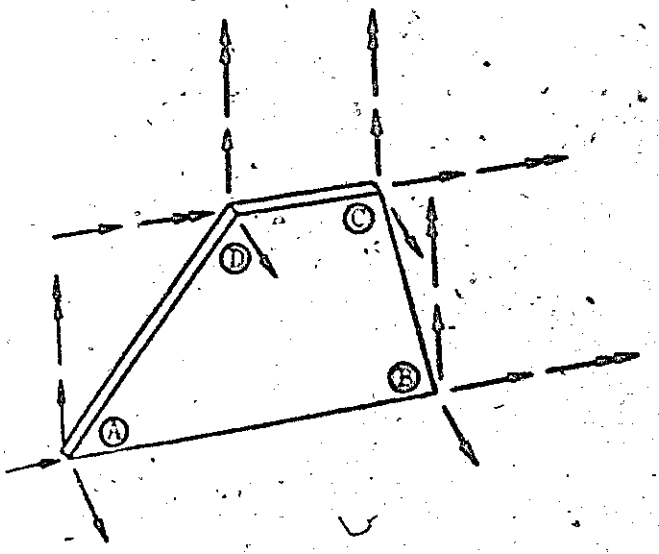

o Quadrilateral Plate
(4 nodes)

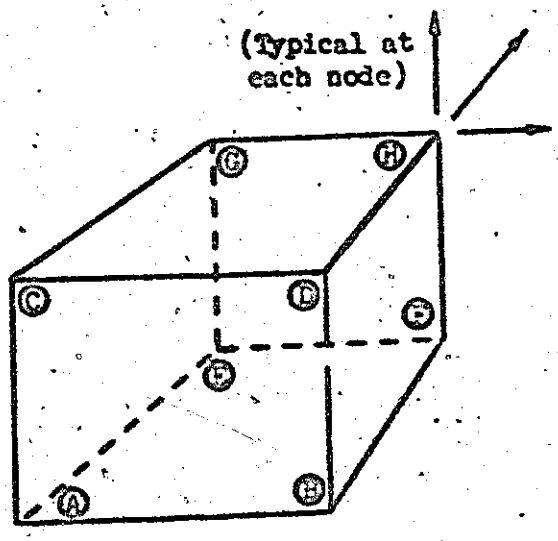

o General Six Sided Solid (Hexahedron)
(8 nodes)

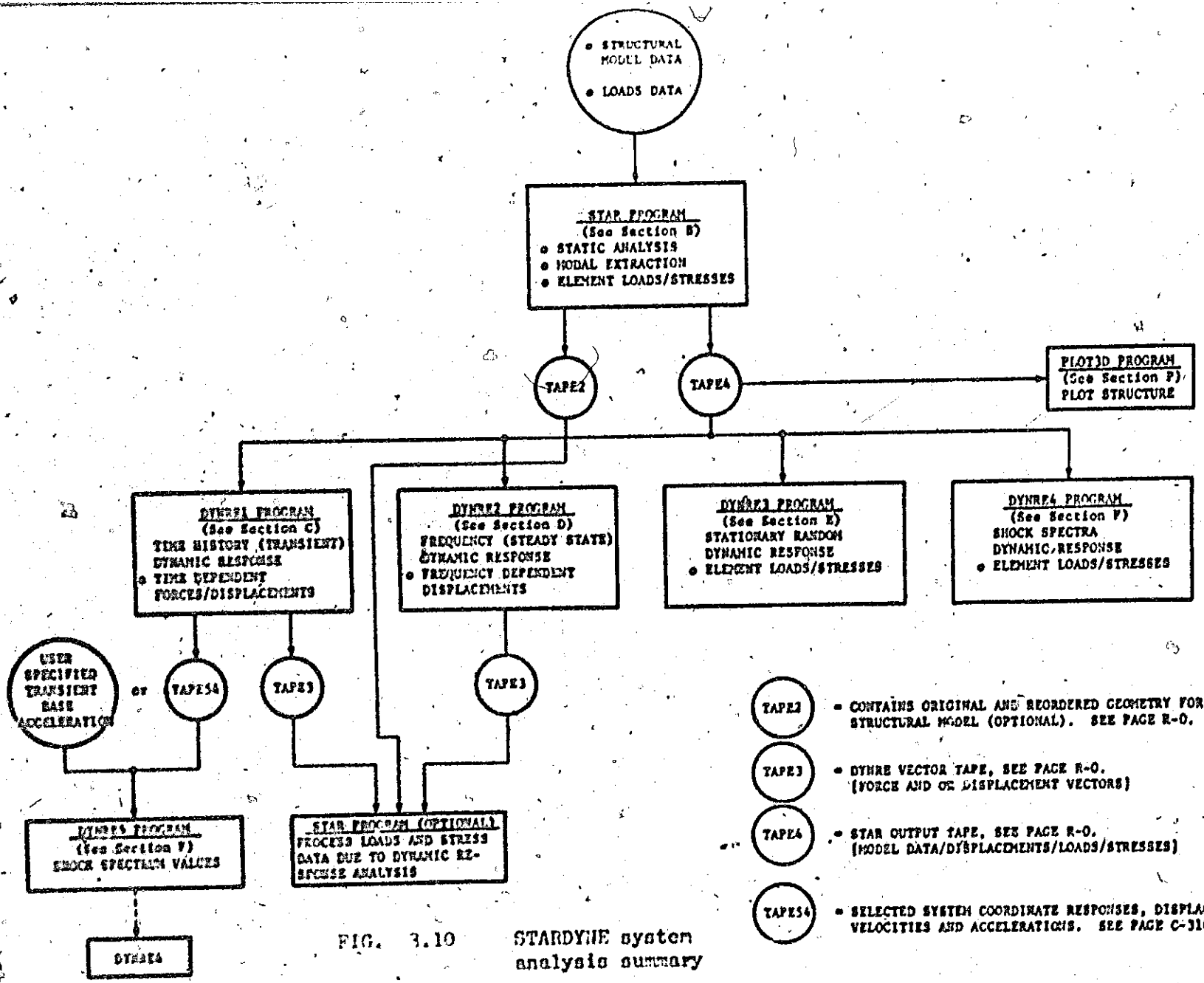

FIG. 3.10 STARDYNE system analysis summary

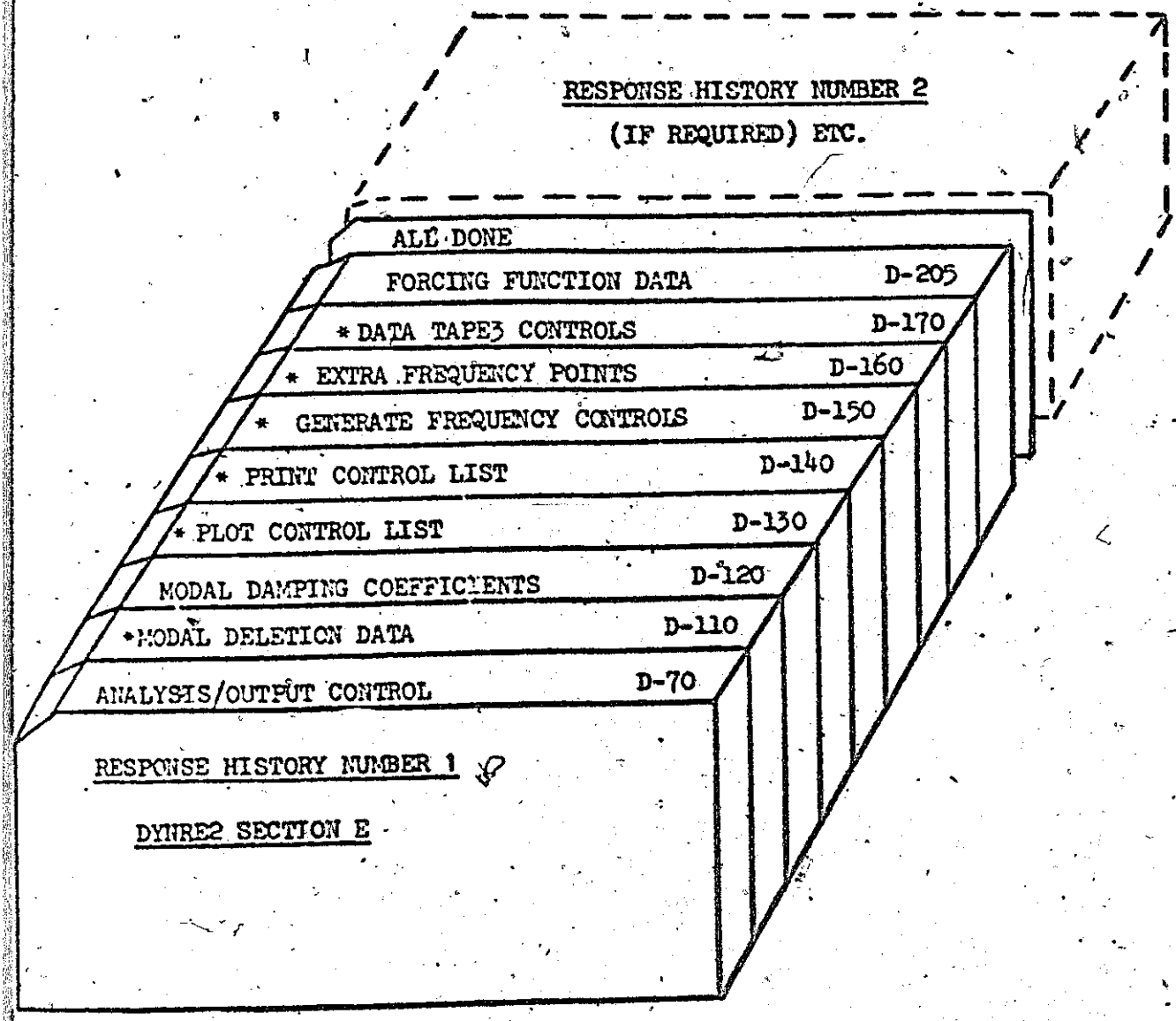

Optional Input Sections

FIG. 3.11 DYNRE2 DECK SETUP DIAGRAM

```
      PROGRAM PROG(INPUT,TAPE5=INPUT,OUTPUT,TAPE6=OUTPUT)
      DIMENSION FP(36),TP(36),AP(36),FQ(36),TQ(36),AQ(36),RR(36),
     1  RI(36),RA(36)
      I=0
      DO 100 L=1,2
      WRITE(6,99)
   99 FORMAT(/,10X,10HINPUT DATA  )
      DO 5 I=1,N
      READ(5,10) FP(I),TP(I),AP(I)
   10 FORMAT(E15.6,E15.6,E15.6)
      TP(I)=(TP(I))*3.1416/180.
      WRITE(6,50) FP(I), TP(I), AP(I)
   50 FORMAT(/,3E15.6)
    5 CONTINUE
      DO 15 I=1,N
      READ(5,20)  FQ(I),TQ(I),AQ(I)
   20 FORMAT (E15.6,E15.6,E15.6)
      TQ(I)=(TQ(I))*3.1416/180.
      WRITE(6,70) FQ(I), TQ(I), AQ(I)
   70 FORMAT(/ 3E15.6)
   15 CONTINUE
      WRITE (6,25)
   25 FORMAT (/10X,5HFREQ.,10X, 7H  REAL   , 7X,7H  IMAG.,10X,7H   ABS
     1      ,/)
      DO 30 I=1,N
      AP(I)=AP(I)*COS(TP(I))-AQ(I)*COS(TQ(I))
      RI(I)=AP(I)*SIN(TP(I))+AQ(I)*SIN(TQ(I))
      RA(I)=SQRT( RR(I)**2 +RI(I)**2)
      WRITE(6,35)  FP(I),AP(I),RI(I),RA(I)
   35 FORMAT (5X,4E15.4)
   30 CONTINUE
  100 CONTINUE
      STOP
      END
```

FIG. 3.12 Computer programme for receptance

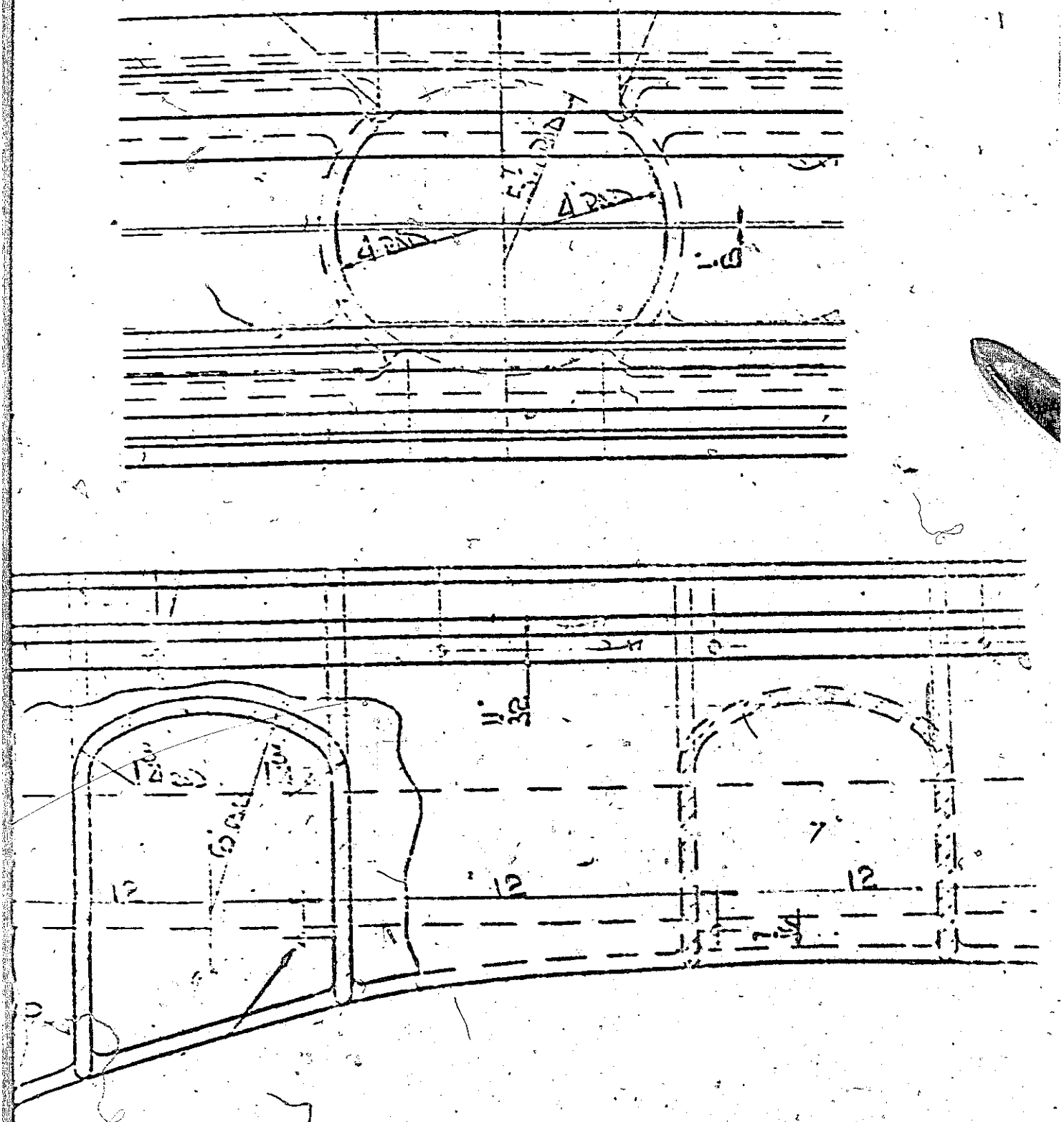

FIG. 3.13, Elliptical cross-ribbing

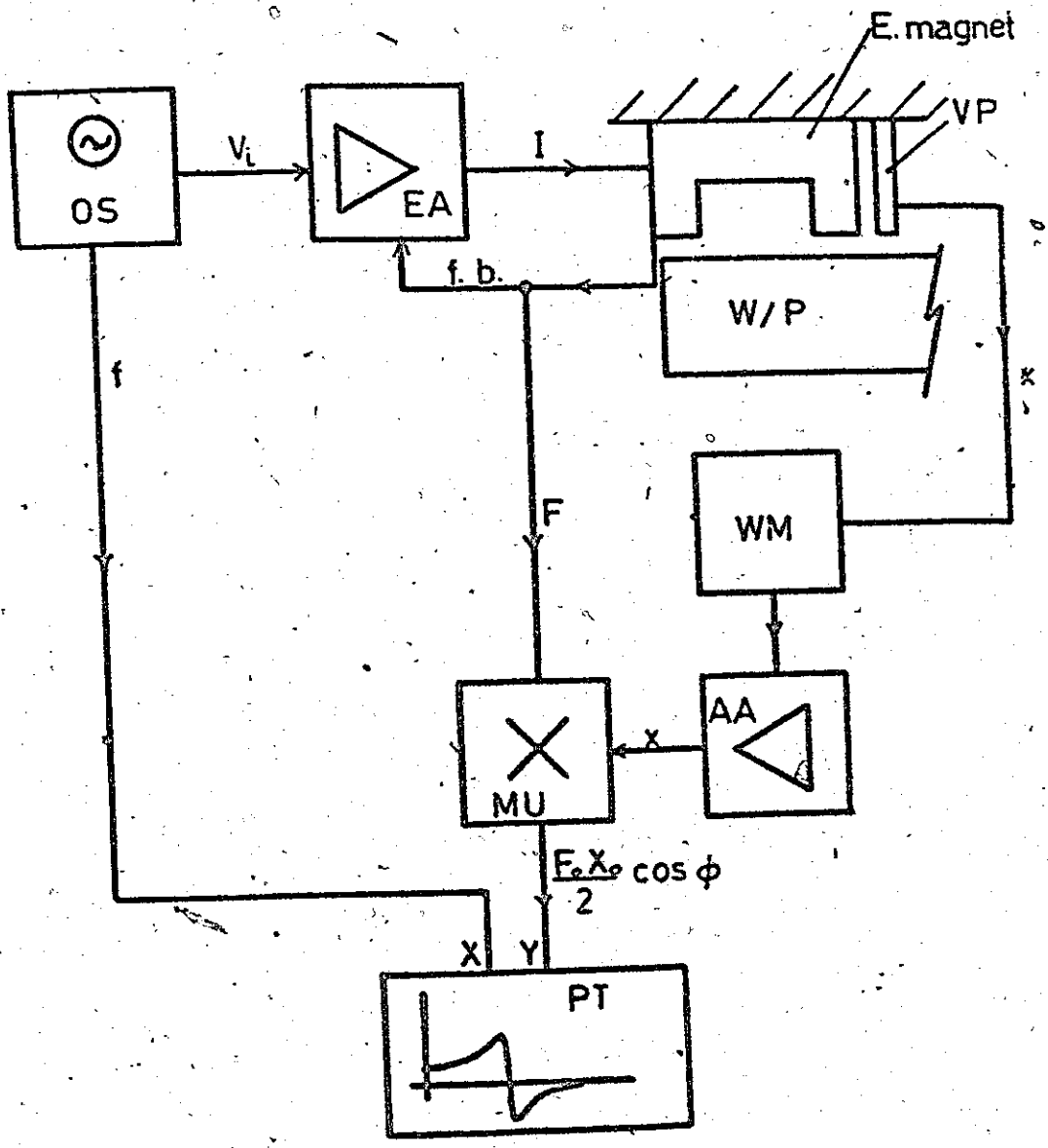

FIG. 3.14 Arrangement of equipment

******* EIGENVALUE SEARCH HAS BEEN COMPLETED *****

THE NUMBER OF EIGENVALUES EXTRACTED = 10.

NUMBER	EIGENVALUE	FREQUENCY(E)	GENERALIZED WEIGHT	FREQUENCY(F)
1	.2969387?E+03	.5?710343?1E+02	.3920977?E+03	53.9103
2	.37A30660E+03	.6?A5483915E+02	.28462734E+03	60.8548
3	.5917?A?4E+03	.7610591441E+02	.26211?88E+03	76.1039
4	.?727?17?E+03	.81142?9795E+02	.5596?961E+03	91.1428
5	.?7345?17E+03	.9761063902E+02	.17777?32E+03	97.6136
6	.14276?22E+04	.1182?46536E+03	.11616269E+03	118.2037
7	.1645?342E+04	.1269?892?1E+03	.15677217E+03	126.9049
8	.?2294222E+04	.1477317?43E+03	.79265277E+02	147.7317
9	.?3573643E+04	.1518980133E+03	.15?82139E+03	151.8990
10	.?6422734E+04	.1609153??8E+03	.6710?998E+02	160.8154

FIG. 3.15 First ten eigenvalues for Colchester Lathe

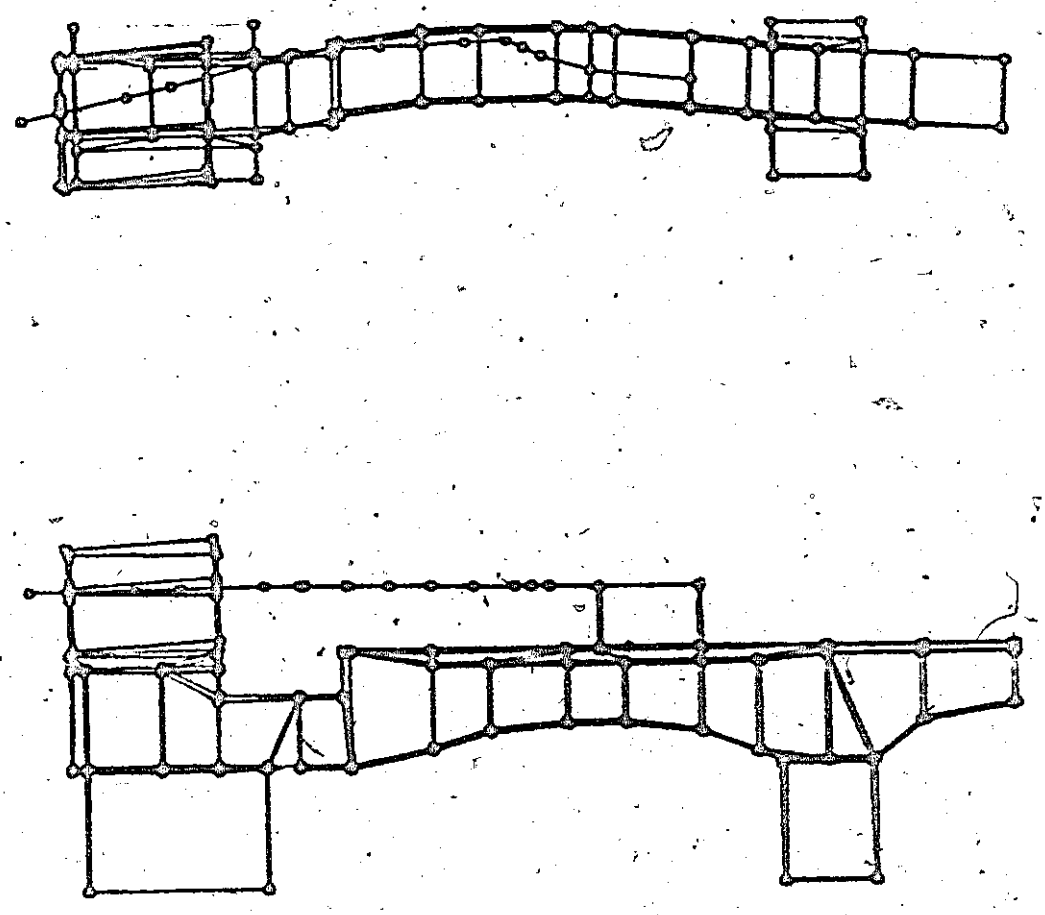

FIG. 3.16 1st Mode 53.9 Hz

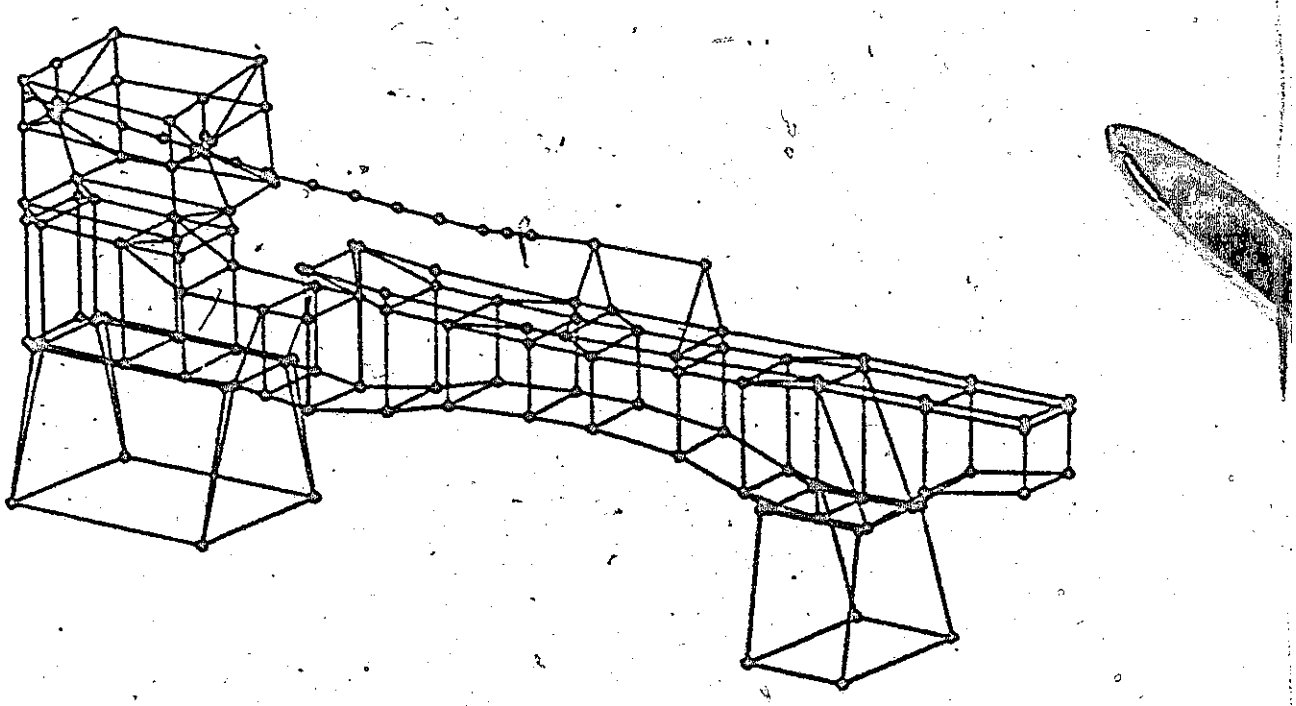

FIG. 3.17 1st Mode 53.9 Hz

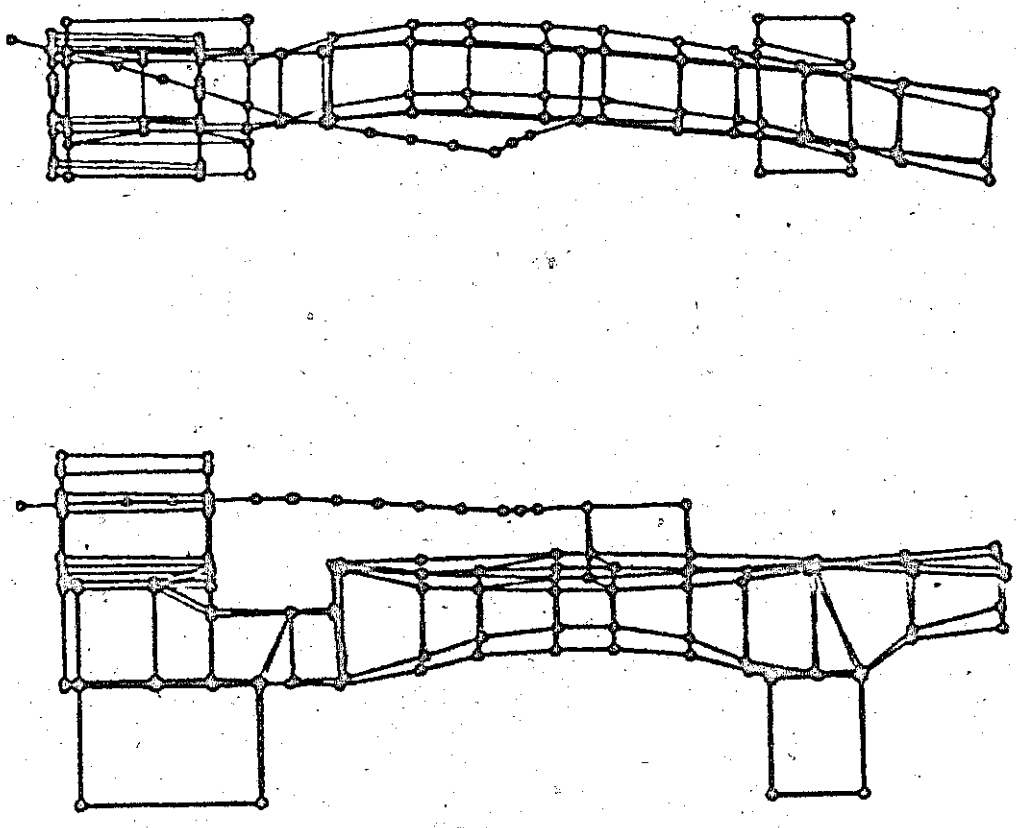

FIG. 3.18 5th Mode 97.6 Hz

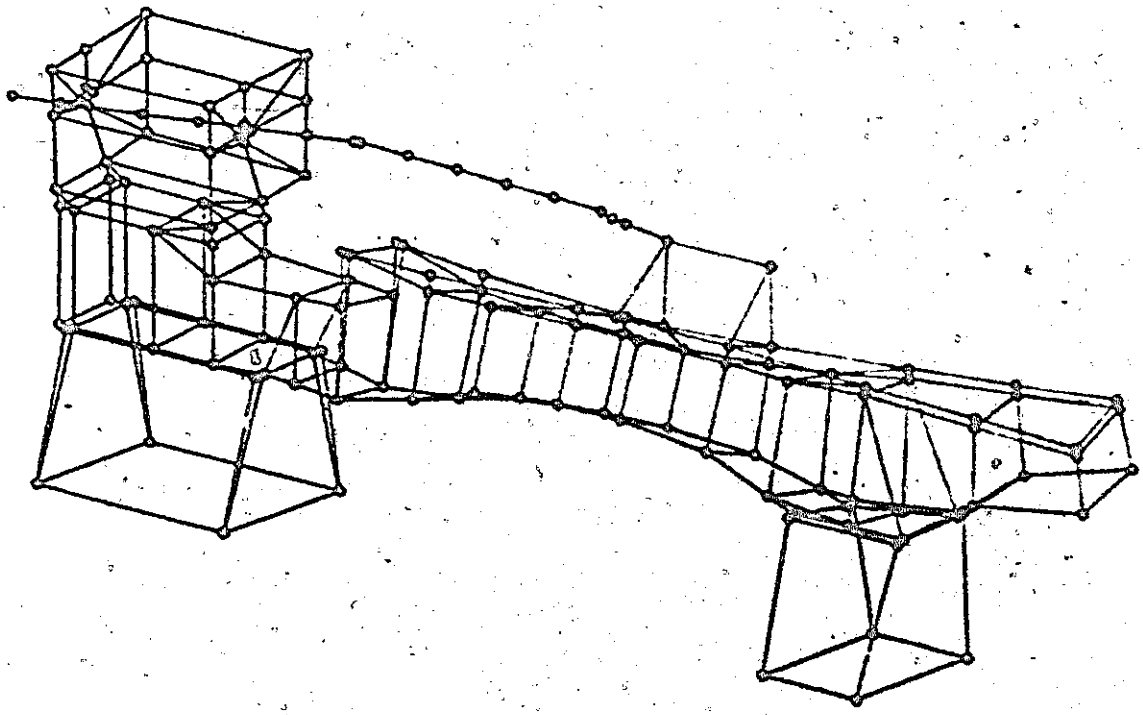

FIG. 3.19 5th Mode 97.6 Hz.

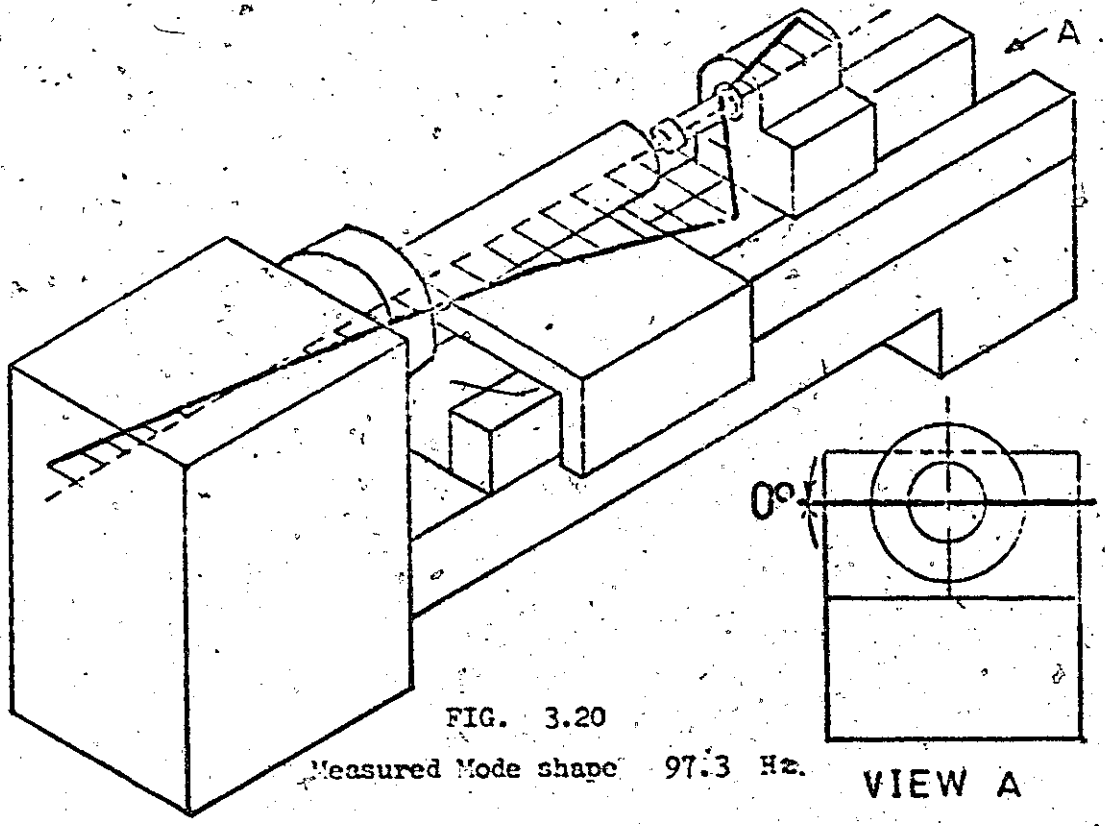

FIG. 3.20

Measured Mode shape 97.3 Hz.

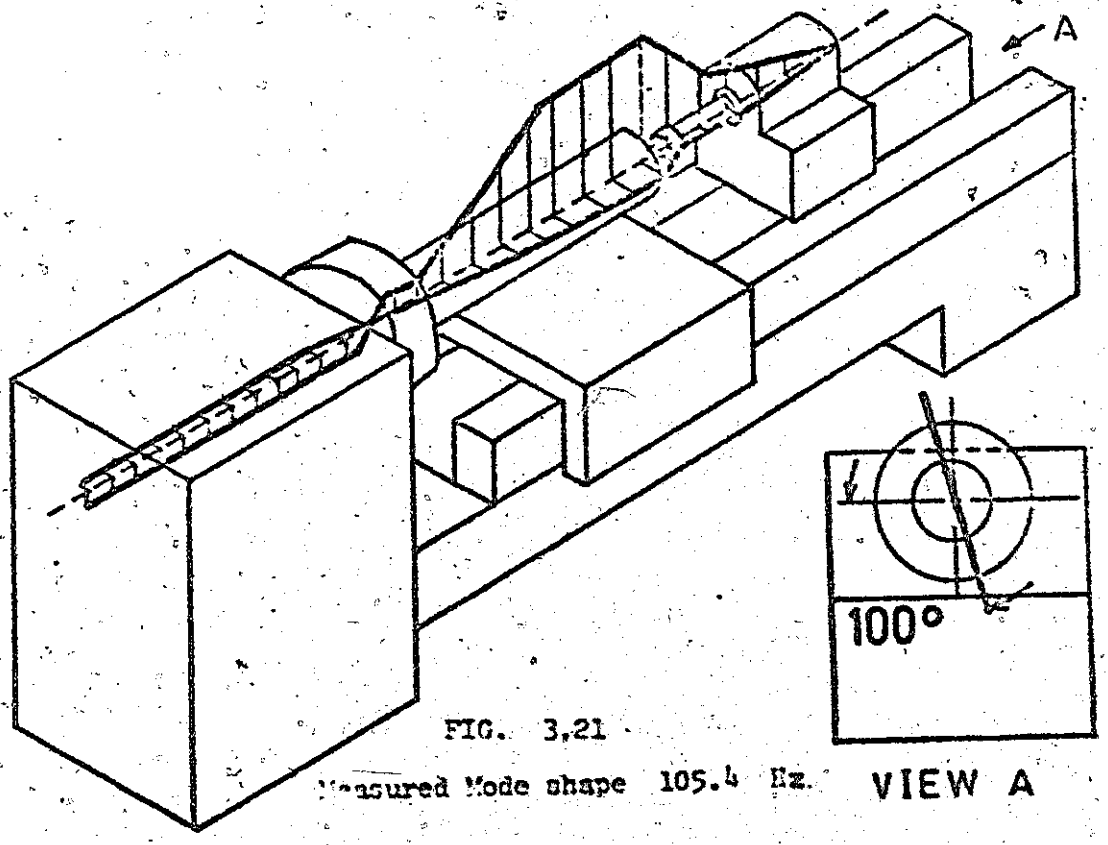

FIG. 3.21

Measured Mode shape 105.4 Hz.

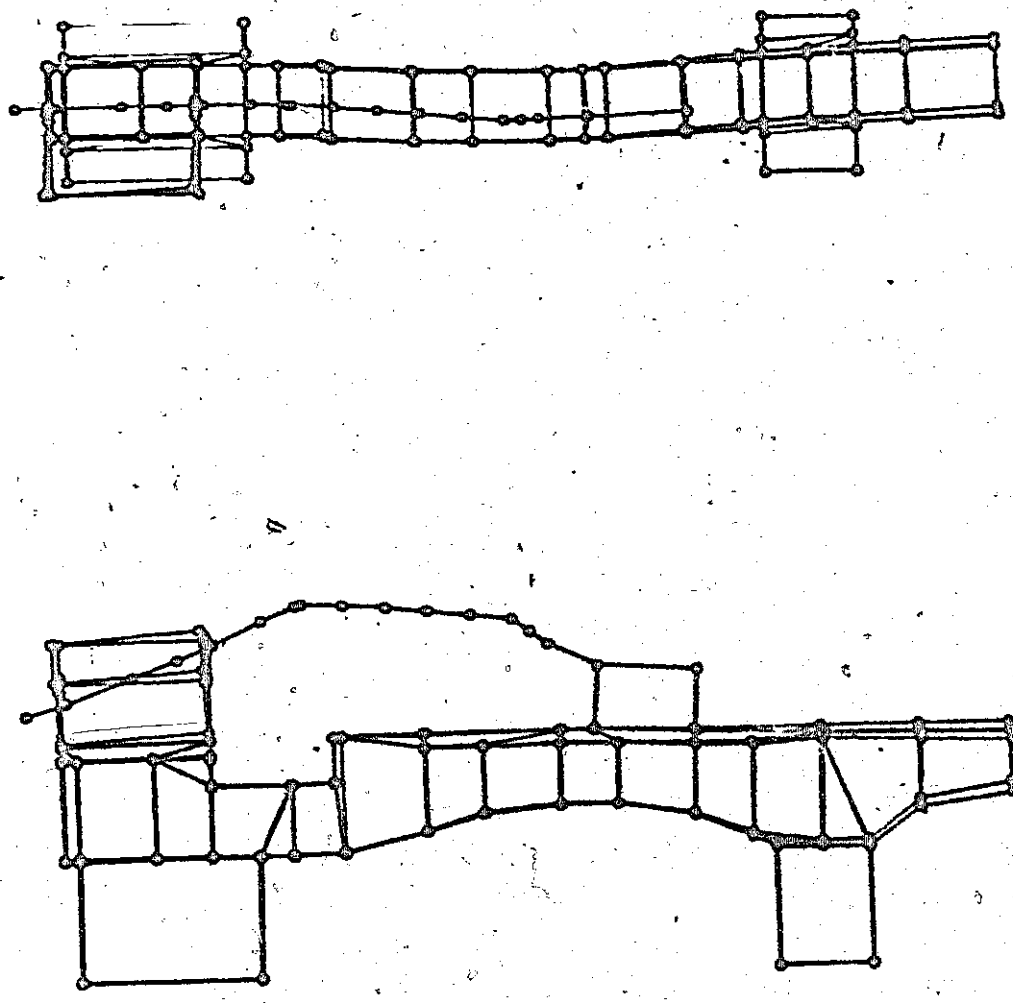

FIG. 3.22 3rd Mode 76.1 Hz

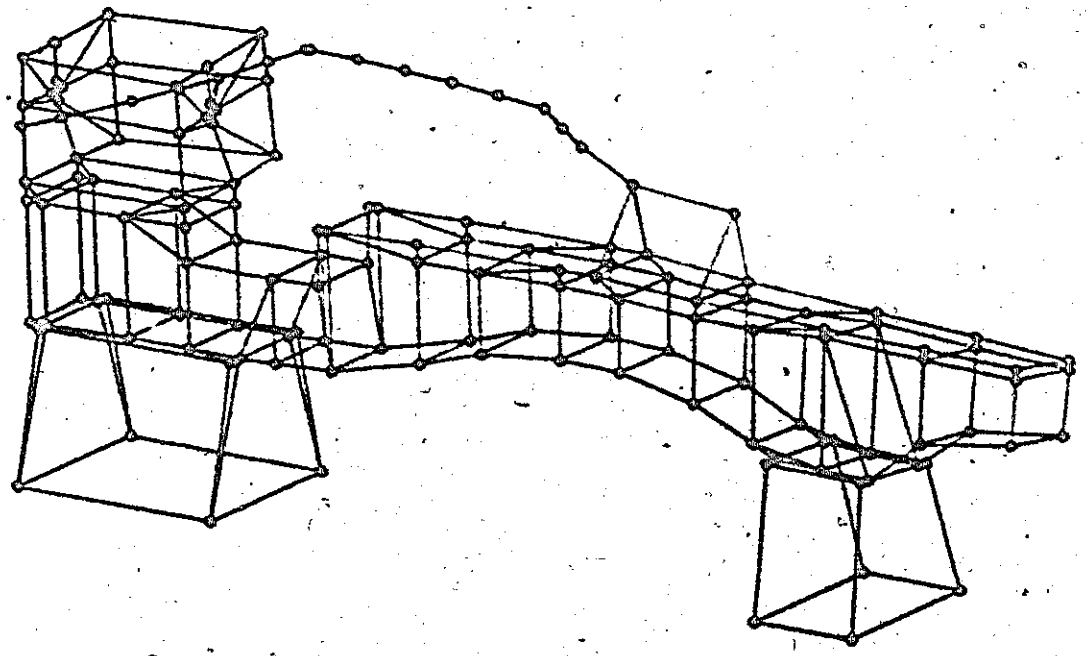

FIG. 3.23 3rd Mode 76.1 Π

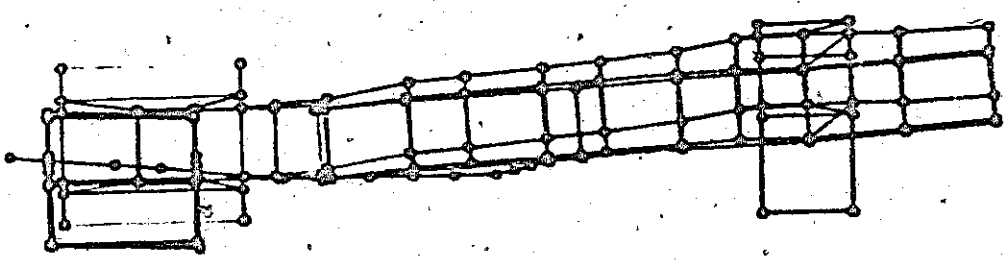

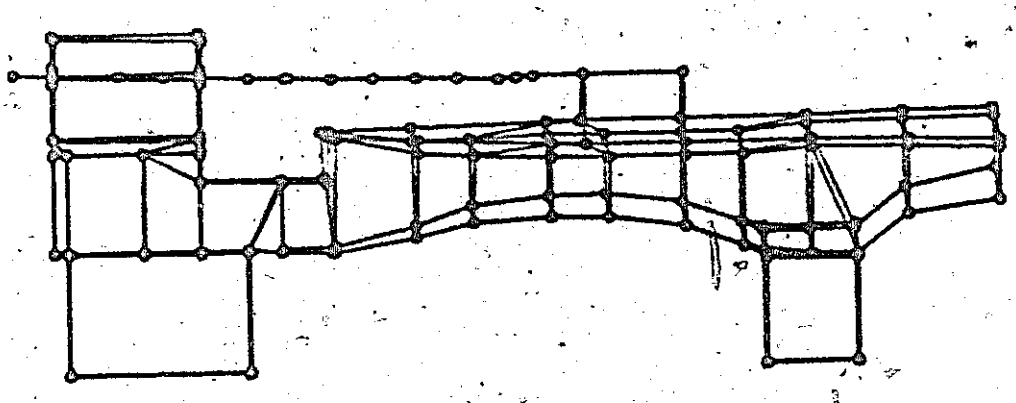

FIG. 3.24 2nd Mode 60.8 Hz.

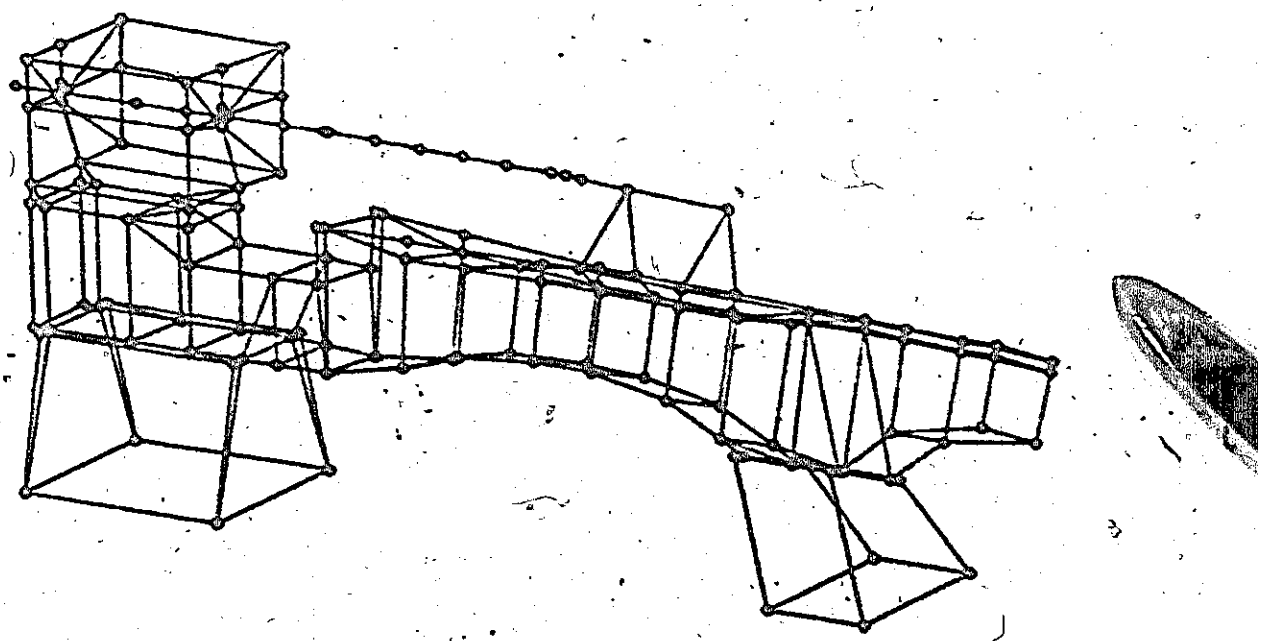

FIG. 3.25 2nd Mode 60.8 Hz.

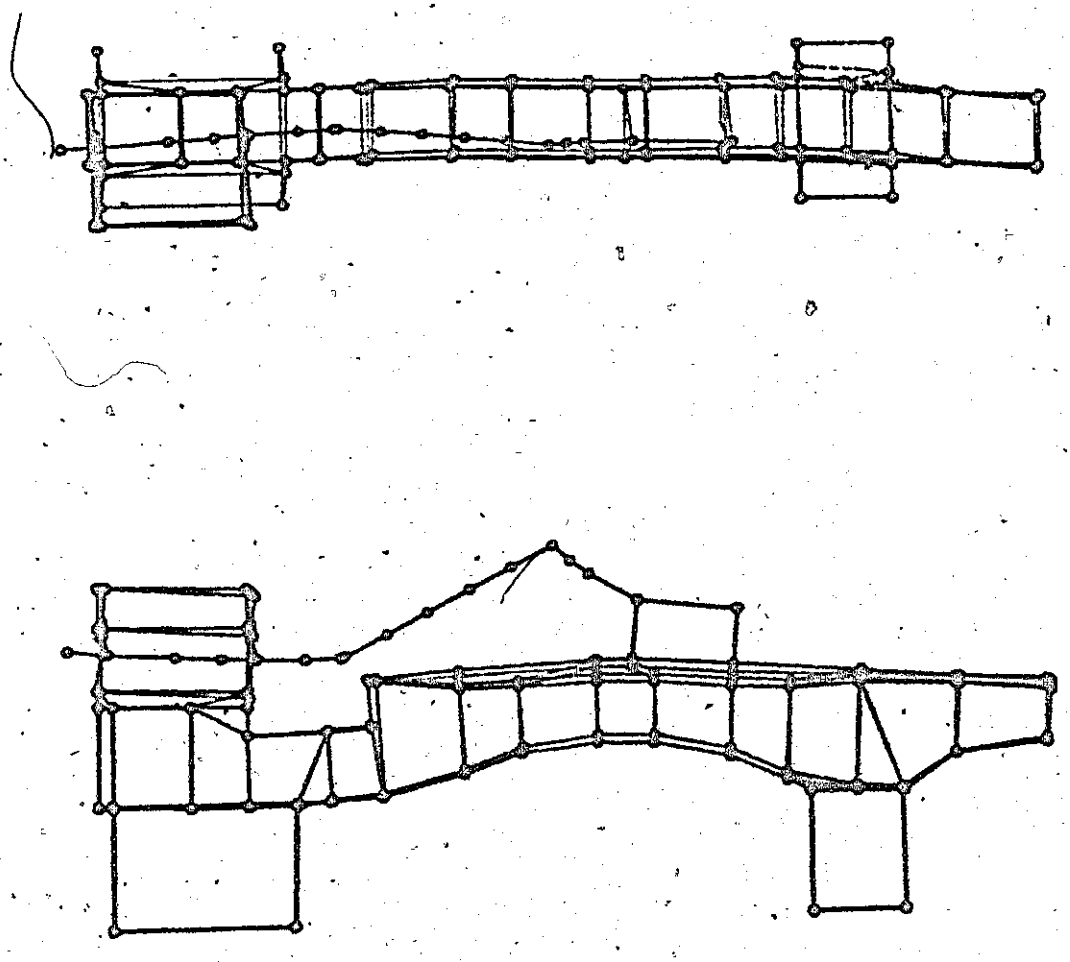

FIG. 3.26 7^{th} Mode 126.9 Hz.

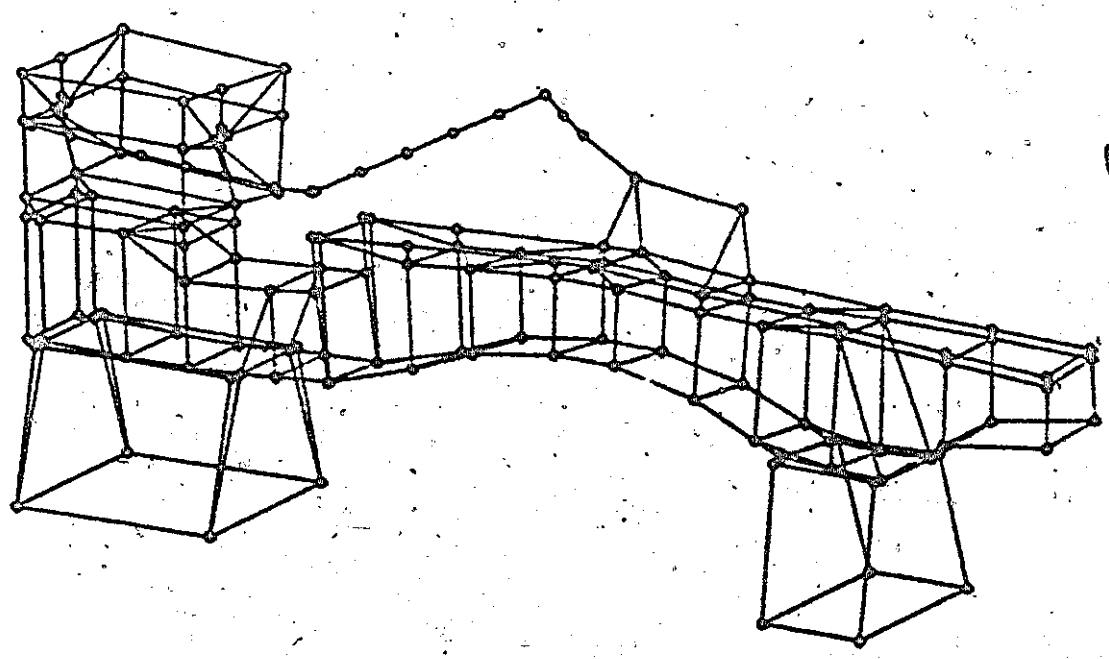

FIG. 3.27 7^{th} Mode 126.9 Hz.

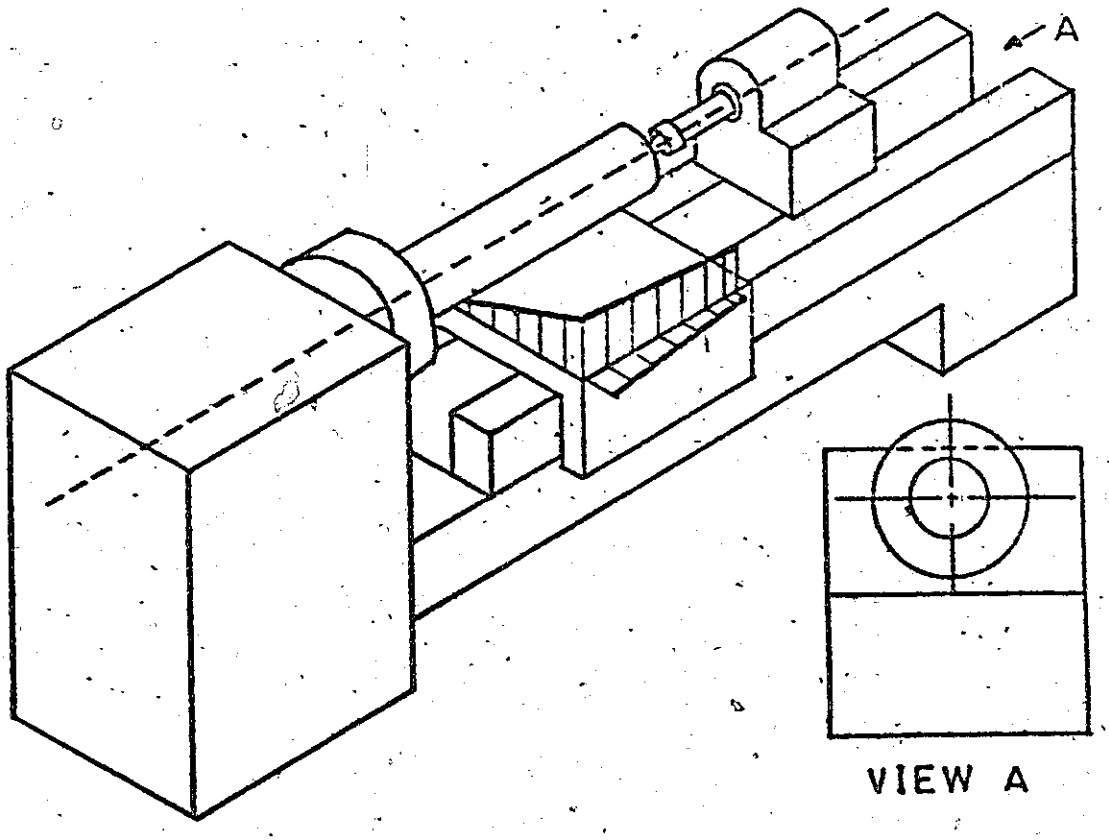

FIG. 3.28 Measured Mode Shape 140 Hz

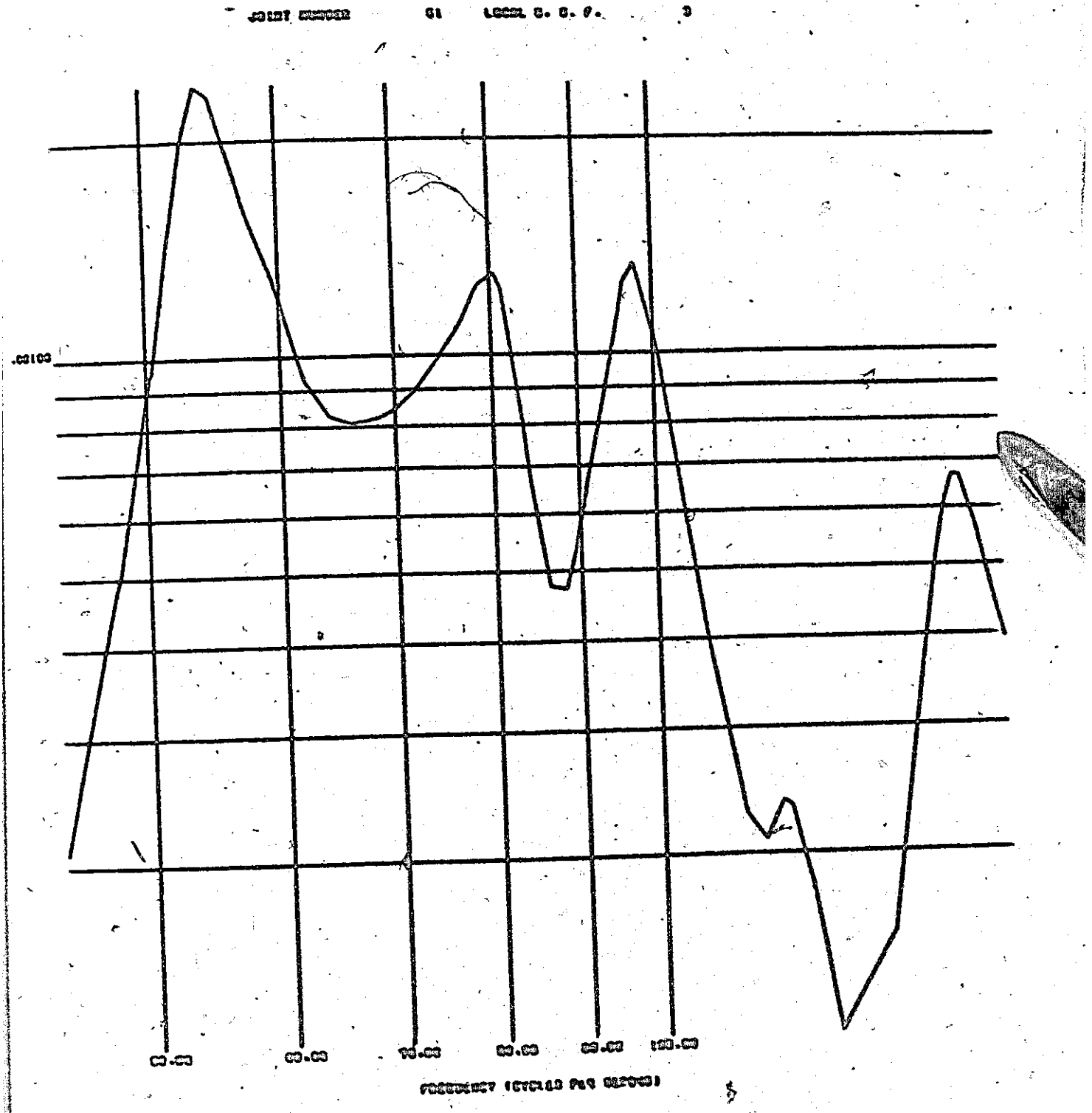

FIG. 3.29 Dynamic Response - Tool Horizontal

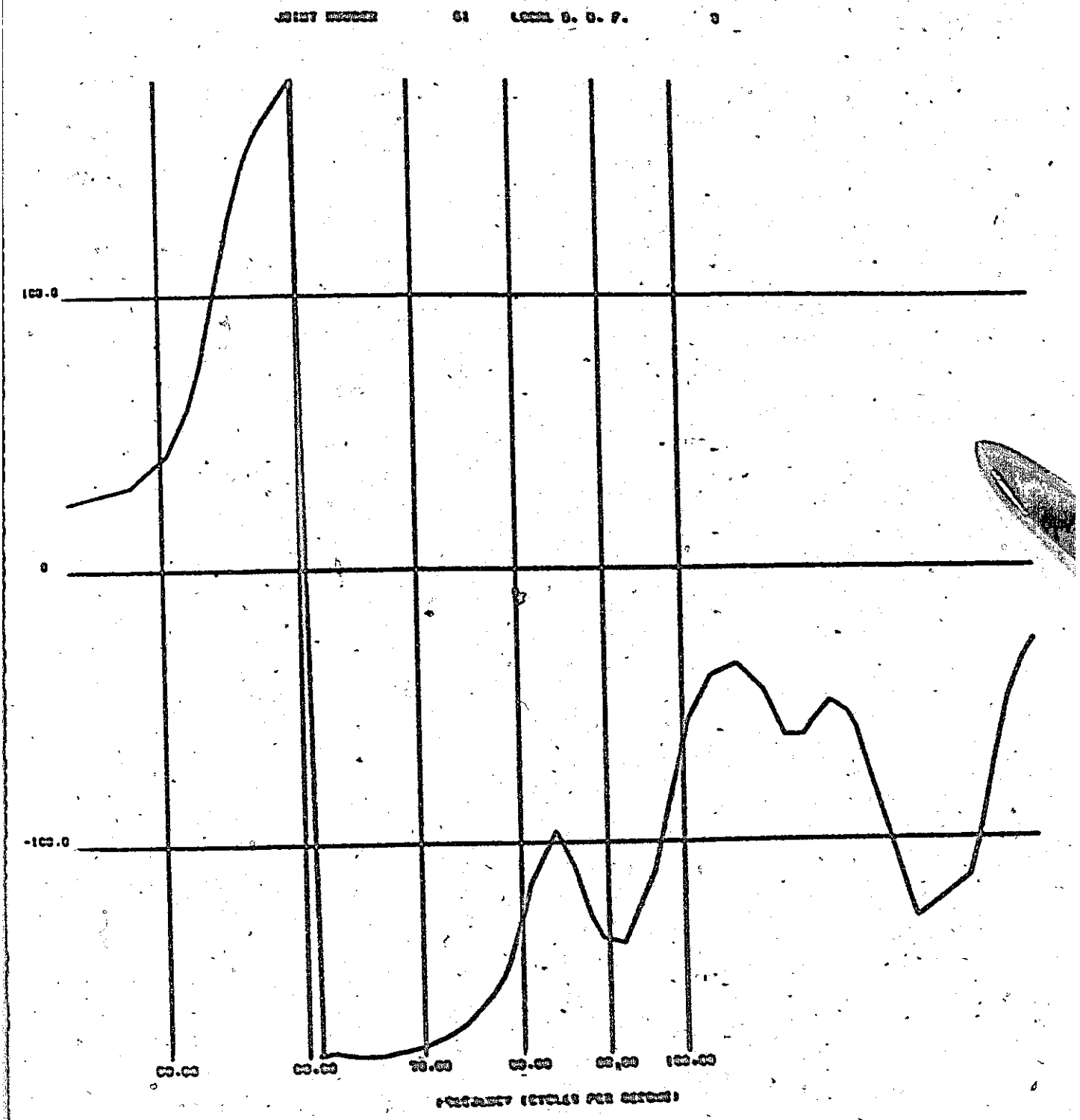

FIG. 3.30 Phase Shift - Tool Horizontal

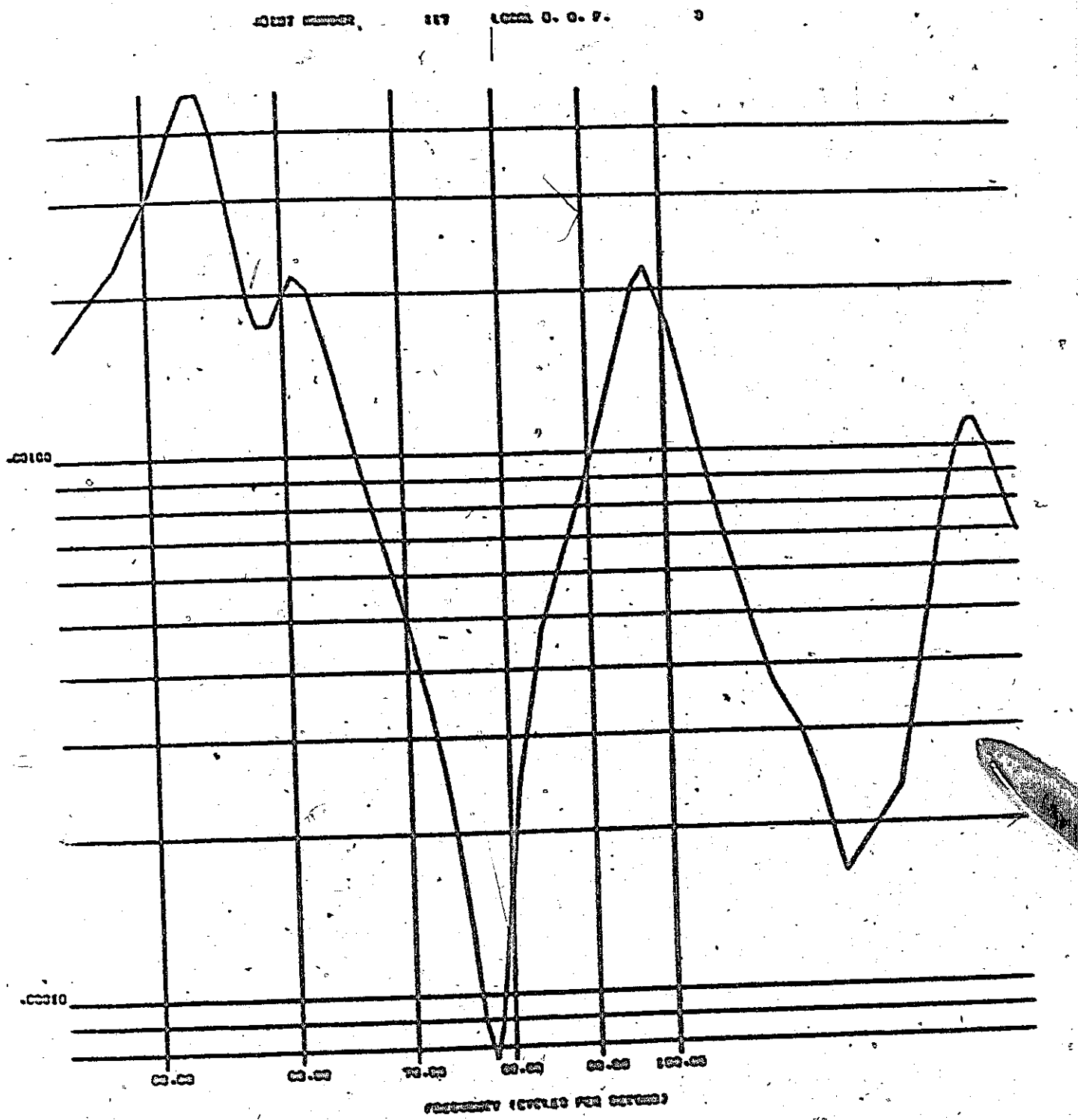

FIG. 3.31 Dynamic Response - Workpiece Horizontal

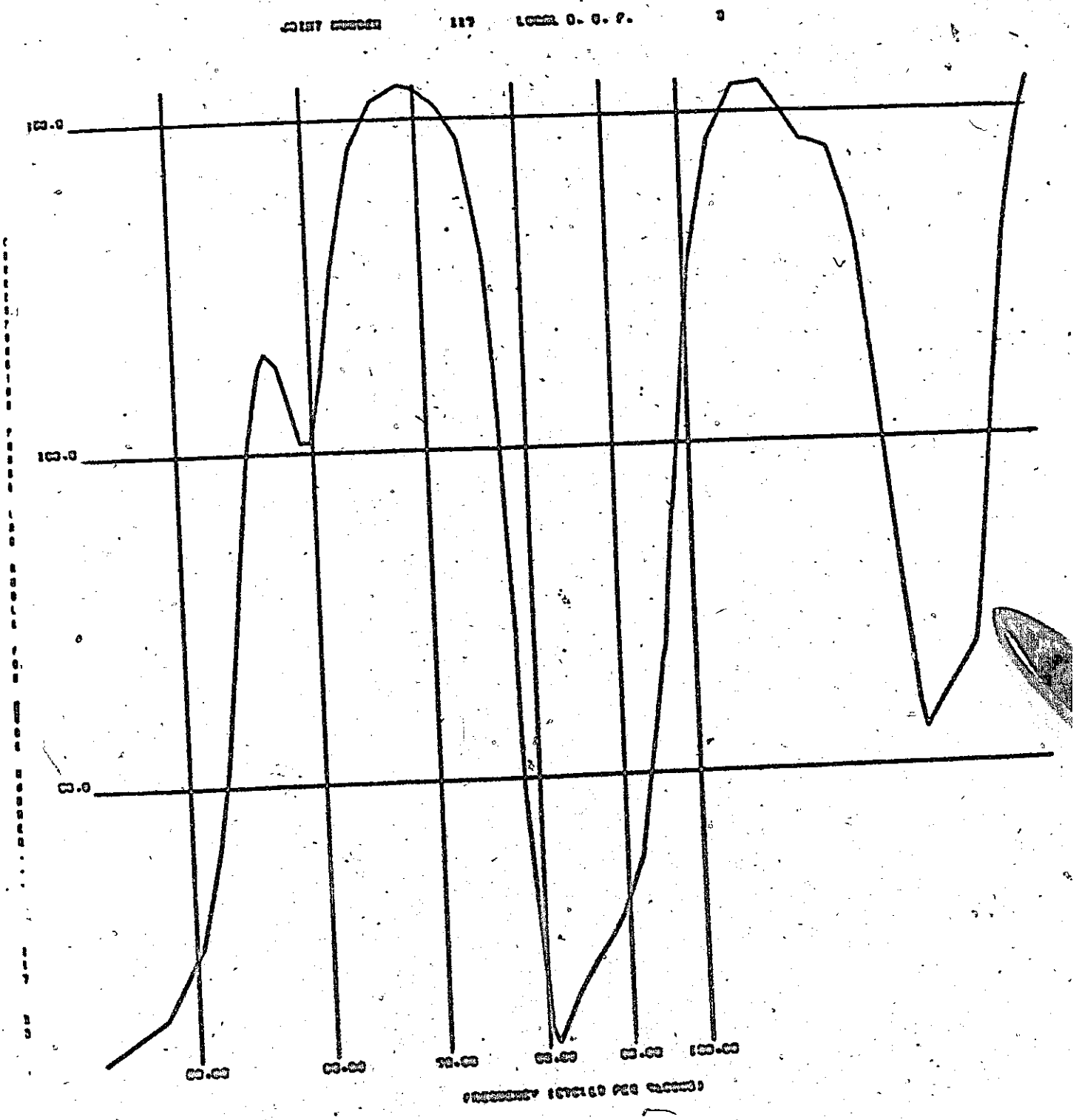

FIG. 3.32 Phase Shift - Workpiece Horizontal

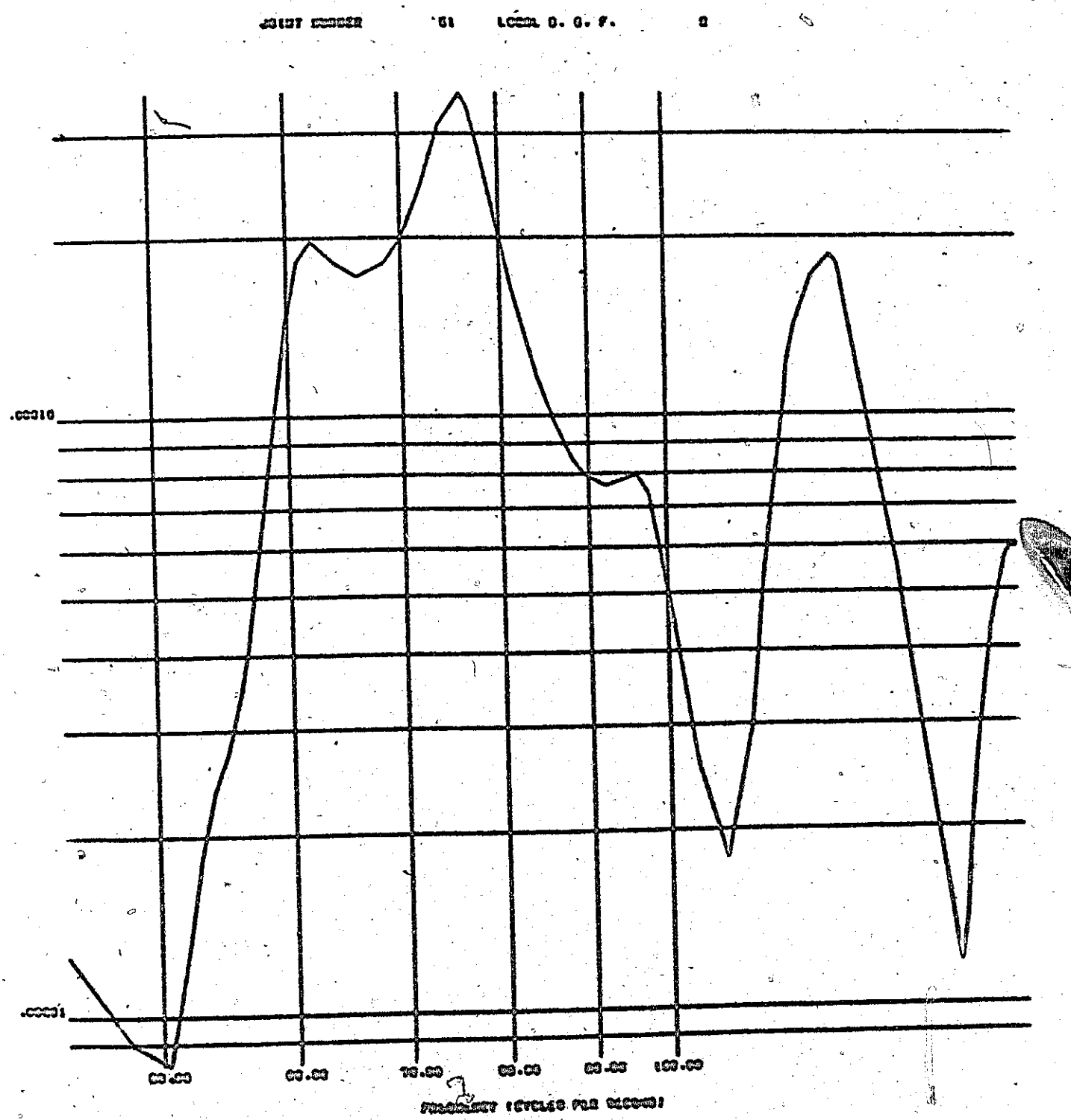

FIG. 3.33 Dynamic Response - Tool Vertical

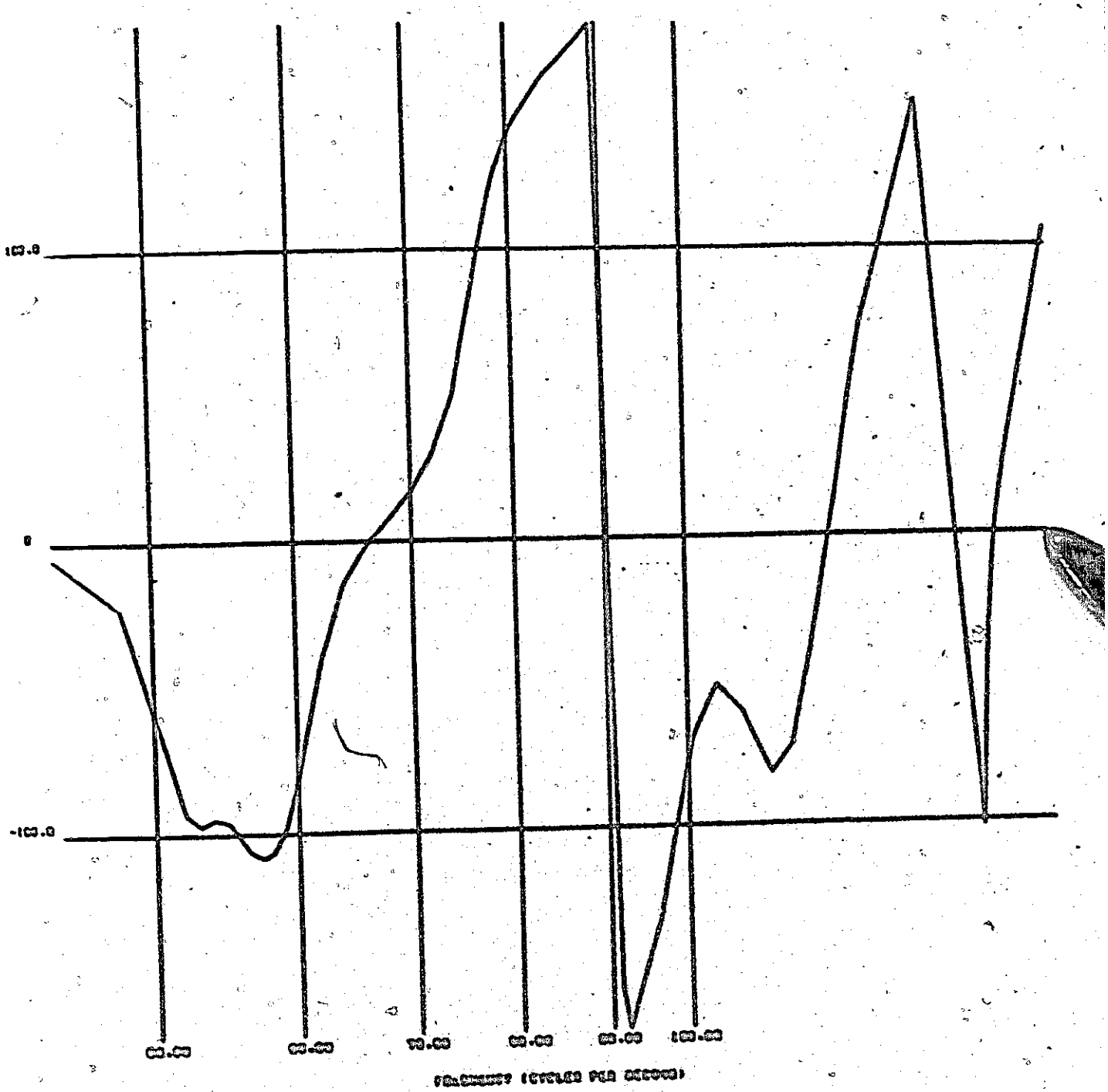

FIG. 3.34 Phase Shift - Tool Vertical

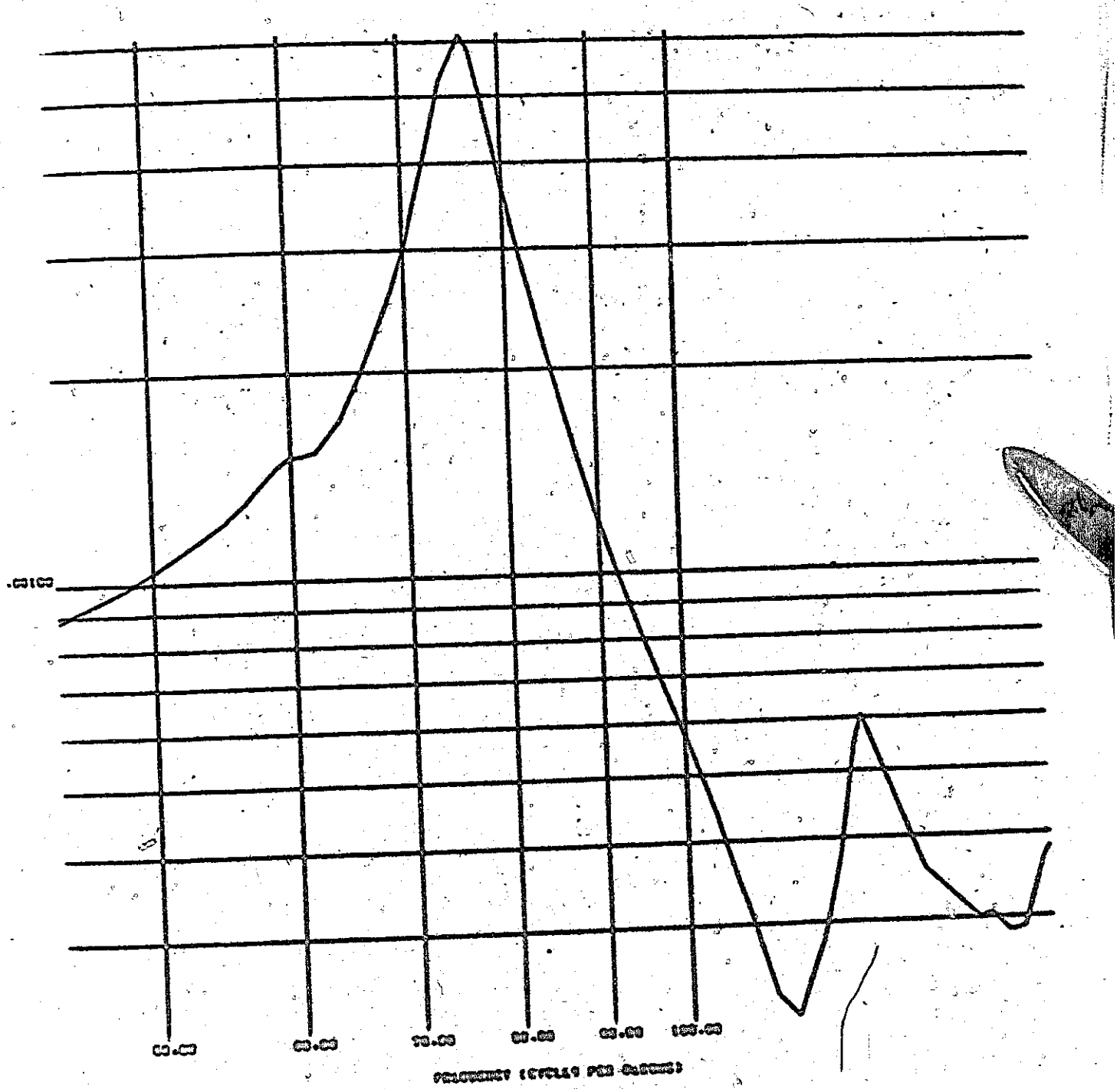

FIG. 3.35 Dynamic Response - Workpiece, Vertical

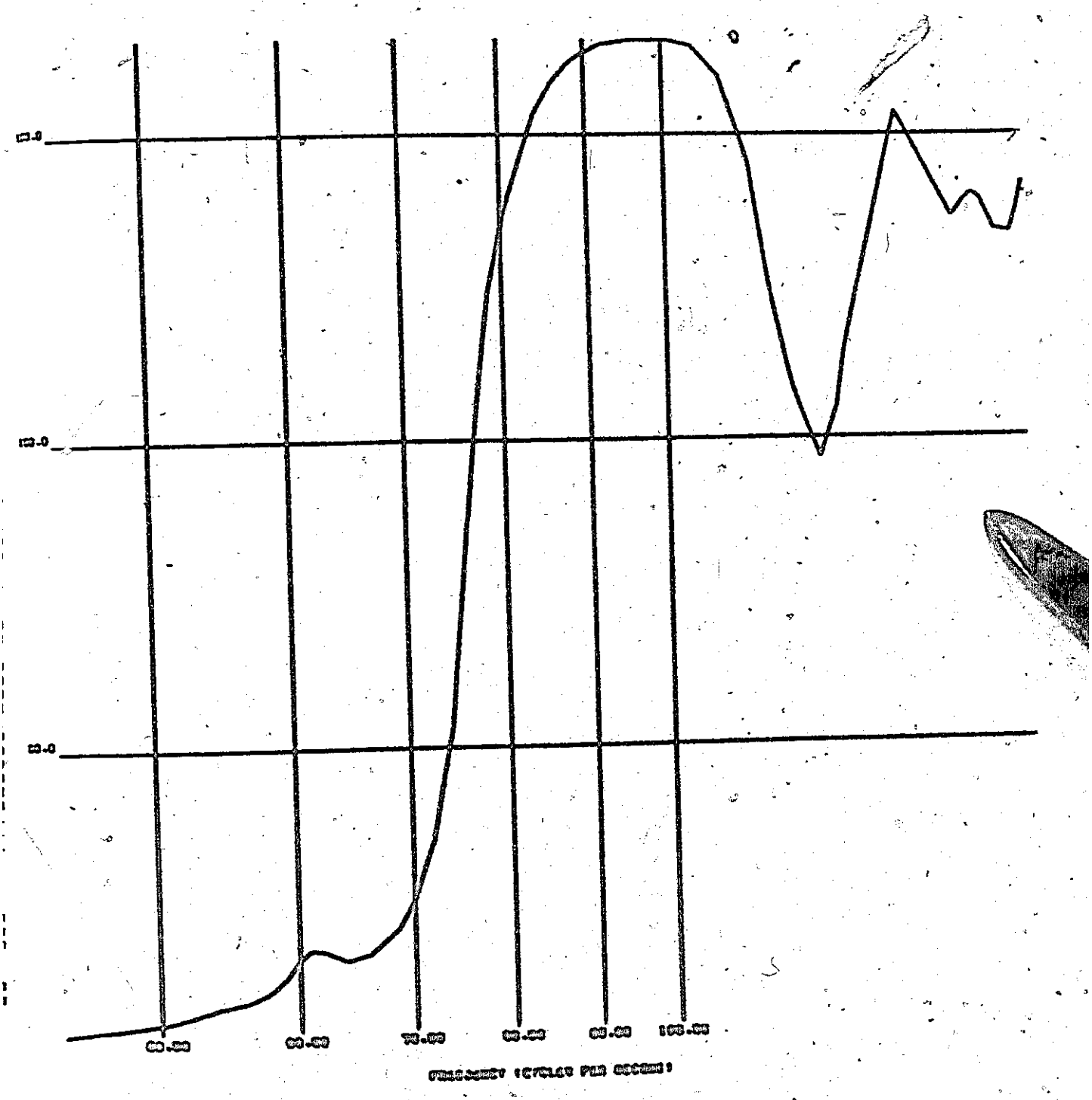

FIG. 3.36 Phase Shift - Workpiece Vertical

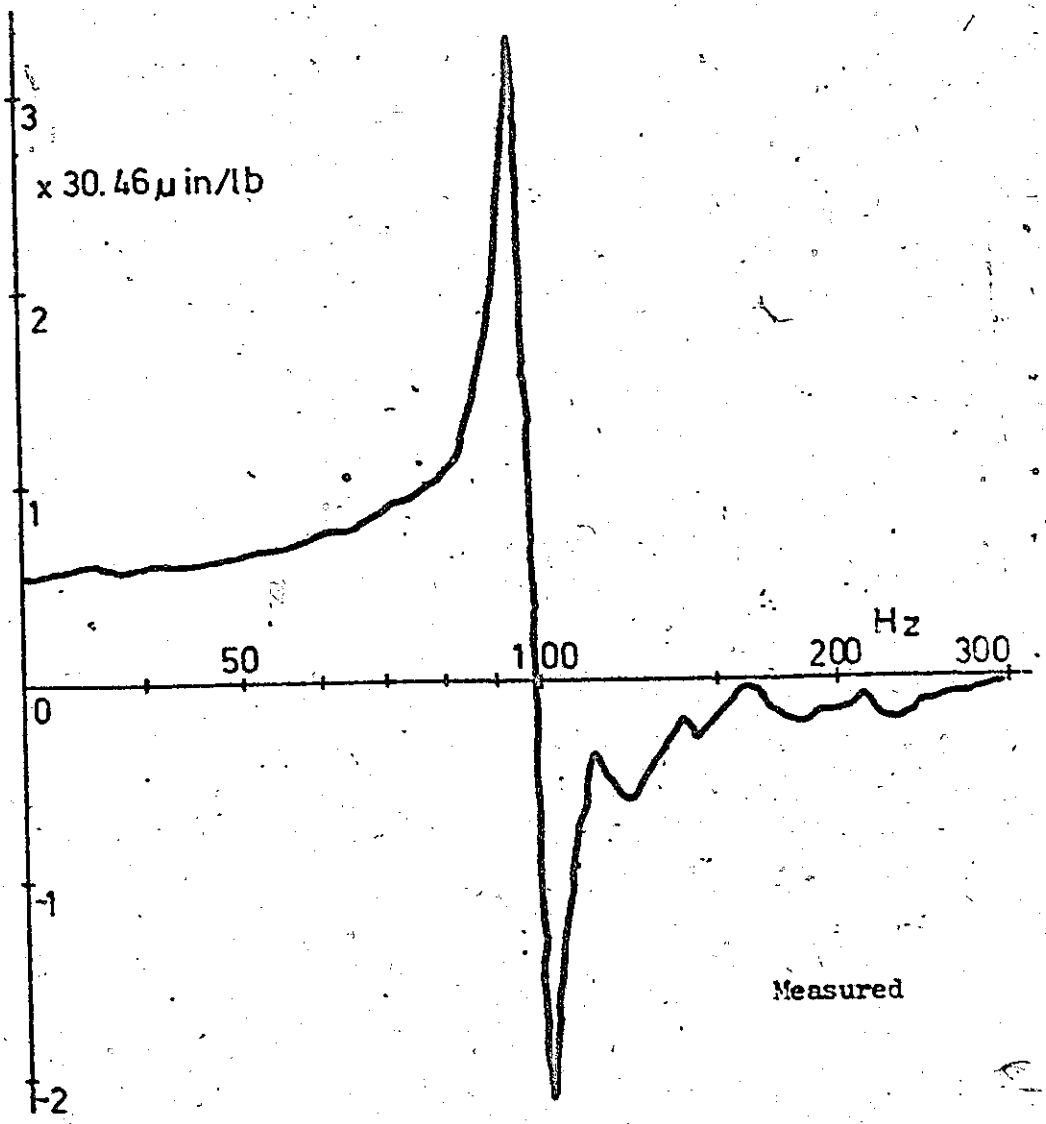

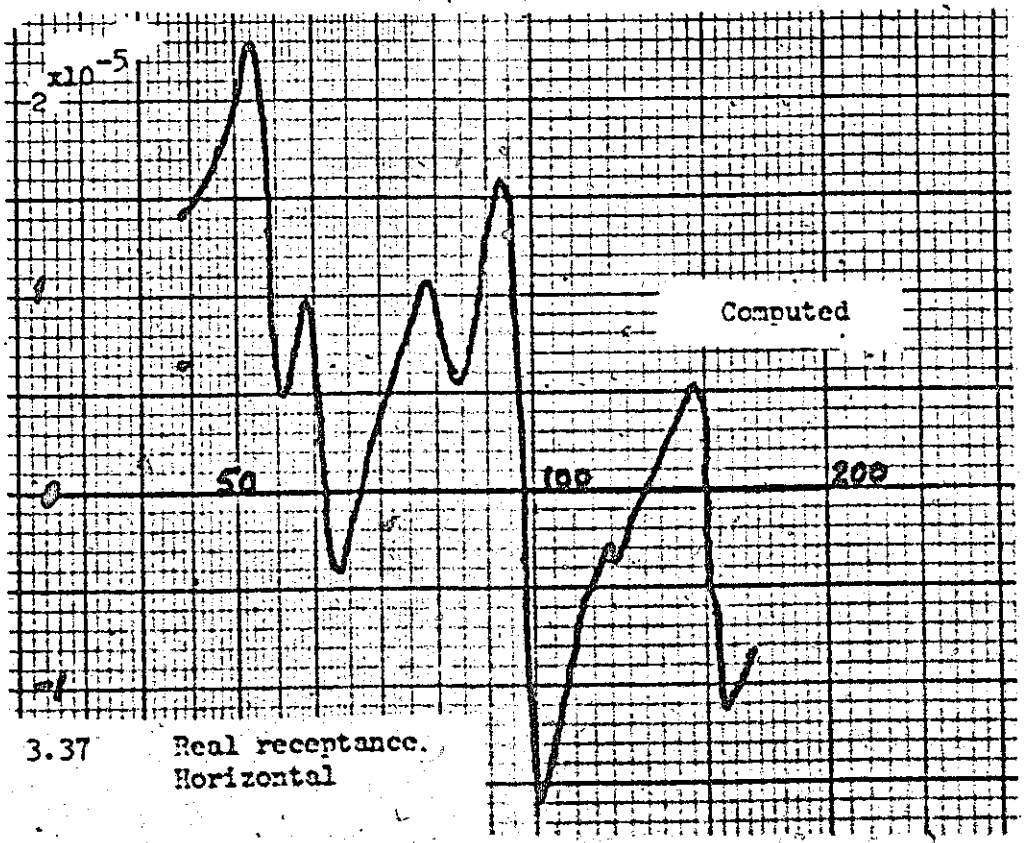

FIG. 3.37 Real receptance. Horizontal

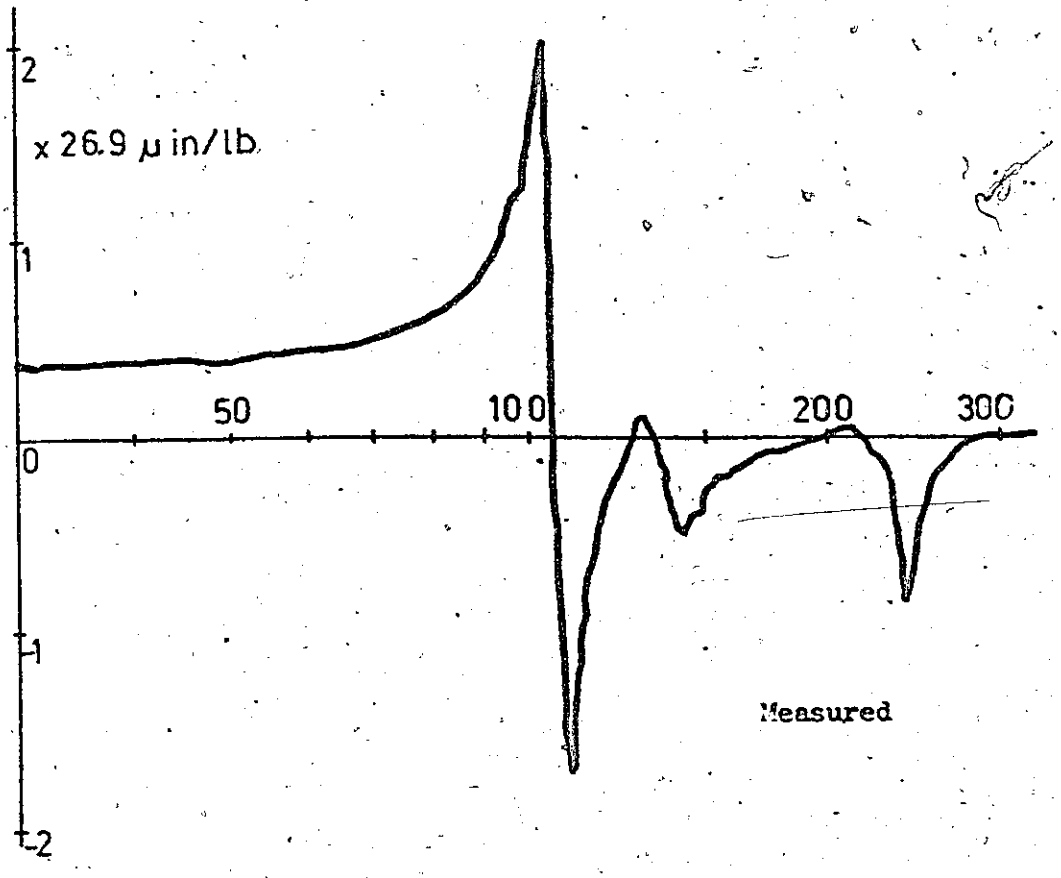

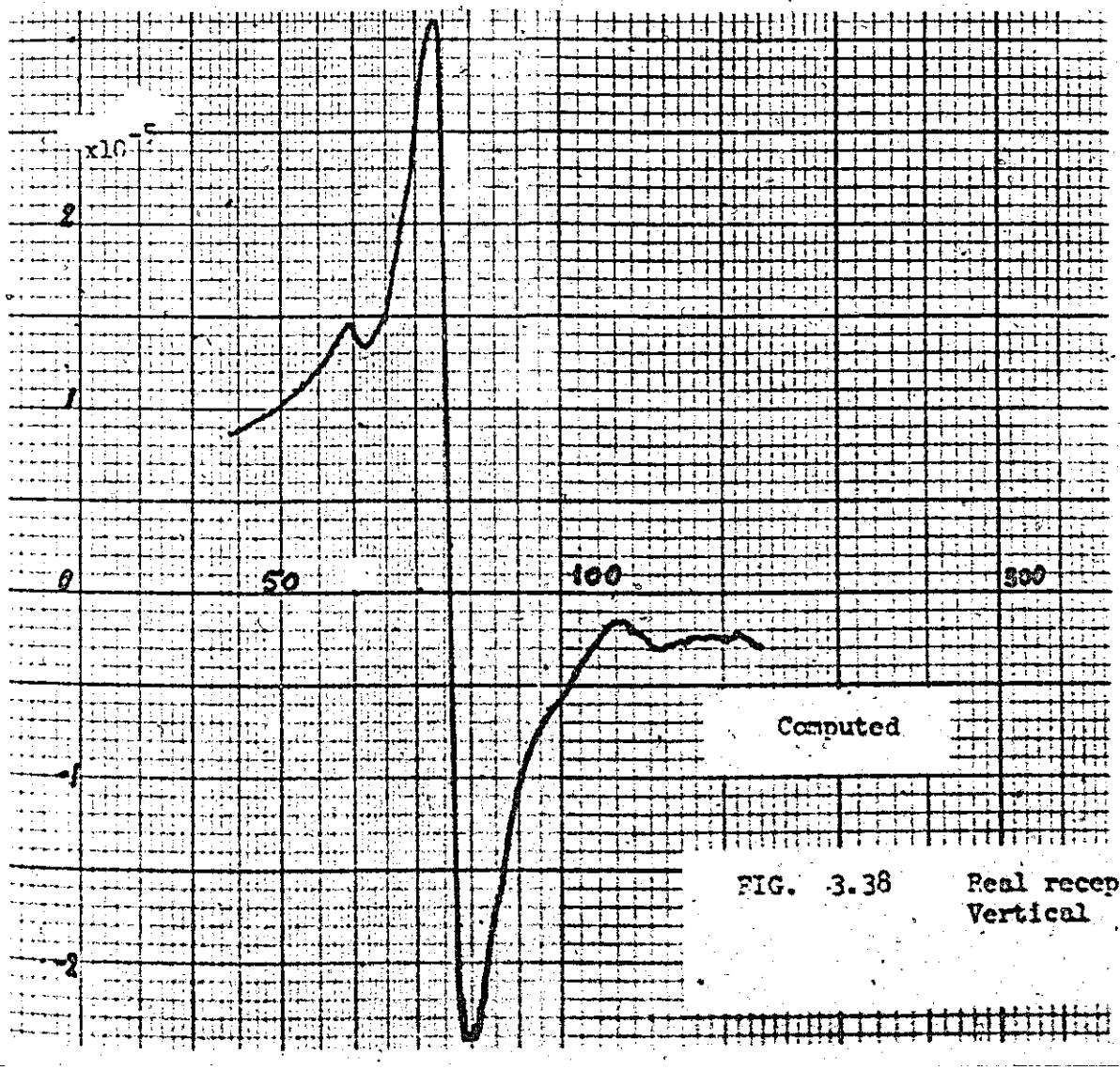

FIG. 3.38 Real receptance Vertical

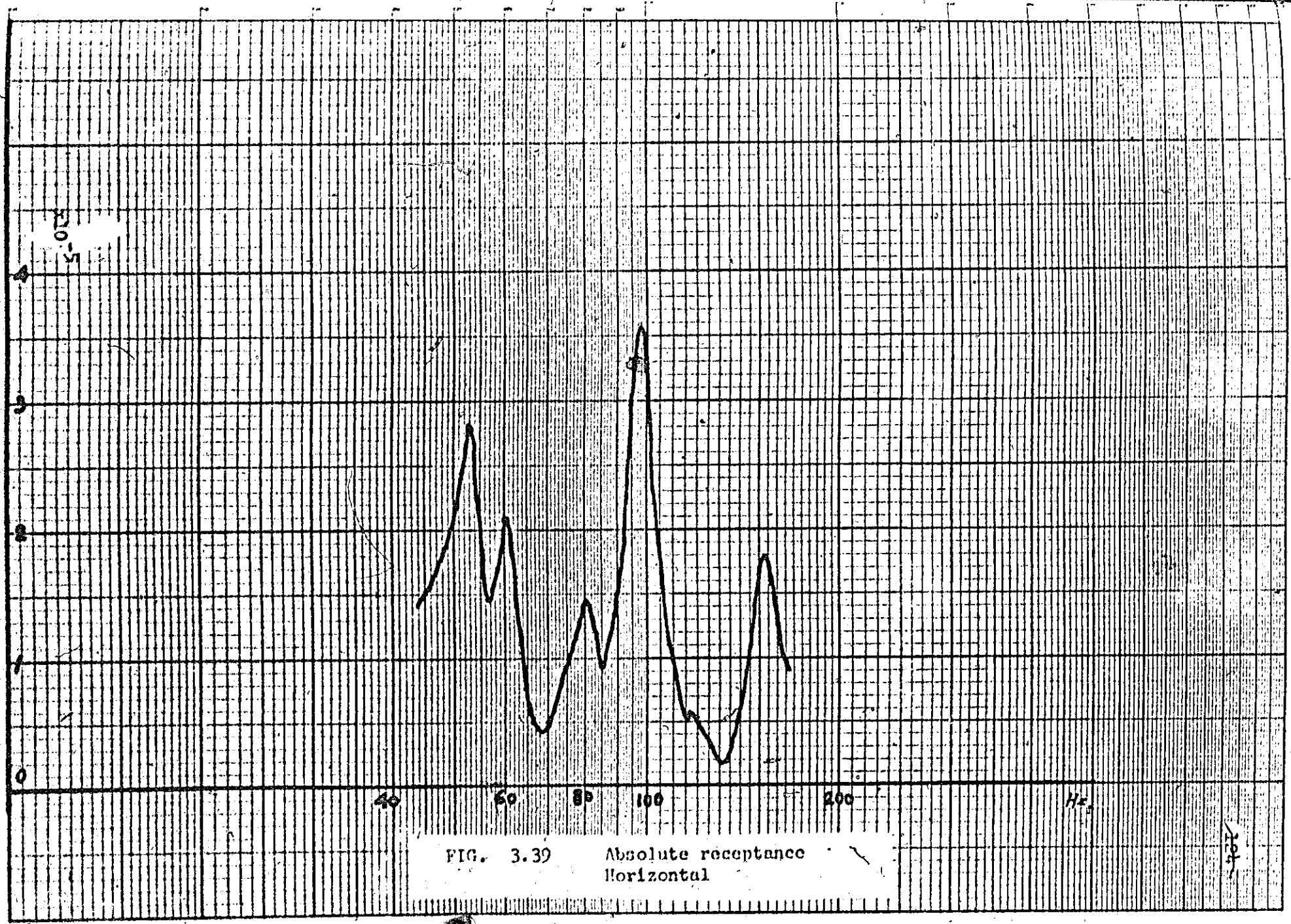

FIG. 3.39 Absolute receptance
Horizontal

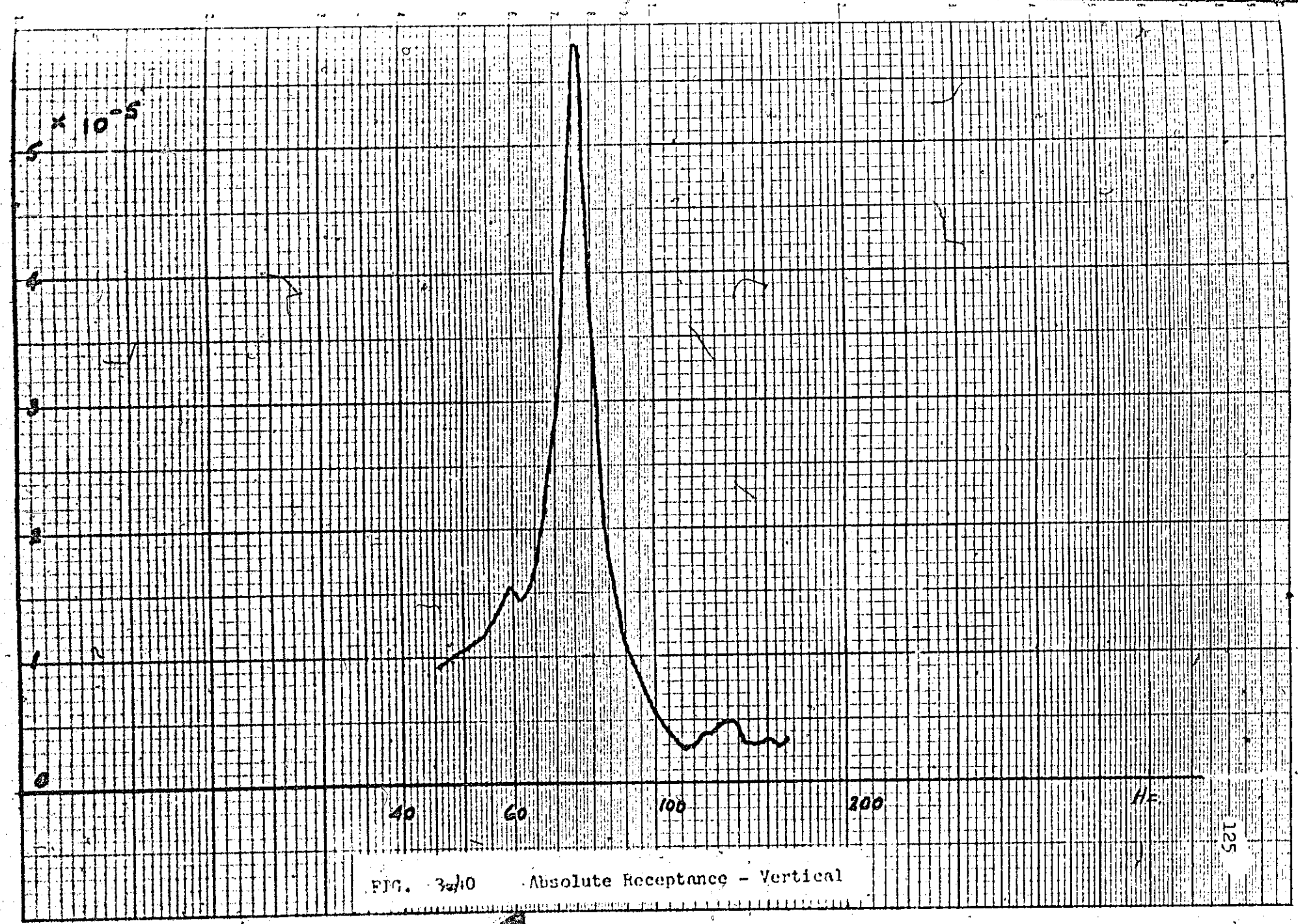

FIG. 3.10 Absolute Receptance - Vertical

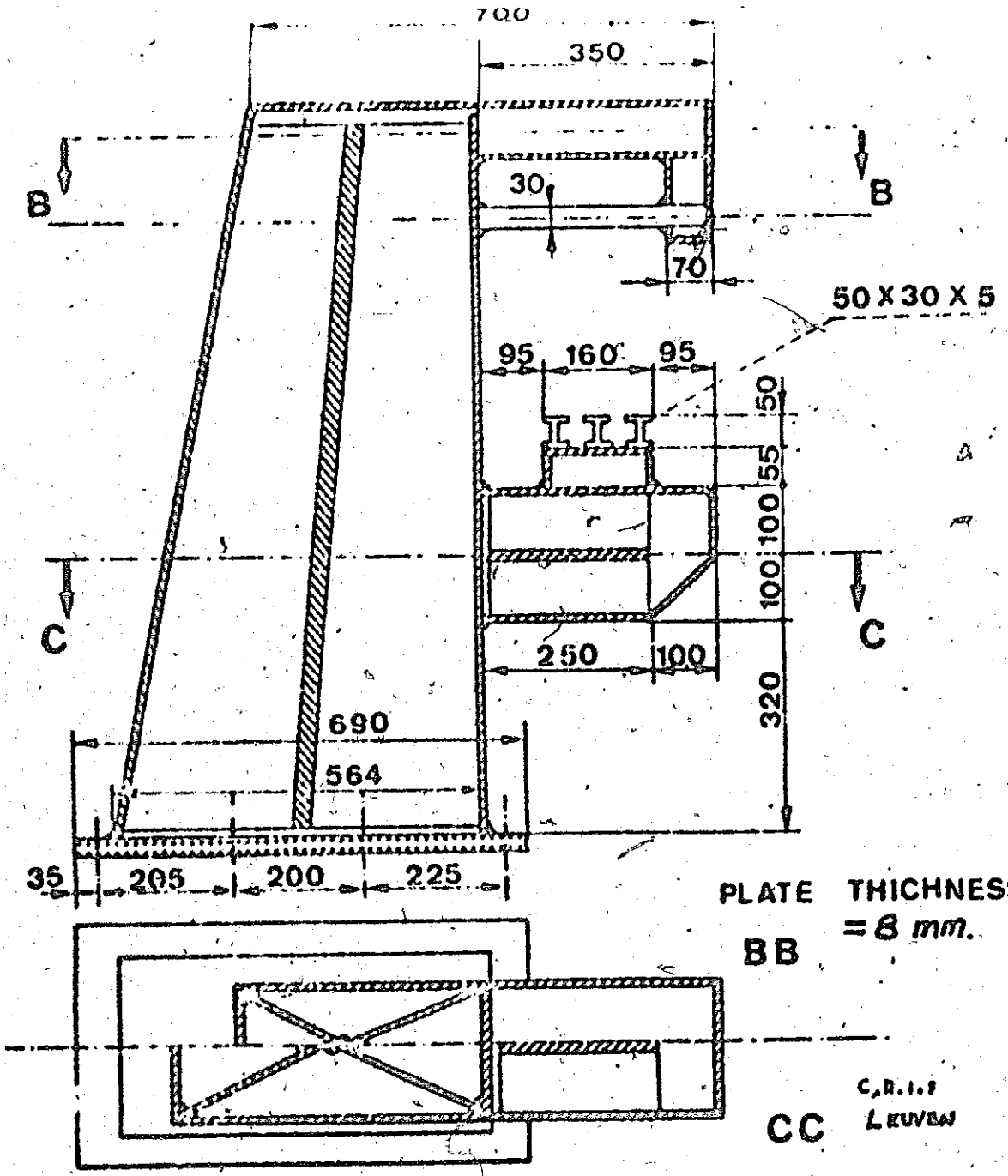

Fig. 4.1 C.I.R.P. Model Milling M/C

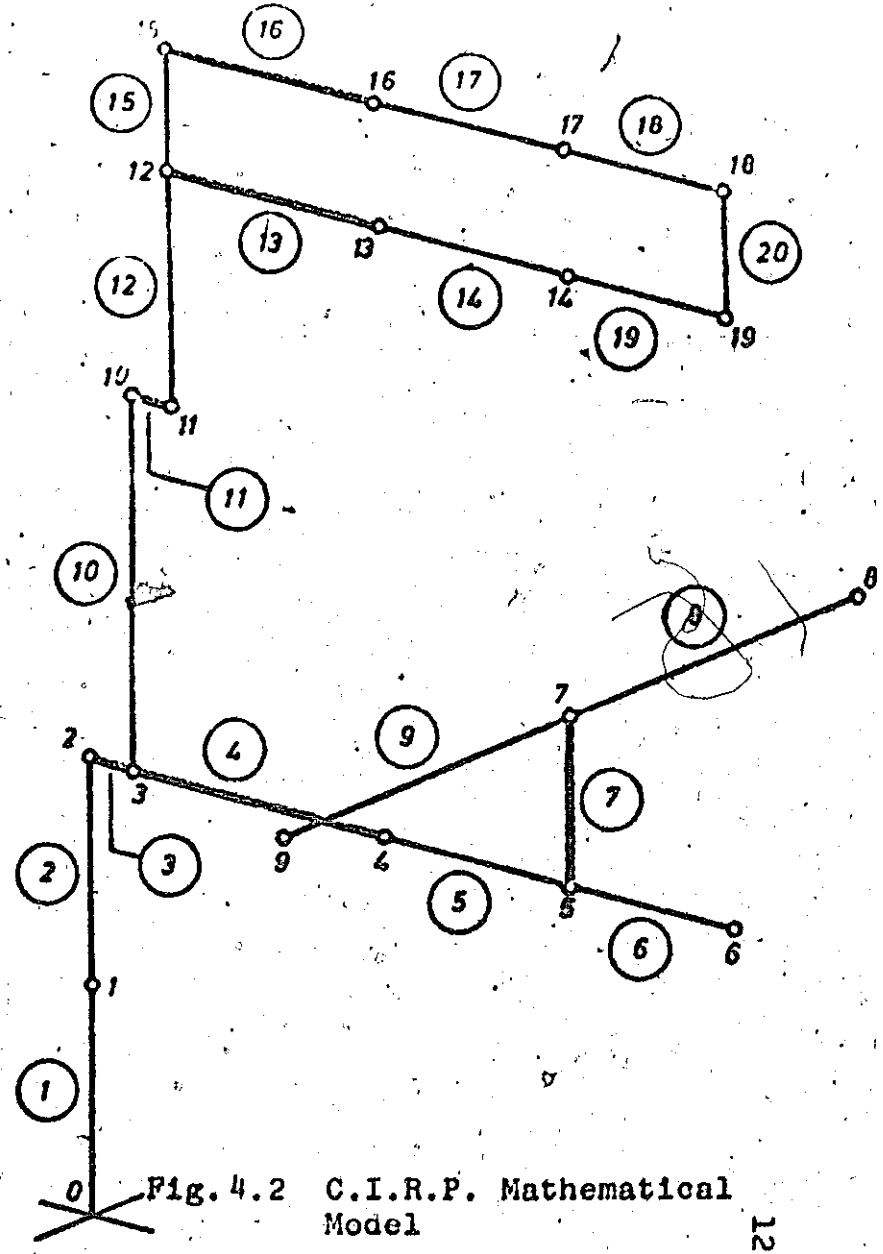

Fig. 4.2 C.I.R.P. Mathematical Model

Fig. 4.3. C.I.R.P. Model, Horizontal loading
Y- displacements

Horizontal Load (Y - axis) - 100 N at node 15

Y - Displacements

Node	U.M.I.S.T.	Leuven	McMaster
1	-.1371 E-06	-.2874 E-06	-.1371 E-06
2	-.5400 E-06	-.8532 E-06	-.5406 E-06
3	-.5400 E-06	-.8532 E-06	-.5406 E-06
4	-.5400 E-06	-.8532 E-06	-.5406 E-06
5	-.5400 E-06	-.8532 E-06	-.5406 E-06
6	-.5400 E-06	-.8532 E-06	-.5406 E-06
7	-.9591 E-06	-.1272 E-05	-.9596 E-06
8	-.9591 E-06	-.1272 E-05	-.9596 E-06
9	-.9591 E-06	-.1272 E05	-.9596 E-06
10	-.1763 E-05	-.2372 E-05	-.1764 E-05
11	-.1763 E-05	-.2372 E-05	-.1764 E-05
12	-.2753 E-05	-.3569 E-05	-.2755 E-05
13	-.2753 E-05	-.3569 E-05	-.2755 E-05
14	-.2752 E-05	-.3569 E.05	-.2754 E-05
15	-.3507 E-05	-.4462 E-05	-.3509 E-05
16	-.3507 E-05	-.4462 E-05	-.3509 E-05
17	-.3507 E-05	-.4462 E-05	-.3509 E-05
18	-.3508 E-05	-.4462 E-05	-.3510 E-05
19	-.2751 E-05	-.3594 E-05	-.2754 E-05

Fig. 4.4 C.I.R.P. Model, Horizontal loading

Z displacements

Horizontal load (y-axis) -1000 N at node 15

Z - Displacements

Node	U.M.I.S.T.	Leuven	McMaster
1	0	0	0
2	0	0	0
3	.9167 E-07	.9297 E-07	.9296 E-07
4	.6875 E-06	.6875 E-06	.6874 E-06
5	.1145 E-05	.1146 E-05	.1146 E-05
6	.1511 E-05	.1512 E-05	.1512 E-05
7	.1145 E-05	.1146 E-05	.1146 E-05
8	.1145 E-05	.1146 E-05	.1146 E-05
9	.1145 E-05	.1146 E-05	.1146 E-05
10	.9167 E-07	.9297 E-07	.9296 E-07
11	.2381 E-06	.2395 E-06	.2395 E-06
12	.2381 E-06	.2395 E-06	.2395 E-06
13	.1303 E-05	.1305 E-05	.1305 E-05
14	.2302 E-05	.2323 E-05	.2305 E-05
15	.2381 E-06	.2395 E-06	.2395 E-06
16	.1338 E-05	.1340 E-05	.1340 E-05
17	.2323 E-05	.2352 E-05	.2325 E-05
18	.3108 E-05	.3197 E-05	.3111 E-05
19	.3108 E-05	.3197 E-05	.3111 E-05

Fig. 4.5 C.I.R.P. Model Vertical loading

Y - displacements

Vertical Load -1000 N at node 6

1000 N at node 19

Y - Displacements

Node	U.M.I.S.T.	Leuven	McMaster
1	0	0	0
2	0	0	0
3	0	0	0
4	0	0	0
5	0	0	0
6	0	0	0
7	.3944 E-06	.3997 E-06	.3998 E-06
8	.3944 E-06	.3997 E-06	.3998 E-06
9	.3944 E-06	.3997 E-06	.3998 E-06
10	-.3523 E-06	-.3540 E-06	-.3541 E-06
11	-.3523 E-06	-.3540 E-06	-.3541 E-06
12	-.9610 E-06	-.9622 E-06	-.9622 E-07
13	-.9610 E-06	-.9622 E-06	-.9622 E-06
14	-.1380 E-06	-.2526 E-06	-.1380 E-06
15	-.1597 E-05	-.1684 E-05	-.1599 E-06
16	-.1597 E-05	-.1684 E-05	-.1599 E-06
17	-.1759 E-05	-.1821 E-05	-.1759 E-06
18	-.1887 E-05	-.1931 E-05	-.1887 E-06
19	.5233 E-06	.3151 E-06	.5214 E-06

Fig. 4.6 C.I.R.P. Model, Vertical Loading

Z - displacements

Vertical Load -1000N at node 6

-1000N at node 19

Z - Displacements

Node	U.M.I.S.T.	Leuven	McMaster	
1	0	0	0	
2	0	0	0	
3	0	0	0	
4	0	0	0	
5	-.2468 E-06	-.5069 E-06	-.2467 E-06	
6	-.6530 E-06	-.1122 E-05	-.6539 E-06	(-6.0mm)
7	-.2468 E-06	-.5069 E-06	-.2467 E-06	
8	-.2468 E-06	-.5069 E-06	-.2467 E-06	
9	-.2468 E-06	-.5069 E-06	-.2467 E-06	
10	.8800 E-07	.8794 E-07	.8794 E-07	
11	.1567 E-06	.1566 E-06	.1566 E-06	
12	.2187 E-06	.2185 E-06	.2185 E-06	
13	.1016 E-05	.1016 E-05	.1016 E-05	
14	.5113 E-05	.6798 E-05	.5113 E-05	
15	.2610 E-06	.2603 E-06	.2606 E-06	
16	.1294 E-05	.1296 E-05	.1294 E-05	
17	.4690 E-05	.6386 E-05	.4694 E-05	
18	.8674 E-05	.1202 E-04	.8677 E-05	
19	.8861 E-05	.1221 E-04	.8862 E-05	(23.0mm)

Natural Frequencies Hz

Mode	Leuven	U.M.I.S.T.	Aachen	Eindhoven	Birmingham	Kyoto	McMaster
1	185/184	184	189	184	184	189	187
2.	334/381	334	318	334	334	352	338
3.	410/425	408	401	408	408	384	400
4.	497/499	478	-	476	485	476	470
5.	529/670	670	-	670	687	761	676
6.	678/720	713	555	713	713	873	712

Fig. 4.7 C.I.R.P. Model Natural frequencies

FIG. 4.8 C.I.R.P. Model First Mode

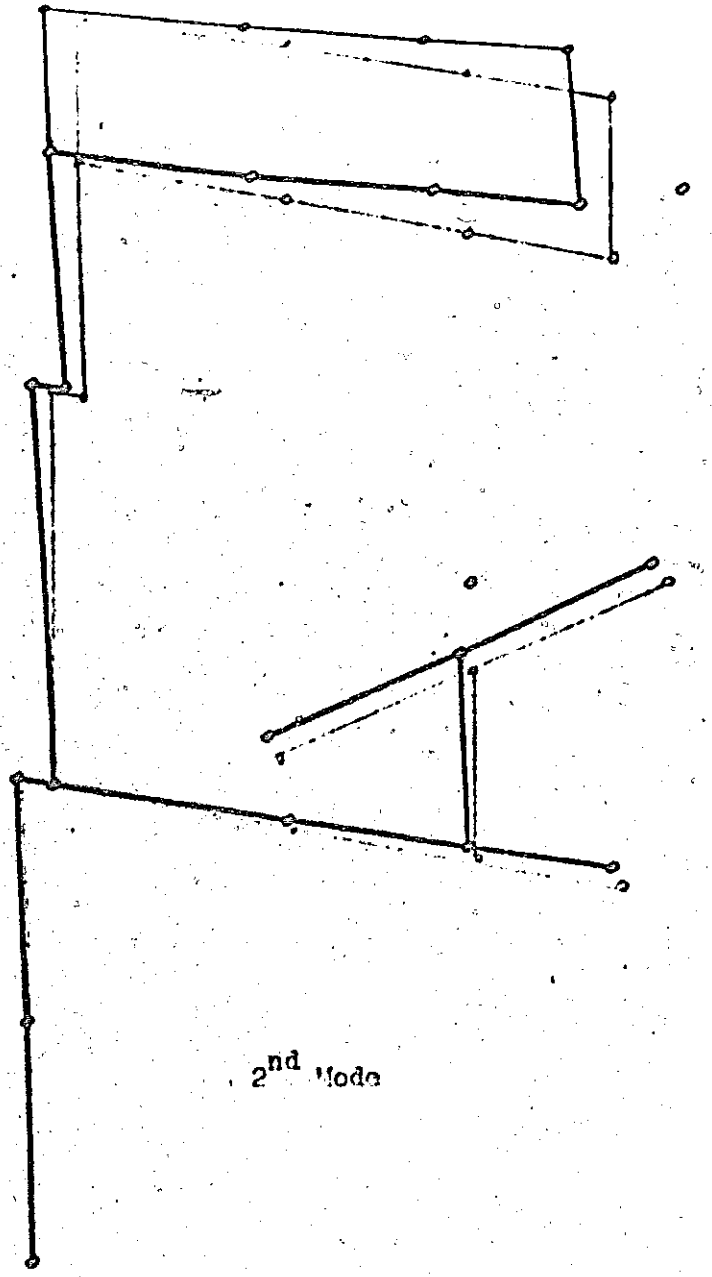

2nd Mode

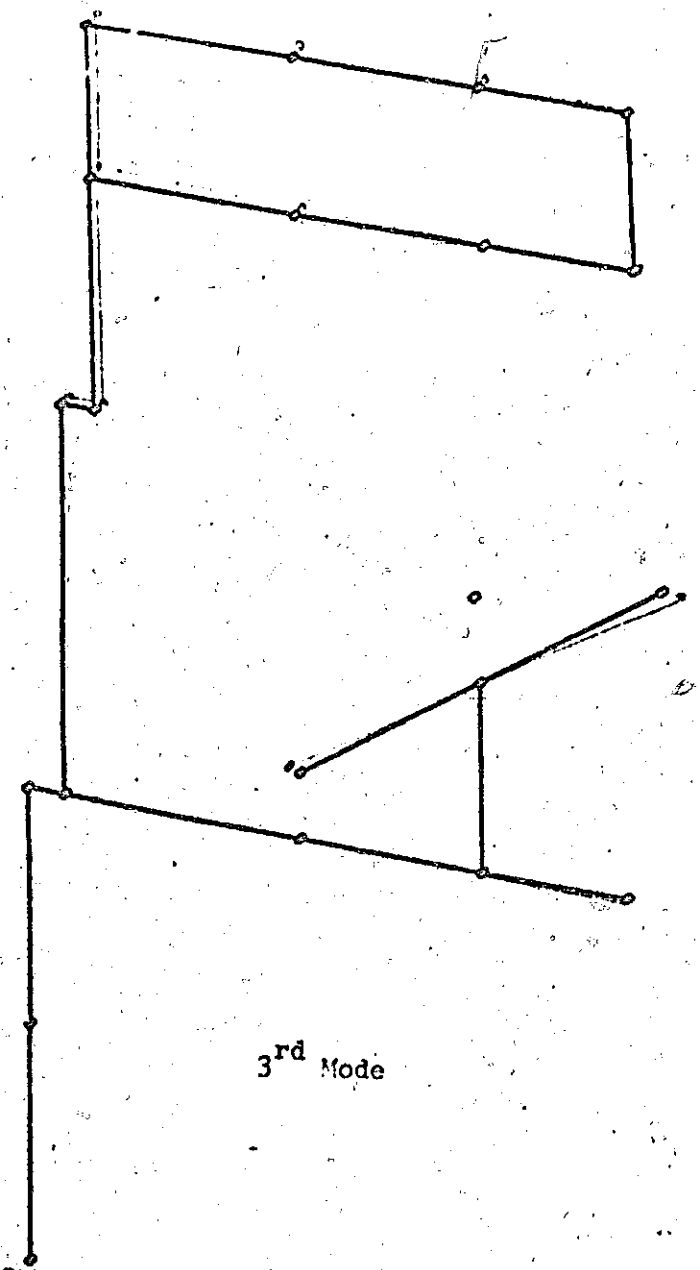

3rd Mode

FIG. 4.9 C.I.R.P. Model

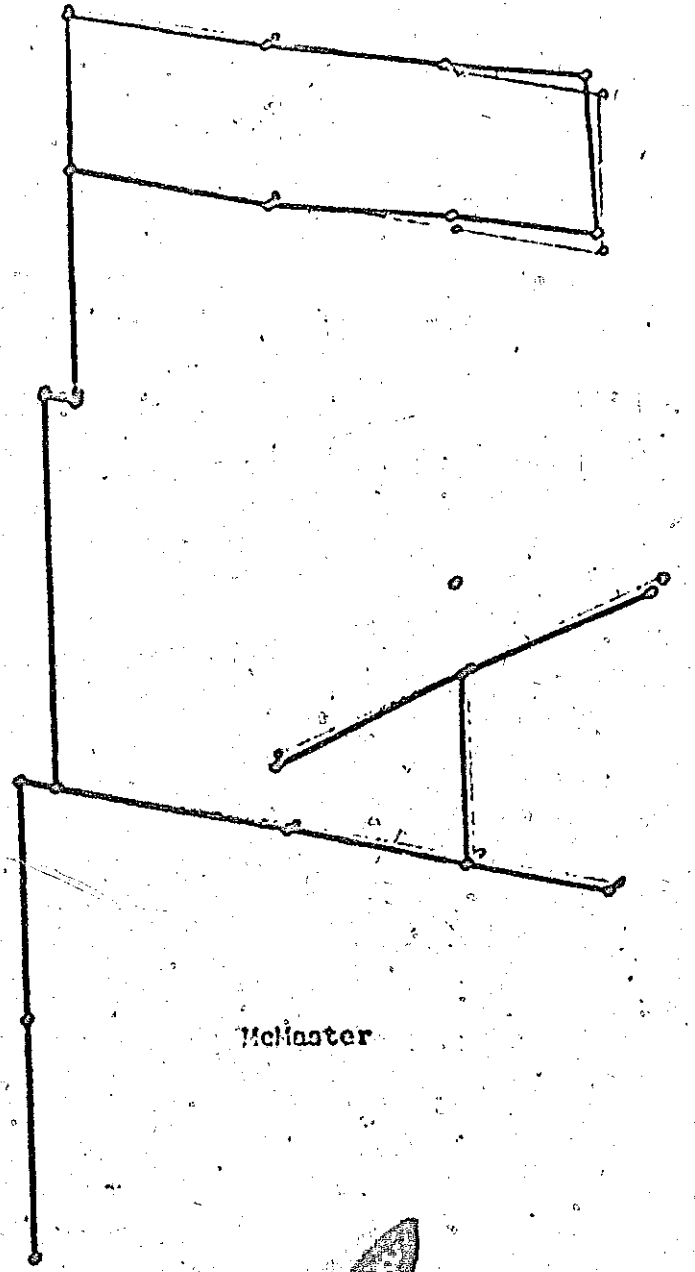

McMaster

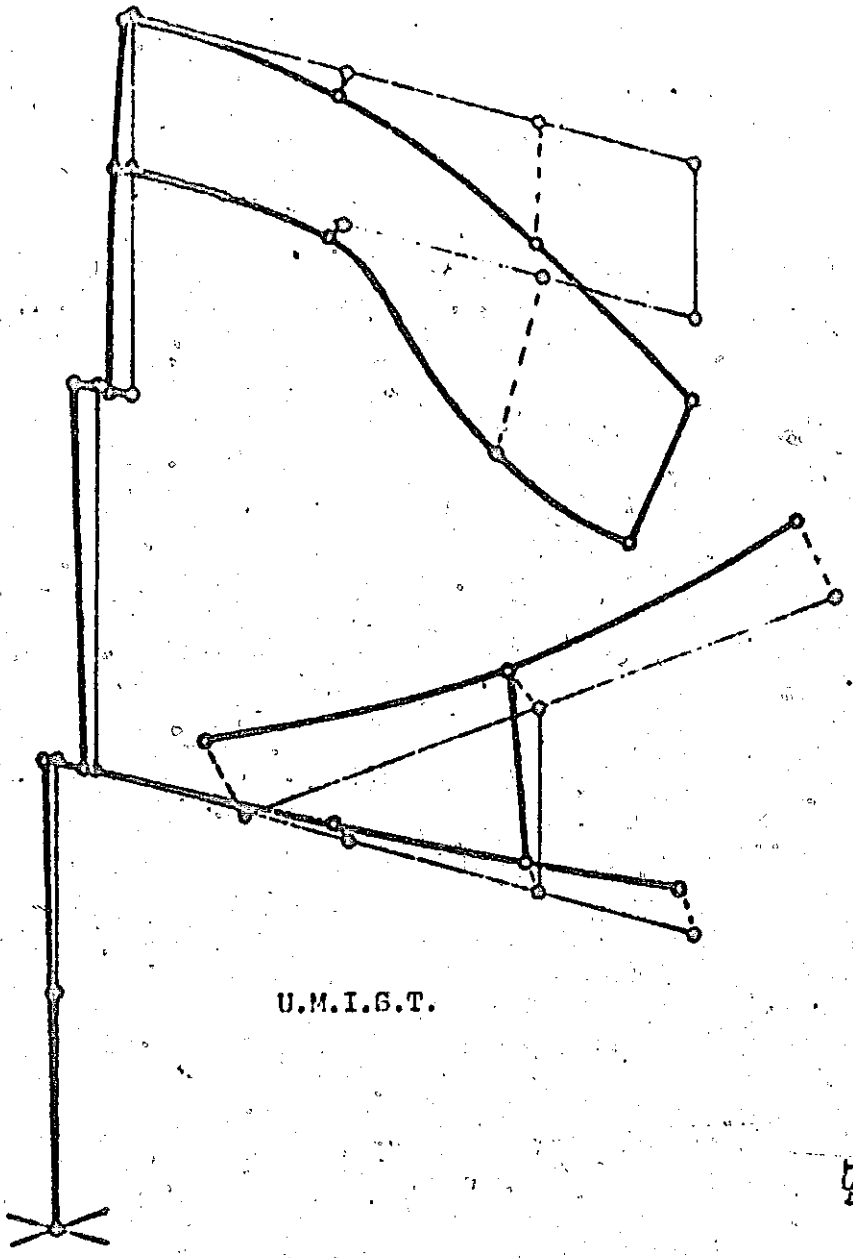

U.M.I.S.T.

FIG. 4.10 C.I.R.P. Model 5th Mode

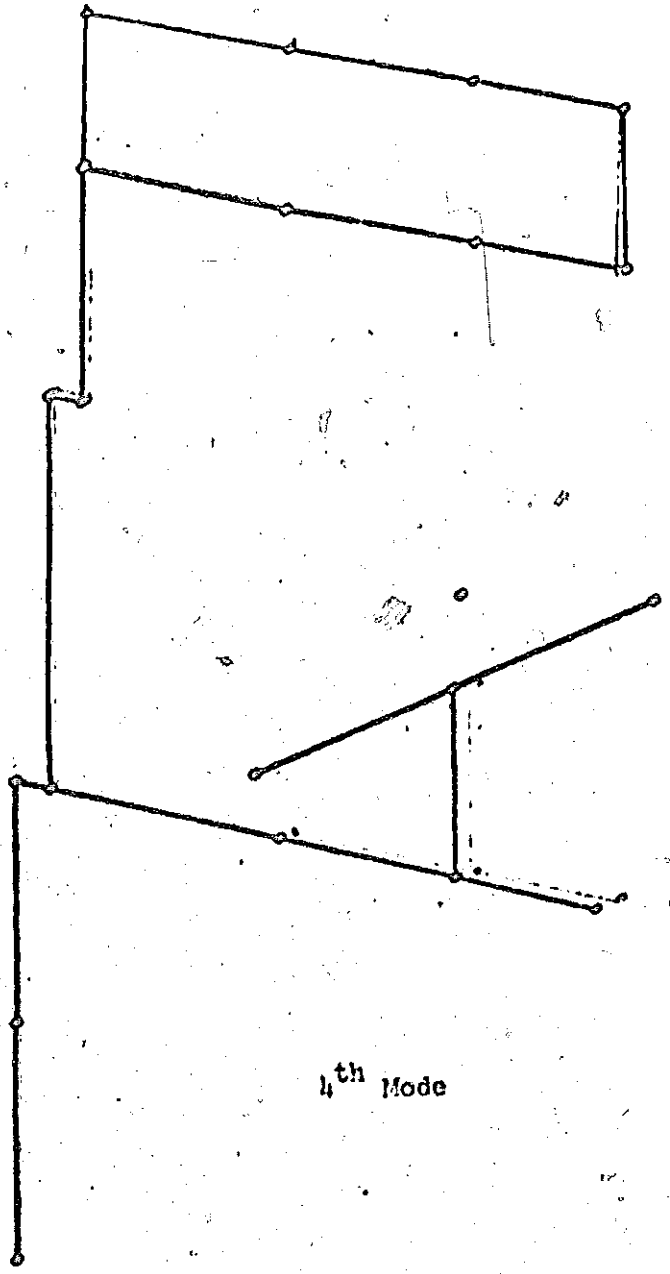

4th Mode

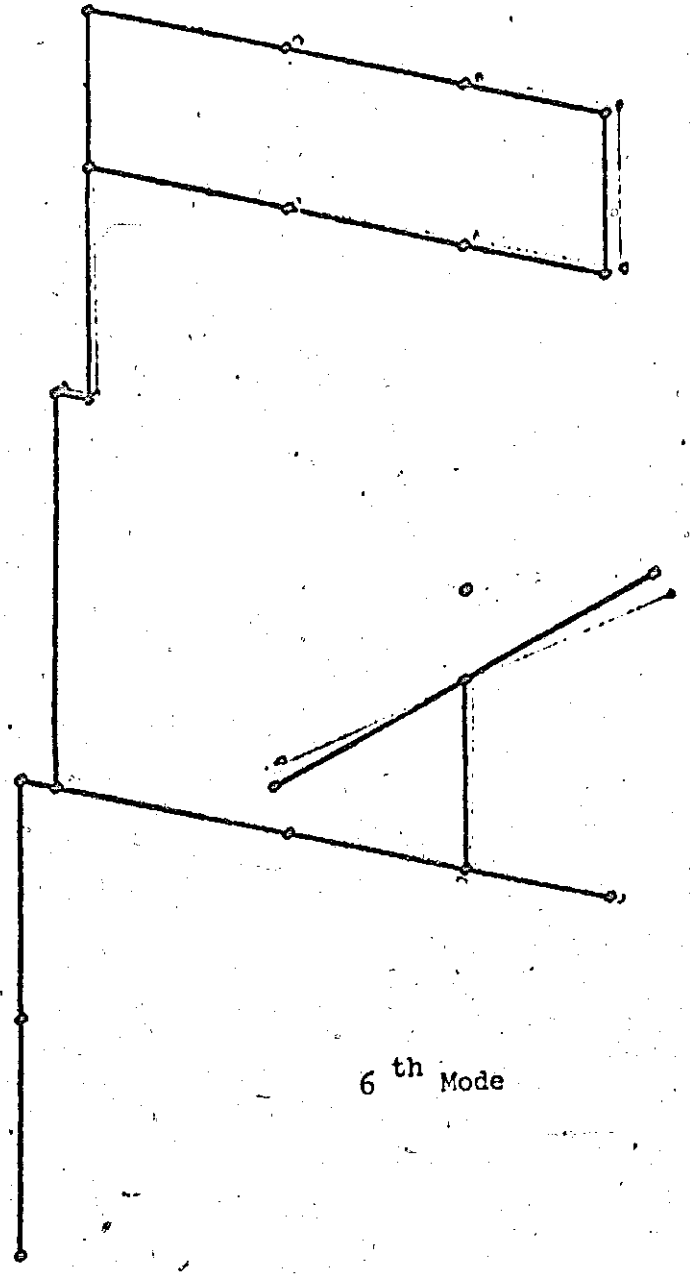

6 th Mode

FIG. 4.11 C.I.R.P. Model

```
6400 END OF RECORD
PROGRAM TST (INPUT,OUTPUT,TAPE5=INPUT,TAPE6=OUTPUT)


      DYNAMIC ANALYSIS OF LATHE SPINDLE


      DIMENSION XI(6),XL(6),S(11,11),B1(4),B2(4),B3(4),XV(7,7),
     1  N1(4),VEC(7,7),A(7,7),CK(4,4),UNIT(4,4),N2(7),
     2 NC(2), BS(2),S1(11,7),S2(11,4),B(7,7),T(7,4),U(4,7),V(4,4),
     3  VU(4,7),TVU(7,7),SP(7,7)

      WRITE(6,301)
  301 FORMAT (1H1,5X,40HSPINDLE SUSPENDED FREELY (WITHOUT GEARS)  ///)
      WRITE(6,303)
  303 FORMAT (5X,11HCHUCK NO. 2  /)
      WRITE(6,306)
  306 FORMAT (5X,15HWORKPIECE NO. 3  /)
      WRITE (6,307)
  307 FORMAT (5X,11HMODEL NO. 1 ///)

         N=NO. OF DEGREES OF FREEDOM, NE =NO. OF BEAM ELEMENTS
      N=11
      NE=6
      EMOD=30.E6
         NB = NO. OF BEARINGS
      NB=0
         TS IS STIFFNESS OF SPIRAL SPRING (WORKPIECE IN CHUCK)
      TS=10.E6
      DO 20 I=1,NE
      READ (5,10) XI(I), XL(I)
   10 FORMAT(2F10.0)
   20 CONTINUE
      NEN=NE-2
      DO 30 I=1,NEN
      B1(I)=EMOD*(XI(I)/XL(I))
      B2(I)=B1(I)/XL(I)
      B3(I)=B2(I)/XL(I)
   30 CONTINUE

         STIFFNESS MATRIX
      DO 35 I = 1,N
      DO 35 J = 1,N
      S(I,J) = 0.0
   35 CONTINUE
         LEADING DIAGONAL
      S(1,1)=12.*B3(1)
      S(2,2)=4.*B1(1)
      S(N-2,N-2)=    12.*B3(NE-2)+TS/(XL(NE)*(XL(NE)+XL(NE-1)))
      S(N-1,N-1)=  4.*B1(NE-2)+TS*((XL(NE)+XL(NE-1))/XL(NE))
      S(N,N)=  TS/(XL(NE)*(XL(NE)+XL(NE-1)))
      DO 40 I=2,NEN
      L=2*I-1
      S(L,L)=12.*(B3(I)+B3(I-1))
```

FIG. A.1 Programme using the reduced mass-matrix method

```
      LL=2*I
      S(LL,LL)=4.*(B1(I)+B1(I-1))
   50 CONTINUE
         FIRST UPPER DIAGONAL
      S(1,2)=6.*B2(1)
      S(N-2,N-1)=-6.*B2(NEN)+TS/XL(NE)
      S(N-1,N)=-TS/XL(NE)
      DO 60 I=1,NEN
      L=2*I
      S(L,L+1)=-6.*B2(I)
   60 CONTINUE
      DO 70 I=2,NEN
      L=2*I
      S(L-1,L)=6.*(B2(I)-B2(I-1))
   70 CONTINUE
         SECOND UPPER DIAGONAL
      S(N-2,N)=-TS/((XL(NE))*(XL(NE)+XL(NE-1)))
      DO 70 I=1,NEN
      L=2*I
      S(L-1,L+1)=-12.*B2(I)
      S(L,L+2)=2.*B1(I)
   80 CONTINUE
         THIRD UPPER DIAGONAL
      DO 80 I=1,NEN
      L=2*I
      S(L-1,L+2)=6.*B2(I)
   80 CONTINUE
         LOWER DIAGONALS
      DO 90 I=2,N
      L=I-1
      DO 90 J=1,L
      S(I,J)=S(J,I)
   90 CONTINUE

         BEARING STIFFNESS
      IF(NB.EQ.0)  GO TO 101
      DO 100 I=1,NB
      READ (5,105) NC(I),BS(I)
  105 FORMAT(I10,F15.0)
      JN=NC(I)
      S(JN,JN) = S(JN,JN) + BS(I)
  100 CONTINUE
  101 WRITE (6,240)
  240 FORMAT (10X,16HSTIFFNESS MATRIX  //)
      DO 92 I=1,N
      WRITE(6,93)  ( S(I,J),J=1,N)
   93 FORMAT (11E11.3 /)
   92 CONTINUE

         INTERCHANGE ROWS AND COLOYNS
      CALL RINT (S,N,N,11,8)
      CALL RINT (S,N,N,8,6)
      CALL RINT (S,N,N,2,9)
      CALL RINT (S,N,N,4,10)
      CALL CINT (S,N,11,8)
      CALL CINT (S,N,8,6)
      CALL CINT (S,N,2,9)
```

```
      CALL CINT (S,N,11,8)

C     PARTITION STIFFNESS MATRIX
      CALL CCUT (S,8,S1,S2,11,11,0 )
      CALL RCUT (S1,8,R,U,11,7,0 )
      CALL RCUT (S2,8,T,V,11,4,0 )
      WRITE (6,535)
535   FORMAT(//10X,8HR MATRIX  */)
      DO 550 I=1,7
      WRITE(6,540)  (R(I,J),J=1,7)
540   FORMAT (7E11.3 /)
550   CONTINUE
      WRITE (6,560)
560   FORMAT(// 10X,8HT MATRIX  */)
      DO 570 I=1,7
      WRITE (6,565)  (T(I,J), J=1,4)
565   FORMAT (4E11.3)
570   CONTINUE
      WRITE (6,575)
575   FORMAT (// 10X, 8HU MATRIX  */)
      DO 580 I=1,4
      WRITE(6,585)  (U(I,J),  J=1,7)
585   FORMAT(7E11.3 /)
580   CONTINUE
      WRITE(6,590)
590   FORMAT (// 10X,8HV MATRIX */)
      DO 595 I=1,4
      WRITE(6,600)  (V(I,J), J=1,4)
600   FORMAT (4E11.3 /)
595   CONTINUE

C     FORM REDUCED STIFFNESS MATRIX
C       INVERT MATRIX V
      DO 96 I = 1,4
      DO 96 J = 1,4
      CK(I,J)=V(I,J)
 96   CONTINUE
      DO 170 I=1,4
      DO 170 J=1,4
      V(I,J) =(V(I,J))/(1.0E6)
170   CONTINUE
      CALL INVMAT(V,4,4,1.E-7,IERR,N11)
      IF (IERR .EQ. 0)  GO TO 160
      WRITE (6,165)  IERR
      GO TO 150
165   FORMAT ( 24HINVERSION FAILS.   IERR=   ,I4)
160   WRITE (6,94)
 94   FORMAT (// 10X,16HV INVERSE MATRIX  */)
      DO 190 I=1,4
      DO 190 J=1,4
      V(I,J)=(V(I,J))/(1.0E6 )
190   CONTINUE
      DO 192 I=1,4
      WRITE(6,193)  (V(I,J),J=1,4)
193   FORMAT( 4E11.3 /)
192   CONTINUE
      DO 200 I=1,4
```

```
      DO 200 J=1,4
      UNIT(I,J)=0.0
      DO 205 K=1,4
      UNIT(I,J)=UNIT(I,J)+(CK(I,K))*(V(K,J))
  205 CONTINUE
  200 CONTINUE
      WRITE (6,106)
  106 FORMAT(/// 10X,13HINVERSE CHECK /)
      DO 108 I = 1,4
      WRITE(6,107)  (UNIT(I,J),J=1,4)
  107 FORMAT( 4E11.4 /)
  108 CONTINUE

          MULTIPLY INVERSE V BY U
      DO 500 I = 1,4
      DO 505 J = 1,7
      VU(I,J)=0.0
      DO 505 K=1,4
      VU(I,J)=VU(I,J)+(V(I,K))*(U(K,J))
  505 CONTINUE
  500 CONTINUE
      WRITE(6,605)
  605 FORMAT(//10X,10HVU PRODUCT ,/)
      DO 610 I=1,4
      WRITE(6,615)  (VU(I,J),  J=1,7)
  615 FORMAT(7E11.3 /)
  610 CONTINUE

          MULTIPLY T BY VU
      DO 510 I=1,7
      DO 510 J=1,7
      TVU(I,J)=0.0
      DO 515 K=1,4
      TVU(I,J)=TVU(I,J)+(T(I,K))*(VU(K,J))
  515 CONTINUE
  510 CONTINUE
      WRITE(6,620)
  620 FORMAT(// 10X,11HTVU PRODUCT ' /)
      DO 625 I=1,7
      WRITE(6,630)  (TVU(I,J),  J=1,7)
  630 FORMAT(7E11.3 KJ)
  625 CONTINUE

          SUBTRACT TVU FROM R.  SR IS REDUCED STIFFNESS MATRIX
      DO 520 I=1,7
      DO 520 J=1,7
      SR(I,J)=R(I,J) - TVU(I,J)
  520 CONTINUE
      WRITE(6,635)
  635 FORMAT(// 10X,24HREDUCED STIFFNESS MATRIX  /)
      DO 640 I=1,7
      WRITE(6,645)  (SR(I,J),  J=1,7)
  645 FORMAT (7E11.3 /)
  640 CONTINUE

          REDUCED MASS MATRIX      (IN NEW ORDER)
      DO 110 I=1,7
```

```
      DO 110 J=1,7
      XM(I,J)=0.0
  110 CONTINUE
      DO 120 I=1,7
      READ(5,125)  XM(I,I)
  125 FORMAT(F12.0)
  120 CONTINUE
      WRITE(6,122)
  122 FORMAT (/// 10X,11HMASS MATRIX /)
      DO 124 I=1,7
      WRITE(6,123) (XM(I,J),J=1,7)
  123 FORMAT ( 7E10.5)
  124 CONTINUE

            INVERT MASS MATRIX
      CALL INVMAT(XM,7,7,1.E-7,IERR,N2)
      IF (IERR .EQ. 0)  GO TO 530
      WRITE (6,165)  IERR
      GO TO 150

            INVERTED MASS --STIFFNESS PRODUCT
  530 WRITE (6,220)
  220 FORMAT(/// 10X,14HMATRIX PRODUCT  //)
      DO 210 I=1,7
      DO 210 J=1,7
      A(I,J)=0.0
      DO 215 K=1,7
      A(I,J)=A(I,J)+(XM(I,K))*(SR(K,J))
  215 CONTINUE
  210 CONTINUE
      WRITE (6,225) ((A(I,J), J=1,7), I= 1,7)
  225 FORMAT ( 7E11.3)
      DO 130 I=1,7
      DO 130 J=1,7
  130 VEC(I,J)=0.0
      DO 135 I=1,7
  135 VEC(I,I)=1.0
      CALL EBEPVC(A,7,1,200,1.E-11,1.E-12,1.,7,VEC,1.)
      WRITE (6,136)
  136 FORMAT(/// 10X,11HEIGENVALUES /)
      WRITE(6,137)((A(I,J),J=1,7), I=1,7)
      WRITE(6,138)
  138 FORMAT (// 10X,12HEIGENVECTORS /)
      WRITE(6,137)  ((VEC(I,J),J=1,7),I=1,7)
  137 FORMAT ( 7E11.3)
      WRITE (6,400)
  400 FORMAT (1H1,5X,27HFREQUENCIES AND MODE SHAPES ///)
      DO 140 I=1,7
      XLIM=1.E-12
      IF (A(I,I) .LE. XLIM)  GO TO 142
      FREQ=(1.0/6.284)*SQRT (A(I,I))
      WRITE(6,145) I,FREQ,(VEC(J,I), J=1,7)
  145 FORMAT (    5X,I4,5X,12HFREQUENCY =    ,E10.3,4H HZ.  /
     1  5X,12HEIGENVECTORS /  4X,  7E11.3/ )
      GO TO 140
  142 WRITE (6,143)I,A(I,I)
  143 FORMAT (    10X,I4,10H  A(I,I)= ,E12.5/)
```

```
140 CONTINUE
150 STOP
    END
      6400 END OF RECORD
.74       8.5
3.25       5.75
5.78      4.6
8.35        6.1
.          4.6
.          5.0
.234
.328
.315
.78
.206
.170
.449
           END OF FILE

                        CD TOT   0305
```

```
      PROGRAM TST (INPUT,OUTPUT,TAPE5=INPUT,TAPE6=OUTPUT)
C
C           DYNAMIC ANALYSIS OF LATHE SPINDLE
C
      DIMENSION XI(9),XL(9),S(20,20),B1(9),B2(9),B3(9),XM(20,20),
     1 N1(20),A(20,20),CK(20,20),UNIT(20,20),B(20,20),
     2 NC(2),BS(2),EY(20),EZ(20),EIGVAL(20,20),
     3          VECR(20,20),VECI(20,20),INDIC(20,20),EVI(20,20),XC(6)
C
      WRITE(6,301)
  301 FORMAT (1H1,5X,40HSPINDLE SUSPENDED FREELY (WITHOUT GEARS) //)
      WRITE(6,303)
  303 FORMAT (5X,11HCHUCK NO. 2  /)
      NO=1
C
C         N=NO. OF DEGREES OF FREEDOM, NE =NO. OF BEAM ELEMENTS
      N=21
      NE=9
      NN=N-1
      EMOD=30.E6
C         NB = NO. OF BEARINGS
      NB=2
      DO 20 I=1,NE
      READ (5,10) XI(I), XL(I)
   10 FORMAT(2F10.0)
   20 CONTINUE
      DO 726 I=1,6
      READ (5,725) XC(I)
  725 FORMAT (F10.0)
  726 CONTINUE
C
C         BEARING STIFFNESS
      WRITE(6,800)
  800 FORMAT(// 5X,51HBEARINGS.LOCATION NODES AND STIFFNESSES IN LB./IN.
     1  /)
      DO 733 I=1,NB
      READ (5,105) NC(I),BS(I)
      WRITE(6,801)   NC(I), BS(I)
  801 FORMAT(10X,I4,F10.2 /)
  105 FORMAT(I10,F15.0)
  733 CONTINUE
C
C         MASS MATRIX
      DO 110 I=1,N
      DO 110 J=1,N
      XM(I,J)=0.0
  110 CONTINUE
      DO 120 I=1,N
      READ(5,125)  XM(I,I)
  125 FORMAT(F12.0)
  120 CONTINUE
      WRITE(6,122)
  122 FORMAT (/// 10X,11HMASS MATRIX /)
```

Fig. A.2

Final programme, used to determine clamping stiffness.

```
      DO 124 I=1,N
      WRITE(6,123) (XM(I,J),J=1,N)
  123 FORMAT (10F10.5/)
  124 CONTINUE
      DO 731 M=1,6
      XI(I)=XC(M)
      DO 30 I=1,NE
      B1(I)=EMOD*(XI(I))/XL(I)
      B2(I)=B1(I)/XL(I)
      B3(I)=B2(I)/XL(I)
   30 CONTINUE
C
C          STIFFNESS MATRIX
      DO 35 I =1,N
      DO 35 J = 1,N
      S(I,J) = 0.0
   35 CONTINUE
C          LEADING DIAGONAL
      S(1,1)=12.*B3(1)
      S(2,2)=4.*B1(1)
      S(N-1,N-1)=12.*B3(NE)
      S(N,N)=4.*B1(NE)
      DO 40 I=2,NE
      L=2*I-1
      S(L,L)=12.*(B3(I)+B3(I-1))
      LL=2*I
      S(LL,LL)=4.*(B1(I)+B1(I-1))
   40 CONTINUE
C          FIRST UPPER DIAGONAL
      S(1,2)=6.*B2(1)
      S(N-1,N)=-6.*B2(NE)
      DO 50 I=1,NE
      L=2*I
      S(L,L+1)=-6.*B2(I)
   50 CONTINUE
      DO 60 I=2,NE
      L=2*I
      S(L-1,L)=6.*(B2(I)-B2(I-1))
   60 CONTINUE
C          SECOND UPPER DIAGONAL
      DO 70 I=1,NE
      L=2*I
      S(L-1,L+1)=-12.*B3(I)
      S(L,L+2)=2.*B1(I)
   70 CONTINUE
C          THIRD UPPER DIAGONAL
      DO 80 I=1,NE
      L=2*I
      S(L-1,L+2)=6.*B2(I)
   80 CONTINUE
C          LOWER DIAGONALS
      DO 90 I=2,N
      L=I-1
      DO 90 J=1,L
      S(I,J)=S(J,I)
```

```
      DO 100 I=1,NB
      JN=NC(I)
      S(JJ,JN) = S(JN,JN) + BS(I)
  100 CONTINUE
  101 DO 96 I = 1,N
      DO 96 J = 1,N
      CK(I,J)=S(I,J)
   96 CONTINUE
      WRITE (6,240)
  240 FORMAT(// 10X,16HSTIFFNESS MATRIX    //)
      DO 92 I=1,N
      WRITE(6,93)  (CK(I,J),J=1,N)
   93 FORMAT ( 7E10.3 /)
   92 CONTINUE
C        TO INVERT MATRIX
      DO 170 I=1,N
      DO 170 J=1,N
      S(I,J) =(S(I,J))/(1.0E6)
  170 CONTINUE
      CALL INVMAT(S,N,N,1.E-7,IERR,N1)
      IF (IERR .EQ. 0)  GO TO 160
      WRITE (6,165)  IERR
      GO TO 150
  165 FORMAT ( 24HINVERSION FAILS.   IERR=   ,I4)
  160 WRITE (6,94)
   94 FORMAT(// 10X,14HINVERSE MATRIX  ,/)
      DO 190 I=1,N
      DO 190 J=1,N
      S(I,J)=(S(I,J))/(1.0E6 )
  190 CONTINUE
      DO 102 I=1,N
      WRITE(6,103)  (S(I,J),J=1,N)
  103 FORMAT ( 7E10.3/)
  102 CONTINUE
      DO 200 I=1,N
      DO 200 J=1,N
      UNIT(I,J)=0.0
      DO 205 K=1,N
      UNIT(I,J)=UNIT(I,J)+(CK(I,K))*(S(K,J))
  205 CONTINUE
  200 CONTINUE
      WRITE (6,106)
  106 FORMAT(/// 10X,13HINVERSE CHECK /)
      DO 108 I = 1,N
      WRITE(6,107)  (UNIT(I,J),J=1,N)
  107 FORMAT ( 7E10.3/)
  108 CONTINUE
C
C        MATRIX PRODUCT
      WRITE (6,220)
  220 FORMAT(/// 10X,14HMATRIX PRODUCT  //)
      DO 210 I=1,N
      DO 210 J=1,N
      A(I,J)=0.0
```

```
      DO 215 J=1,N
      A(I,J)=(I,J)+(S(I,K))*(XM(K,J))
  215 CONTINUE
  210 CONTINUE
      WRITE (6,225) ((A(I,J), J=1,N), I=1,N)
  225 FORMAT ( 7E10.3/)
      CALL EIGENP( N, N,A,48.0,EIGVAL,EVI,VECR,VECI,INDIC)
      WRITE (6,135)
  136 FORMAT(/// 10X,11HEIGENVALUES /)
      WRITE(6,508)   (EIGVAL(I),I=1,N)
  508 FORMAT (E11.3)
      WRITE(6,138)
  138 FORMAT (// 10X,12HEIGENVECTORS /)
      WRITE(6,137)   ((VECR(J,I),J=1,N),I=1,N)
  137 FORMAT ( 7E10.3/)
      WRITE (6,400)
  400 FORMAT (1H1,5X,27HFREQUENCIES AND MODE SHAPES ///)
      WRITE(6,333)   NO
  333 FORMAT(5X,18HMODEL TRY-OUT NO.  ,I2//)
      DO 140 I=1,N
      XLIM=1.E-12
      IF(EIGVAL(I) .LE. XLIM)  GO TO 142
      FREQ=(1.0/6.284)*SQRT(1.0/EIGVAL(I))
      WRITE(6,145) I,FREQ
  145 FORMAT (//  5X,I4,5X,12HFREQUENCY =   ,E10.3,4H HZ.  /
     1   5X,12HEIGENVECTORS   )
      WRITE(6,146)     (VECR(J,I),    J=1,NN,2)
  146 FORMAT(/ 4X,10F11.3)
      GO TO 140
  142 WRITE (6,143)I,EIGVAL(I)
  143 FORMAT (     10X,I4,10H EIGVAL =   ,E12.5/)
  140 CONTINUE
      DO 732 I=1,NE
      WRITE(6,723)    XI(I), XL(I)
  723 FORMAT(10X,2F12.5)
  732 CONTINUE
  731 CONTINUE
  150 STOP
      END
```

MODEL TRY-OUT NO. 1

1 FREQUENCY = .582E+00 HZ.
EIGENVECTORS

-.632	-.544	-.393	-.292	-.210	-.102	-.021	-.012	.032

2 FREQUENCY = .164E+00 HZ.
EIGENVECTORS

.390	.281	.097	-.027	-.127	-.259	-.358	-.369	-.423

3 FREQUENCY = .445E+03 HZ.
EIGENVECTORS

.635	.366	-.004	-.131	-.156	-.103	.037	.071	.299

4 FREQUENCY = .772E+03 HZ.
EIGENVECTORS

.671	.204	-.212	-.230	-.144	.067	.157	.122	-.220

5 FREQUENCY = .134E+04 HZ.
EIGENVECTORS

.622	.038	-.414	-.221	-.000	.149	-.211	-.216	.093

6 FREQUENCY = .192E+04 HZ.
EIGENVECTORS

-.780	.116	.493	.014	-.210	.015	-.009	-.026	.023

7 FREQUENCY = .449E+04 HZ.
EIGENVECTORS

.673	-.421	.394	-.156	-.248	.074	.017	.016	.005

8 FREQUENCY = .346E+04 HZ.
EIGENVECTORS

-.788	.384	-.031	-.303	-.105	.009	-.039	-.031	-.012

9 FREQUENCY = .412E+04 HZ.
EIGENVECTORS

.410	-.232	.140	.072	-.006	.312	-.517	-.441	-.156